

C.C. TAŐAN

PRODUCTION AND CHARACTERIZATION OF  
RESOL TYPE PHENOLIC RESIN / LAYERED SILICATE  
NANOCOMPOSITES

CEMAL CEM TAŐAN

METU 2005

APRIL 2005

PRODUCTION AND CHARACTERIZATION OF  
RESOL TYPE PHENOLIC RESIN / LAYERED SILICATE  
NANOCOMPOSITES

A THESIS SUBMITTED TO  
THE GRADUATE SCHOOL OF NATURAL AND APPLIED SCIENCES  
OF  
MIDDLE EAST TECHNICAL UNIVERSITY

BY

CEMAL CEM TAŞAN

IN PARTIAL FULFILLMENT OF THE REQUIREMENTS  
FOR  
THE DEGREE OF MASTER OF SCIENCE  
IN  
METALLURGICAL AND MATERIALS ENGINEERING

APRIL 2005

Approval of the Graduate School of Natural and Applied Science

---

Prof. Dr. Canan Özgen  
Director

I certify that this thesis satisfies all the requirements as a thesis for the degree of Master of Science.

---

Prof. Dr. Tayfur Öztürk  
Head of Department

This is to certify that we have read this thesis and that in our opinion it is fully adequate, in scope and quality, as a thesis for the degree of Master of Science.

---

Assoc. Prof.Dr. Cevdet Kaynak  
Supervisor

Examining Committee Members

Prof. Dr. Ülkü Yılmaz (METU, CHE) \_\_\_\_\_

Assoc.Prof.Dr. Cevdet Kaynak (METU, METE) \_\_\_\_\_

Prof. Dr. Asuman Türkmenoğlu (METU, GEOE) \_\_\_\_\_

Assoc.Prof. Dr. Göknur Bayram (METU, CHE) \_\_\_\_\_

Asst.Prof. Dr. Caner Durucan (METU, METE) \_\_\_\_\_

**I hereby declare that all information in this document has been obtained and presented in accordance with academic rules and ethical conduct. I also declare that, as required by these rules and conduct, I have fully cited and referenced all material and results that are not original to this work.**

Name, Surname: C.Cem Taşan

Signature :

## **ABSTRACT**

### **PRODUCTION AND CHARACTERIZATION OF RESOL TYPE PHENOLIC RESIN / LAYERED SILICATE NANOCOMPOSITES**

Taşan, Cemal Cem

M.S., Department of Metallurgical and Materials Engineering

Supervisor: Assoc.Prof. Cevdet Kaynak

April 2005, 133 Pages

Polymer / layered silicate (P/LS) nanocomposites belong to one of the most promising group of materials of the past few decades and most probably for the near future. Combining two of the most widely studied topics of material science: composite materials and nanotechnology; P/LS research have drawn great attention starting with the pioneering works of Toyota Research Group in 1980's. The research is now being carried out world wide; since the excellent properties of these new materials, which is achieved by using very low amounts of a cheap reinforcement material (clay), increases the interest on these materials everyday after.

In this present study, the object was to investigate the production parameters of phenol formaldehyde based layered silicate nanocomposites. For this purpose, 14 different specimen groups were produced; using two different resol type phenolic resins (PF76 and PF76TD) as the matrix; and 9 different montmorillonite clays (Rheospan, Resadiye, Cloisite Na<sup>+</sup>, 10A, 15A, 20A, 25A, 30B, 94A) as the reinforcement phase. Initially the curing schedules for the available resins were experimentally determined. Then, a short and effective mixing procedure for the

thermosetting resin and the montmorillonite clay was developed. The effects of several processing parameters; such as clay type, clay source, clay content, clay modification, resin type, resin cure type, cure cycle and mixing cycle were determined by X-ray Diffraction, Scanning Electron Microscopy and Mechanical Tests. Then, Transmission Electron Microscopy was used to investigate the level of intercalation and/or exfoliation of the layered silicates. Finally, Differential Scanning Calorimetry was also carried out to analyse thermal properties of the specimens.

It was concluded that, a partially intercalated and/or exfoliated structure could be obtained in resol type phenolic resin based systems at very low clay contents (such as 0,5%) leading to remarkable increases in mechanical properties (e.g. 66% increase in fracture toughness).

**Keywords:** Nanocomposites, phenolic resin, resol, montmorillonite, layered silicate, clay modification, fracture toughness

## ÖZ

### RESOL TİPİ FENOLİK REÇİNE / KATMANLI SİLİKAT NANOKOMPOZİTLERİNİN ÜRETİMİ VE KARAKTERİZASYONU

Taşan, Cemal Cem

Yüksek Lisans, Metalurji ve Malzeme Mühendisliği Bölümü

Tez Yöneticisi: Doç.Dr.Cevdet Kaynak

Nisan 2005, 133 Sayfa

Polimer / katmanlı silikat (P/KS) nanokompozitleri, son yirmi yılın ve büyük ihtimalle yakın geleceğin, en umut vadeden malzeme gruplarından. Malzeme biliminin son dönemde en geniş çapta çalışılan iki konusunu; kompozit malzemeler ve nanoteknolojiyi biraraya getiren P/KS nanokompozitlerine ilgi 1980'li yıllarda Toyota Araştırma Grubunun öncülük ettiği çalışmalarla filizlendi. Günümüzde ise, üstün özellikleri ve bu özelliklerin ucuz bir güçlendirici malzemesinin (kil), çok düşük miktarlarda (0,5%) kullanılmasıyla elde edilebilmesi sayesinde, bu konudaki çalışmalar dünya çapında sürdürülmektedir ve ilgi her geçen gün artmaktadır.

Bu çalışmanın amacı fenol formaldehit bazlı katmanlı silikat nanokompozitlerin üretim parametrelerini incelemektir. Bu amaçla, matriks olarak 2 farklı resol tip fenolik reçine (PF76 ve PF76TD), ve güçlendirici faz olarak ta 9 farklı montmorilonit kili (Rheospan, Resadiye, Cloisite Na<sup>+</sup>, 10A, 15A, 20A, 25A,

30B, 94A) kullanılarak 14 farklı numune grubu üretilmiştir. Öncelikle elde bulunan reçinelerin pişirme süreçleri deneysel olarak belirlenmiştir. Ardından, termoset reçine ile kil için kısa ama etkili bir karıştırma yöntemi geliştirilmiştir. Kil tipi, kil kaynağı, kil miktarı, kil modifikasyonu, reçine türü, reçine pişirme etmenleri ve karıştırma işlemi gibi üretim parametrelerin etkisi X-Işınları Kırınımı, Taramalı Elektron Mikroskobu ve Mekanik Testlerin sonuçlarıyla incelenmiştir. Daha sonra, kil tabaka ayrışması ve/veya tabaka dağılması seviyelerinin tespiti için Geçirimli Elektron Mikroskobu kullanılmıştır. Diferansiyel Taramalı Kalorimetre ile termal özellikler incelenmiştir.

Sonuç olarak resol tipli fenolik reçine bazlı sistemlerde tabaka ayrışması ve/veya dağılması düşük kil miktarlarında (Ör. 0,5%) kısmi olarak elde edilebilmiş, ve bu malzemelerin mekanik özelliklerinde dikkat çekici artışlar gözlemlenmiştir (ör. Kırılma tokluğunda 66%).

**Anahtar Kelimeler:** Nanokompozit, fenolik reçine, resol, montmorilonit, kil modifikasyonu, kırılma tokluğu



*in memory of*  
*Barış Güvendi & Timur Ertürk*

## ACKNOWLEDGEMENTS

I am deeply thankful to Assoc.Prof.Cevdet Kaynak for his guidance and encouragement throughout the research and especially for his efforts in organizing the thesis in the final run.

I would like to thank POLİSAN Boya Sanayi ve Ticaret A.Ş., for kindly providing the phenolic resins; and to KARAKAYA Bentonit Sanayi ve Ticaret A.Ş. for providing the Resadiye clay.

I wish to express my special thanks to Assist.Prof.Dr. Selçuk Aktürk and Erdem Yaşar from Kırıkkale University for the TEM analysis; and to Hüseyin Solmaz from Ankara University Faculty of Medicine for the preparation of TEM specimens. I am also grateful to Prof.Dr. Şakir Bor and Elif Tarhan for their helps with the TEM analysis.

I would also like to thank Prof.Dr. Asuman Türkmenoğlu from Geological Engineering Department, not only for providing us her laboratory for clay purification, but also for her valuable comments; to Prof.Dr. Teoman Tinçer from Chemistry Department for providing the Charpy Impact Test Machine and Prof.Dr. Ali Usanmaz from the same department for his valuable helps and comments on the XRD analysis. I would like to thank the staff of Metallurgical and Materials Engineering Department, especially Prof.Dr.Vedat Akdeniz for the DSC analysis and Nevzat Akgün for the mechanical tests.

I am also thankful to my lab friends İpek Selimoğlu and Onur Çağatay for sharing the toughest and miserable moments of lab life with me, and to Zeynep Kavalcı for consistently showing me the right direction whenever I fell into despair.

I would like to acknowledge the helps of my very special friends; Coşku Özdemir for bringing two huge buckets of clay all the way from San Fransisco to Ankara,

Nigel Robinson for checking the spelling and grammer of this work, Ahmet Peynirciođlu for looking after my cat in my frequent absences; Ümit Güder, Emek Can Ecevit, Özlem Esmâ GÜngör and many others, for being around and being themselves.

I am deeply indebted to Can Ayas, my dear *cancancan*, for walking all the way with me, making it fun and much easier to handle than it originally is. It would be *tuhaf* without his company.

I express my special thanks to Seçkin Özdamar, not only for converting the dull process of thesis writing to a rather peaceful journey, but also for rapidly covering every single absent thing in my life, and doing it so smoothly.

Finally, I would like to express my deepest gratitude to Asuman and Mevlüt Taşan, for the love and support they have given me in every occasion; and to Melek Tuna Taşan-Kok and Yusuf Caner Taşan; for being so caring and funny. They have always shown the way...

This study was supported by METU Scientific Research Projects Funds BAP-2004-07-02-00-111 and BAP-2004-03-08-03.

## TABLE OF CONTENTS

<b>PLAGIARISM.....</b>	<b>iii</b>
<b>ABSTRACT.....</b>	<b>iv</b>
<b>ÖZ.....</b>	<b>vi</b>
<b>ACKNOWLEDGEMENTS.....</b>	<b>iv</b>
<b>TABLE OF CONTENTS.....</b>	<b>xi</b>
<b>LIST OF TABLES.....</b>	<b>xiv</b>
<b>LIST OF FIGURES.....</b>	<b>xv</b>
 <b>CHAPTERS</b>	
<b>1. INTRODUCTION.....</b>	<b>1</b>
<b>1.1 Nanocomposites.....</b>	<b>1</b>
1.1.1 Definition.....	1
1.1.2 Types of Nanocomposites.....	1
1.1.3 Properties of Nanocomposites.....	2
1.1.3.1 Mechanical Properties of Nanocomposites.....	2
1.1.3.2 Other Properties of Nanocomposites.....	4
<b>1.2 Polymer / Layered Silicate Nanocomposites.....</b>	<b>5</b>
1.2.1 Definition.....	5
1.2.2 Types of P/LS Nanocomposites.....	6
1.2.3 Constituents of P/LS Nanocomposites.....	7
1.2.3.1 Polymeric Matrices.....	7
1.2.3.2 Modified Clay Reinforcements.....	8
1.2.4 Production of P/LS Nanocomposites.....	10
1.2.5 Properties of P/LS Nanocomposites.....	12
1.2.6 Application Fields of P/LS Nanocomposites.....	14
<b>1.3 Previous Works on P / LS Nanocomposites.....</b>	<b>17</b>
1.3.1 Milestone Studies on P / LS Nanocomposites.....	17
1.3.2 Studies on P/ LS Nanocomposites with Phenolic Matrices.....	18
<b>1.4 Important Parameters in Property Enhancement of Phenolic Resin/Organoclay Nanocomposites.....</b>	<b>21</b>
1.4.1 Microstructure of the Polymer.....	21
1.4.2 Molecular Weight of the Polymer.....	22
1.4.3 Rate of Curing Reaction.....	22

1.4.4 Degree of Crosslinking.....	22
1.4.5 Clay Type.....	23
1.4.6 Clay Source.....	23
1.4.7 Interlayer Spacing of the Clay.....	23
1.4.8 Modifier of the Clay.....	24
1.4.9 CEC of the Clay.....	24
<b>1.5 Aim of the Study.....</b>	<b>24</b>
<b>2. EXPERIMENTAL WORK.....</b>	<b>25</b>
<b>2.1 Materials.....</b>	<b>25</b>
2.1.1 The Matrix; Phenol Formaldehyde Resin.....	25
2.1.2 The Curing Agent; Methyl-4-Toluenesulfonate.....	25
2.1.3 The Reinforcement; Layered Silicates (Na-Montmorillonite) .....	26
<b>2.2 Production of the Nanocomposite Specimens.....</b>	<b>30</b>
<b>2.3 Specimen Characterization.....</b>	<b>32</b>
2.3.1 X-ray Analysis.....	32
2.3.2 SEM Analysis.....	32
2.3.3 TEM Analysis.....	33
2.3.4 DSC Analysis.....	33
2.3.5 Mechanical Testing.....	33
2.3.5.1 Flexural Tests.....	34
2.3.5.2 Charpy Impact Tests.....	35
2.3.5.3 Fracture Toughness Tests.....	35
<b>3. RESULTS AND DISCUSSION.....</b>	<b>36</b>
<b>3.1 Production of the Specimens.....</b>	<b>36</b>
<b>3.2 Characterization of the Specimens.....</b>	<b>41</b>
3.2.1 Morphological Analysis.....	41
3.2.1.1 XRD Analysis.....	41
3.2.1.2 SEM Analysis.....	52
3.2.1.3 TEM Analysis.....	65
3.2.2 Mechanical Testing.....	73
3.2.2.1 Effect of Resin Type.....	73
3.2.2.2 Effect of Cure Method.....	76
3.2.2.3 Effect of Clay Source.....	78
3.2.2.4 Effect of Clay Concentration.....	80

3.2.2.5 Effect of Clay Modification.....	87
3.2.3 Thermal Analysis.....	98
<b>4. CONCLUSIONS.....</b>	<b>103</b>
<b>5. FUTURE WORK.....</b>	<b>107</b>
<b>6. REFERENCES.....</b>	<b>109</b>
<b>7. APPENDIX.....</b>	<b>113</b>

## LIST OF TABLES

### TABLE

1.1 - Examples of layered host crystals susceptible to intercalation by a polymer...	2
1.2 - Property enhancements of different polymer matrices.....	16
2.1 - Product Data of Polisan Phenolic Resins.....	25
2.2 - Product Data of Curing Agent.....	26
2.3 - Product Data of Cloisite Clays.....	27
2.4 - Product Data of Rheospan (Nanomer I.33M) Clay.....	27
2.5 - Modifiers of Cloisite Clays.....	28
3.1 - The Heat Cure Cycle for the phenolics resins of PF76 and PF76TD.....	37
3.2 - The Acid Cure Cycle for the phenolic resins of PF76 and PF76TD.....	40
3.3 - All the specimens produced for evaluation in this study.....	42
3.4 - X-ray analysis data and <i>d</i> -spacings of the clays used.....	44
3.5 - Mechanical properties of 14 different specimen groups produced.....	74
3.6 - Mechanical properties of the two resol type phenol formaldehyde neat resin specimens produced with acid curing route.....	76
3.7 - Mechanical properties of heat and acid cured PF76TD resin with 0.5% Cloisite 10A specimens.....	77
3.8 - Mechanical properties of PF76TD resin with 0.5% unmodified Cloisite Na+ and Resadiye clays.....	79
3.9 - Mechanical properties of PF76TD resin with 0%, 0.5%, 1% and 1.5% Rheospan clay produced by acid cure route.....	81
3.10 - Interlayer spacing and modifier types of the clays used together with the mechanical properties of PF76TD resin reinforced with 0.5wt% of these clays.....	89

## LIST OF FIGURES

### Figure

1.1 - Schematic picture of a polymer-clay nanocomposite with completely exfoliated clay sheets within the polymer matrix material.....	5
1.2 - Scheme of different types of composite arising from the interaction of layered silicates and polymers: (a) phase separated microcomposite; (b) intercalated nanocomposite and (c) exfoliated nanocomposite.....	6
1.3 - Structure of 2:1 phyllosilicates.....	9
1.4 - Schematic picture of an ion-exchange reaction. The inorganic, relatively small (sodium) ions are exchanged against more voluminous organic onium cations.....	10
1.5 - The flowsheet of solution approach.....	11
1.6 - The flowsheet of in-situ polymerization approach.....	11
1.7 - The flowsheet of melt intercalation approach.....	12
1.8 - The flowsheet of template synthesis approach.....	12
1.9 - The proposed model of torturous zigzag diffusion path in an exfoliated polymer clay nanocomposite when used as a gas barrier.....	13
1.10 - Comparison of the tensile strength and modulus of the best clay/nylon-6 nanocomposites and a glass fiber reinforced nylon-6 composite with 48 wt% fiber content. The properties of the original nylon-6 are also shown.....	14
1.11 - Comparison of the Young's modulus of clay/nylon-6 nanocomposites and glass reinforced nylon-6 composites with low filler loading.....	15
1.12 - Molecular structures of resol and novalac type phenolic esins.....	22
2.1 - Flowchart of the Purification Procedure of Resadiye Clay.....	29
2.2 - Flowcharts of the Heat Cure and Acid Cure Routes of the Nanocomposite Specimen Production.....	31
2.3 - Two examples of the Mean Curves determined by the procedure used; (a) PF76 and (b) PF76TD neat resin specimens.....	34



3.1 - Polymer – clay microstructures, starting from a low magnification SEM picture in (a) to the atomic structures shown in (f).....	43
3.2 - Interpretation of XRD analysis of polymer/layered silicate nanocomposites....	44
3.3 - XRD diffractograms of Rheospan clay and the composite specimens with different Rheospan clay contents (1.5%, 1%, 0.5%).....	45
3.4 - XRD diffractograms of neat PF76TD resin, Cloisite clay and composite specimens with 0.5% Cloisite clay; for (a) Organoclay Cloisite 93A and (b) Unmodified Cloisite Na+.....	47
3.5 - XRD diffractograms of composite specimens in the form of powder and bulk; for three different Rheospan clay contents (a) 0.5% , (b) 1% , (c) 1.5%.....	49
3.6 - XRD diffractograms of composite specimens with high clay contents; 3% and 10%.....	51
3.7 - Comparison of the void formation for the two different neat resin specimens (a) PF76, and (b) PF76TD.....	56
3.8 - Comparison of the void formation and fracture surface roughness for the specimens of (a) neat PF76TD resin and (b) 1% Rheospan clay composite.....	57
3.9 - Comparison of the two different curing routes used for the PF76TD resin, (a) Heat Cure and (b) Acid Cure.....	58
3.10 - (a) Layer formation in Heat Cured PF76TD-0.5% Cloisite 10A and (b) Closer View of this Clay Rich Region.....	59
3.11 - Weak interfacial adhesion between PF76TD resin and tactoids of (a) Cloisite 10A and (b) Cloisite 30B clays.....	60
3.12 - Proper interfacial adhesion between PF76TD resin and (a) Rheospan (b) Cloisite 15A clays.....	61
3.13 - Comparison of the fracture surface roughness of the PF76RD resin specimens reinforced with (a) less compatible Cloisite 10A and (b) more compatible Rheospan clays.....	62
3.14 - (a) and (b) Crack Pinning or crack deflection at the tactoids of Rheospan organoclay in PF76TD resin.....	63
3.15 - Large amount of debonding and particle cracking at a Resadiye clay tactoid in PF76TD matrix.....	64

3.16 - TEM micrographs of the layered structure of Rheospan clay, (a) and (b) general views, (c) and (d) closer views.....	67
3.17 - (a), (b) TEM micrographs of intercalated and/or exfoliated Rheospan clay.	69
3.18 - (a), (b), (c) and (d) TEM micrographs showing large scale layered structure morphology.....	70
3.19 - TEM Diffraction patterns of the large scale layered structures shown in Figure 3.18.....	72
3.20 - Flexural stress-strain curves of PF76 and PF76TD neat resin specimens produced with acid curing route.....	75
3.21 - Flexural stress-strain curves of heat and acid cured PF76TD resin with 0.5% Cloisite 10A specimens.....	77
3.22 - Flexural stress-strain curves of PF76TD resin with 0.5% unmodified Cloisite Na+ and Resadiye clays.....	78
3.23 - Flexural stress-strain curves of PF76TD resin with 0%, 0.5%, 1% and 1.5% Rheospan clay produced by acid cure route.....	80
3.24 - Effects of Clay (Rheospan) concentration on the mechanical properties of PF76TD resin specimens produced with acid curing route; (a) Flexural Strength, (b) Flexural Modulus, (c) Flexural Strain at Break, (d) Charpy Impact Strength, and (e) Fracture Toughness.....	82
3.25 - Relative hydrophobicity levels of the Cloisite clays (provided by SCP), and the estimated levels for Resadiye and Rheospan clays.....	90
3.26 - Effect of increasing relative clay surface hydrophobicity level on (a) Flexural Strength, (b) Flexural Modulus, (c) Flexural Strain-at- Break, (d) Fracture Toughness, (e) Impact Toughness of the composite specimens. Note that the values in the insets are for the neat PF76TD resin.....	90
3.27 - Curing reaction steps between phenol and formaldehyde [40, 35] .....	94
3.28 - Correlation between the clay interlayer spacing and their relative surface hydrophobicity levels.....	96
3.29 - Two typical examples of glass transition temperature determination.....	99

3.30 - DSC curves of PF76TD resin specimens with (a) no clay content (b) 0.5% and (c) 1.5% Rheospan clay. Note that the $T_g$ calculations were carried out by the software of the equipment.....	99
3.31 - Comparison of the DSC curves of three acid cured PF76TD resin specimens of increasing Rheospan clay concentration.....	101
A.1 - XRD diffractogram of Rheospan clay.....	113
A.2 - XRD diffractogram of Cloisite Na <sup>+</sup> clay.....	113
A.3 - XRD diffractogram of Cloisite 10A clay.....	114
A.4 - XRD diffractogram of Cloisite 15A clay.....	114
A.5 - XRD diffractogram of Cloisite 20A clay.....	115
A.6 - XRD diffractogram of Cloisite 25A clay.....	115
A.7 - XRD diffractogram of Cloisite 30B clay.....	116
A.8 - XRD diffractogram of Cloisite 93A clay.....	116
A.9 - XRD diffractogram of Resadiye clay.....	117
B.1 - XRD diffractogram of PF76 neat resin specimen.....	118
B.2 - XRD diffractogram of PF76TD neat resin specimen.....	118
B.3 - XRD diffractogram of PF76TD-0,5% Rheospan specimen.....	119
B.4 - XRD diffractogram of PF76TD-1,0% Rheospan specimen.....	119
B.5 - XRD diffractogram of PF76TD-1,5% Rheospan specimen.....	120
B.6 - XRD diffractogram of PF76TD-0,5% Cloisite 10A (acid cured) specimen....	120
B.7 - XRD diffractogram of PF76TD-0,5% Cloisite 10A (heat cured) specimen....	121
B.8 - XRD diffractogram of PF76TD-0,5% Cloisite 20A specimen.....	121
B.9 - XRD diffractogram of PF76TD-0,5% Cloisite 25A specimen.....	122
B.10 - XRD diffractogram of PF76TD-0,5% Cloisite 93A specimen.....	122
B.11 - XRD diffractogram of PF76TD-0,5% Cloisite Na <sup>+</sup> specimen.....	123
B.12 - XRD diffractogram of PF76TD-0,5% Cloisite Na <sup>+</sup> specimen.....	123
C.1 - Flexural Stress vs Strain Curves of neat PF76 specimen.....	124
C.2 - Flexural Stress vs Strain Curves of neat PF76TD specimen.....	124
C.3 - Flexural Stress vs Strain Curves of PF76TD – 0.5% Rheospan specimen.....	124
C.4 - Flexural Stress vs Strain Curves of PF76TD – 1.0% Rheospan specimen.....	125
C.5 - Flexural Stress vs Strain Curves of PF76TD – 1.5% Rheospan specimen.....	125

C.6 - Flexural Stress vs Strain Curves of PF76TD- 0.5% Cloisite Na+ Specimen.....	125
C.7 - Flexural Stress vs Strain Curves of heat cured PF76TD - 0.5% Cloisite 10A Specimen.....	126
C.8 - Flexural Stress vs Strain Curves of acid cured PF76TD - 0.5% Cloisite 10A Specimen.....	126
C.9 - Flexural Stress vs Strain Curves of PF76TD- 0.5% Cloisite 15A Specimen.....	126
C.10 - Flexural Stress vs Strain Curves of PF76TD - 0.5% Cloisite 20A Specimen..	127
C.11 - Flexural Stress vs Strain Curves of PF76TD - 0.5% Cloisite 25A Specimen..	127
C.12 - Flexural Stress vs Strain Curves of PF76TD -0.5% Cloisite 30B Specimen	127
C.13 - Flexural Stress vs Strain Curves of PF76TD -0.5% Cloisite 93A Specimen	128
C.14 - Flexural Stress vs Strain Curves of PF76TD - 0.5% Resadiye Specimen....	128
D.1 - Flexural Load vs Deflection Curves of neat PF76 specimen.....	129
D.2 - Flexural Load vs Deflection Curves of neat PF76TD specimen.....	129
D.3 - Flexural Load vs Deflection Curves of PF76TD – 0.5% Rheospan.....	129
D.4-Flexural Load vs Deflection Curves of heat cured PF76TD –0.5% Cloisite 10A	130
D.5-Flexural Load vs Deflection Curves of acid cured PF76TD –0.5% Cloisite 10A	130
D.6 - Flexural Load vs Deflection Curves of PF76TD – 0.5% Cloisite Na+.....	130
D.7 - Flexural Load vs Deflection Curves of PF76TD – 1.0% Rheospan.....	131
D.8 - Flexural Load vs Deflection Curves of PF76TD – 1.5% Rheospan.....	131
D.9 - Flexural Load vs Deflection Curves of PF76TD – 0.5% Cloisite 15A.....	131
D.10 - Flexural Load vs Deflection Curves of PF76TD – 0,5% Cloisite 20A specimen.....	132
D.11 - Flexural Load vs Deflection Curves of PF76TD –0,5% Cloisite 25A specimen.....	132
D.12 - Flexural Load vs Deflection Curves of PF76TD – 0,5% Cloisite 30B specimen.....	132
D.13 - Flexural Load vs Deflection Curves of PF76TD –0,5% Cloisite 93A specimen.....	133
D.14 - Flexural Load Deflection Curves of PF76TD – 0,5% Resadiye Specimen.....	133

## CHAPTER 1

### INTRODUCTION

#### 1.1 Nanocomposites

##### 1.1.1 Definition

A composite material is basically the combination of two or more materials, differing in form or composition on a macro scale, in which the constituents retain their identities [1]. Nanocomposites are a new class of composites, which are particle-filled polymers for which at least one dimension of the dispersed particles is in the nanometer range.

##### 1.1.2 Types of Nanocomposites

Three types of nanocomposites may be distinguished, depending on how many dimensions of the dispersed particles are in the nanometer range [2]. All three dimensions may be in the order of nanometers, such as isodimensional spherical silica nanoparticles obtained by in-situ sol-gel methods [3]. When two dimensions of the dispersed particles are in the nanometer scale and the third is larger, the formed elongated structure is called nanofibers. Nanocomposites reinforced with carbon nanotubes [4] or cellulose whiskers [5] are among this group of materials, which are extensively studied due to their exceptional properties. The third type of nanocomposites is characterized by only one dimension in the nanometer range. In this case the filler, which is referred to as nanolayer, is present in the form of sheets of one to a few nanometers thick to hundreds to thousands nanometers long. These materials are almost exclusively obtained by the intercalation of a polymer inside the galleries of layered host crystals. There are a wide variety of both synthetic and natural crystalline fillers to intercalate a polymer (Table 1.1).

**Table 1.1** Examples of layered host crystals susceptible to intercalation by a polymer [2]

CHEMICAL NATURE	EXAMPLE
Element	Graphite
Metal chalcogenides	$(\text{PbS})_{1.18}(\text{TiS}_2)_2$ , $\text{MoS}_2$
Carbon oxides	Graphite oxide
Metal phosphates	$\text{Zr}(\text{HPO}_4)$
Clays and layered silicates	Montmorillonite, hectorite, saponite, fluoromica, fluorohectorite, vermiculite, kaolinite, magadiite
Layered double hydroxides	$\text{M}_6\text{Al}_2(\text{OH})_{16}\text{CO}_3 \cdot n\text{H}_2\text{O}$ ; $\text{M}=\text{Mg}, \text{Zn}$

### 1.1.3 Properties of Nanocomposites

Materials with features on the scale of nanometers often have properties different from their macro scale counterparts. Nanocomposites are among nanoscale materials in which the constituents are mixed on a nanometer-length scale. These materials often exhibit properties superior to conventional composites, such as strength, stiffness, thermal and oxidative stability, barrier properties, as well as unique properties like self-extinguishing behavior and tunable biodegradability [6].

#### 1.1.3.1 Mechanical Properties of Nanocomposites

In composite materials, the reinforcing phase, as its name implies, enhances or reinforces the mechanical properties of the matrix. In most cases the reinforcement is the harder, stronger and stiffer constituent and the principal load bearer; whereas the matrix simply transfers the load to the reinforcement. In other words, the mechanical properties of composites are a function of the size, shape and dimensions of the reinforcement [7].

In general, macroscopic reinforcing elements always contain imperfections. Structural perfection is however more and more reachable as the reinforcing elements become smaller and smaller. The ultimate properties of reinforcing composite elements may be expected, if their dimensions reach atomic or molecular levels [8].

What makes nanocomposites so special are the large number of available elements for carrying an applied load and deflecting cracks; and a tremendous surface area between the matrix and the reinforcement, facilitating stress transfer effectively, allowing for such tensile and toughening improvements [9]. Good examples of such mechanical behavior have been shown with nanocomposites reinforced with nanotubes, whiskers and layered silicates.

Although there are varying reports in the literature on the exact properties of carbon nanotubes, theoretical and experimental results have shown extremely high modulus, greater than 1TPa (the elastic modulus of diamond is 1.2 TPa) and reported strengths 10-100 times higher than the strongest steel at a fraction of the weight [4].

The ultrahigh strength of whiskers, which are the strongest form of solids yet discovered, approaching to the theoretical cohesive strength of solid matter, is attributed to their crystalline perfection and small dimensions, which minimize the occurrence of the defects that are responsible for the low strength of materials in bulk form. It is these extremely high strengths, together with high elastic moduli, low densities and high melting points that make whiskers, which are basically single crystal fibers, as attractive as strengthening agents for metals, plastics and ceramics [10].

The high mechanical properties of nanocomposites reinforced with nanolayers, such as polymer / layered silicate nanocomposites, are due to the high aspect ratio of the dispersed particles and large surface area between the matrix phase and the

reinforcement. Even with the earlier studies [11] very good mechanical properties were obtained due to the advantages of such nanocomposites, such as a doubled modulus and strength increased more than 50% compared to the pristine polymer. The greatest increases observed in mechanical properties were a 103% increase in Young's modulus and a 49% increase in tensile strength [12].

### **1.1.3.2 Other Properties of Nanocomposites**

The reduced gas and liquid permeability of nanofilled polymers make them attractive as membrane materials. The large change in permeability of liquid or gas through a composite material is due to the existence of a filler material with very high aspect ratio, which simply stops all the pathways for transport. The barrier properties are very sensitive to the degree of dispersion and the alignment of the plates.

Dimensional stability is critical in many applications and nanocomposites provide methods for improving both thermal and environmental dimensional stability. There are two mechanisms, which cause this improvement. The first mechanism is the change of the coefficient of thermal expansion (CTE) of the composite material, according to the volume average of the two CTE's. The second is due to the interfacial region between the constituents, which causes increasing volumes of polymer to behave similar to a thin film and has a lower coefficient of thermal expansion than the bulk matrix.

Nanocomposites also have significantly higher thermal stability and flammability values. This increase in stability may be due to the improved barrier characteristics of the composites; when oxygen cannot penetrate, it cannot cause oxidation of the resin. In addition, the inorganic phase can act as a radical sink to prevent polymer chains from decomposing. Flammability is decreased due to the collapsing of the layered silicates during combustion. These collapsed silicates form a uniform layered structure, which acts to reinforce the char and reduce the permeability of the char, reducing the rate of volatile product release. Combining



traditional flame retardants with intercalated or exfoliated clays can result in further improvements in flame retardance [13].

## 1.2 Polymer / Layered Silicate Nanocomposites

### 1.2.1 Definition

Polymer / layered silicate (P/LS) nanocomposites are new hybrid polymeric materials with the layered silicates in the form of sheets of one to several nanometers thick and hundreds of nanometers long (Figure 1.1). Due to the unique nanometer-size dispersion of the layered silicate with high aspect ratio, high surface area and high strength in the polymer matrix, nanocomposites generally exhibit improvements in properties of polymeric materials even at very low volume fraction loading (1-5%) of layered silicates in contrast to the high volume fraction loading (~50%) in the traditional advanced composites [2].

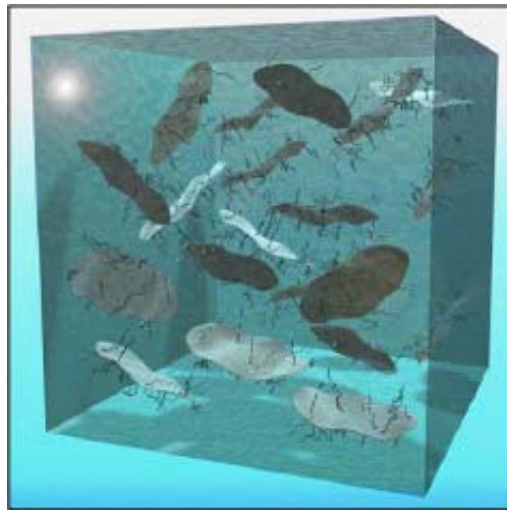


**Figure 1.1** Schematic picture of a polymer-clay nanocomposite with completely exfoliated (molecular dispersed) clay sheets within the polymer matrix material [14].

### 1.2.2 Types of P/LS Nanocomposites

P/LS composites may be grouped into three categories according to their microstructures. If the polymer can penetrate in between the layers of clay, then the material formed is referred to as an *intercalated nanocomposite*. If the polymer enters the layers, which are also called clay galleries, and causes them to separate and disperse in the continuous matrix then it is called an *exfoliated* or *delaminated nanocomposite*. It is also possible that the physical mixture of a polymer and layered silicate not form a nanocomposite. If the layered silicates exist in their original aggregated state with no intercalation of polymer matrix into the galleries of the clay, then the material formed is a *conventional composite*. All three types of polymer – layered silicate composites are shown in Figure 1.2.

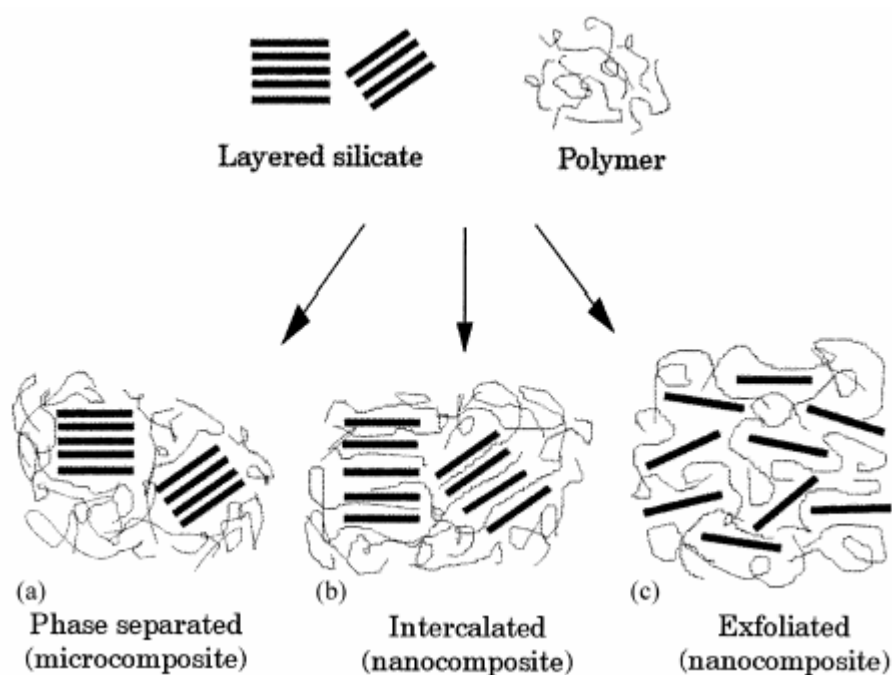


**Figure 1.2** Scheme of different types of composite arising from the interaction of layered silicates and polymers: (a) phase separated microcomposite; (b) intercalated nanocomposite and (c) exfoliated nanocomposite [2].

### **1.2.3 Constituents of P/LS Nanocomposites**

As with all other composite materials, the choice of matrix material and reinforcement material is the main parameter, which determines the properties of nanocomposites. The individual material properties play an important role in the final characteristics of the composite material; as well as the interface between these two materials. The strength, stiffness, fracture behavior and other properties of a composite, such as resistance to creep, fatigue and environmental degradation, are also affected by the characteristics of the interface; which is determined by the chemistry between these constituents.

#### **1.2.3.1 Polymeric Matrices**

The most common matrix materials for composites are polymeric. This is mainly because of their inadequate mechanical properties; which makes them suitable for being reinforced, and the ease of processing of polymer matrix composites; which does not require high pressures or temperatures [7].

For a P/LS nanocomposite to have the highest degree of property enhancement, clay layers must be forced apart and no longer interact with each other. This occurs only when the polarity of the organoclay sufficiently matches the monomer or prepolymer, which will intercalate into the galleries, fully wetting the clay tactoids [9]. So far, the most successful P/LS nanocomposites were produced with nylon 6 [15] and epoxy [16] matrices, which achieved exfoliation leading to remarkable properties. However, studies using other polymers including polyimides [17], polyurethane [18], polyethylene [19], polystyrene [20] and phenolics [21, 22, 23, 24] were also conducted with certain improved properties.

### 1.2.3.2 Modified Clay Reinforcements

Clays have long been used as fillers in polymer systems because of low cost and the improved mechanical properties of resulting polymer composites. The term clay implies a natural earthy fine-grained material, which develops plasticity when mixed with a limited amount of water [25]. Clay minerals are phyllosilicates or sheet silicates with stacking of octahedral and tetrahedral sheets which are two basic building blocks making up the basic structural units. Depending on the combination of these tetrahedral and octahedral sheets, the clay mineral structures may be of type 1:1, 2:1 and 2:1:1 types. 1:1 types consist of one octahedral sheet and one tetrahedral sheet. The 2:1 type is the stacking of an octahedral sheet sandwiched between two tetrahedral sheets. The 2:1:1 structure consists of a 2:1 layer arrangement with an additional octahedral sheet between the 2:1 layers [26].

The commonly used layered silicates for the preparation of P/LS's belong to the same general family of 2:1 phyllosilicates. **Montmorillonite**, **hectorite** and **saponite** are the most commonly used layered silicates. Their crystal structure, shown in Figure 1.3, consists of layers made up of two tetrahedrally coordinated silicon atoms fused to an edge-shared octahedral sheet of either aluminium or magnesium hydroxide. The layer thickness is around 1nm, and the lateral dimensions of these layers may vary from 30nm to several microns or larger, depending on the particular layered silicate. Stacking of these layers leads to a regular Van der Waals gap between the layer, which is called the interlayer or gallery. Isomorphic substitution within the layers (for example,  $\text{Al}^{3+}$  replaced by  $\text{Mg}^{2+}$  or by  $\text{Fe}^{2+}$ , or  $\text{Mg}^{2+}$  replaced by  $\text{Li}^+$ ) generates negative charges that are counterbalanced by alkali or alkaline earth cations situated in the interlayer. As the forces that hold the stacks together are relatively weak, the intercalation of small molecules between the layers is easy [2, 27].

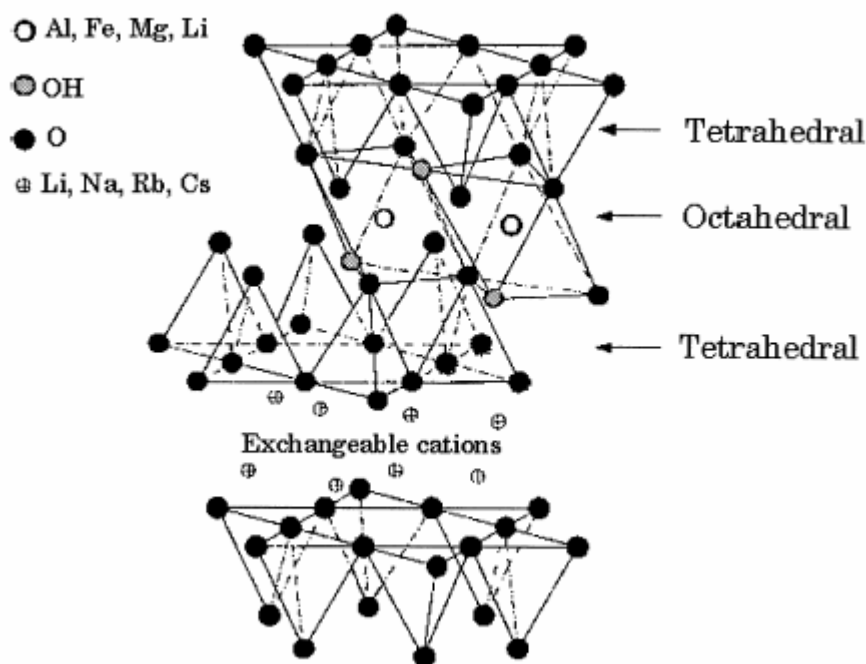


**Figure 1.3** Structure of 2:1 phyllosilicates [2]

### **Organic Modification of the Clay**

Pristine layered silicates usually contain hydrated  $\text{Na}^+$  or  $\text{K}^+$  ions. Obviously, in this pristine state, layered silicates are only miscible with hydrophilic polymers, such as polyethylene oxide (PEO), or polyvinyl alcohol (PVA). To render layered silicates miscible with other polymer matrices, one must convert the normally hydrophilic silicate surface to an organophilic one, making the intercalation of many engineering polymers possible. Generally, this can be done by ion-exchange reactions with cationic surfactants including primary, secondary, tertiary, and quaternary alkylammonium or alkylphosphonium cations. Alkylammonium or alkylphosphonium cations in the organosilicates lower the surface energy of the inorganic host and improve the wetting characteristics of the polymer matrix and result in a larger interlayer spacing (Figure 1.4). Additionally, the alkylammonium or alkylphosphonium cations can provide functional groups that can react with the polymer matrix, or in some cases initiate the polymerization of monomers to improve the strength of the interface between the inorganic and the polymer matrix [27].

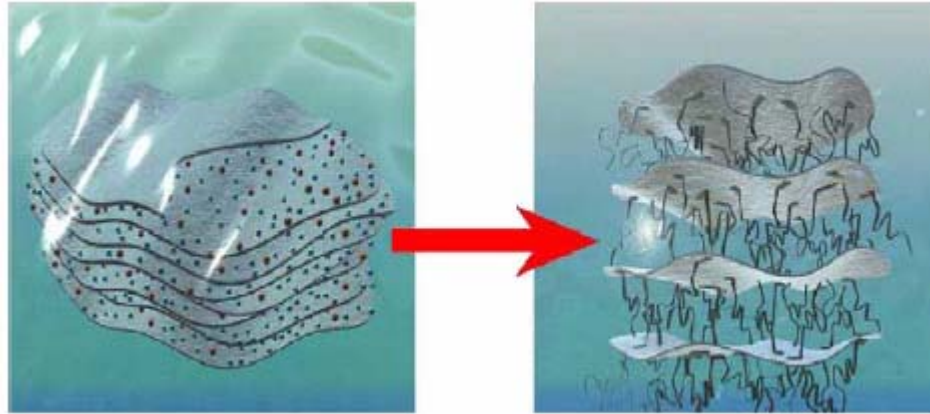


**Figure 1.4** Schematic picture of an ion-exchange reaction. The inorganic, relatively small (sodium) ions are exchanged against more voluminous organic onium cations [8].

#### **1.2.4 Production of P/LS Nanocomposites**

There are four main processes by which polymer / layered silicate nanocomposites are produced: [2]

In **solution method**, shown in Figure 1.5, the layered silicate is exfoliated into single layers using a solvent in which the polymer (or a prepolymer in case of insoluble polymers such as polyimide) is soluble. It is well known that such layered silicates, owing to the weak forces that stack the layers together, can be easily dispersed in an adequate solvent. The polymer then adsorbs into the delaminated sheets and when the solvent is evaporated (or the mixture precipitated), the sheets reassemble, sandwiching the polymer to form, in the best case, an ordered multilayer structure. Under this process are also gathered the nanocomposites obtained through emulsion polymerization where the layered silicate is dispersed in the aqueous phase.

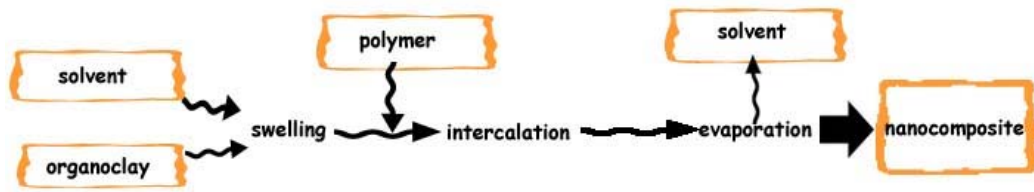


**Figure 1.5** The flowsheet of solution approach

By the **in-situ intercalative polymerization**, shown in Figure 1.6, the layered silicate is swollen within the liquid monomer (or a monomer solution) so that the polymer formation can occur in between the intercalated sheets. Polymerization can be initiated either by heat or radiation, by the diffusion of a suitable initiator or by an organic initiator or catalyst fixed through cationic exchange inside the interlayer before the swelling step by the monomer.

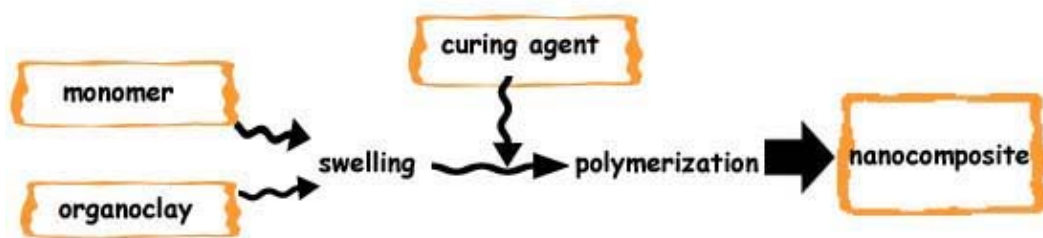


**Figure 1.6** The flowsheet of in-situ polymerization approach

In **melt intercalation method**, shown in Figure 1.7, the layered silicate is mixed with the polymer matrix in the molten state. Under these conditions and if the layer surfaces are sufficiently compatible with the chosen polymer, the polymer can crawl into the interlayer space and form either an intercalated or an exfoliated nanocomposite. In this technique, no solvent is required.

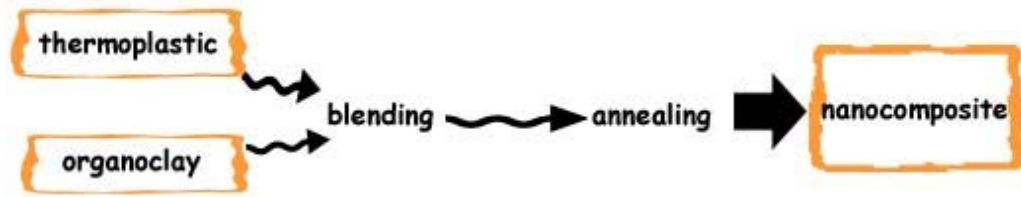


**Figure 1.7** The flowsheet of melt intercalation approach

**Template synthesis**, shown in Figure 1.8, is a technique where the silicates are formed in situ in an aqueous solution containing the polymer and the silicate building blocks. This technique has been widely used for the synthesis of double-layer hydroxide-based nanocomposites but is far less developed for layered silicates. In this technique, based on self-assembly forces, the polymer aids the nucleation and growth of the inorganic host crystals and gets trapped within the layers as they grow.

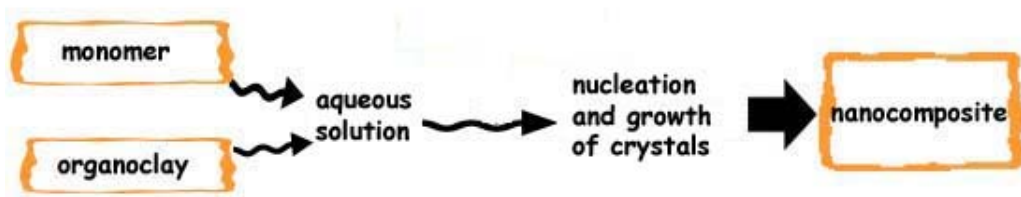


**Figure 1.8** The flowsheet of template synthesis approach

### 1.2.5 Properties of P/LS Nanocomposites

Conventional polymer-clay composites containing aggregated nanolayer tactoids ordinarily improve rigidity, but they often sacrifice strength, elongation and toughness. However, exfoliated clay nanocomposites have shown improvements in all aspects of their mechanical performance. Large numbers of reinforcing elements for carrying an applied load, the high surface area of the interface between the constituents and the high aspect ratio of the nanolayers provide properties that are not possible for large-scaled composites. The clay layers form



a rather difficult path for permeant materials to diffuse through the composite (Figure 1.9). The enhanced barrier characteristics, chemical resistance, reduced solvent uptake and flame retardance of clay-polymer nanocomposites all benefit from the hindered diffusion pathways through the nanocomposite [9].

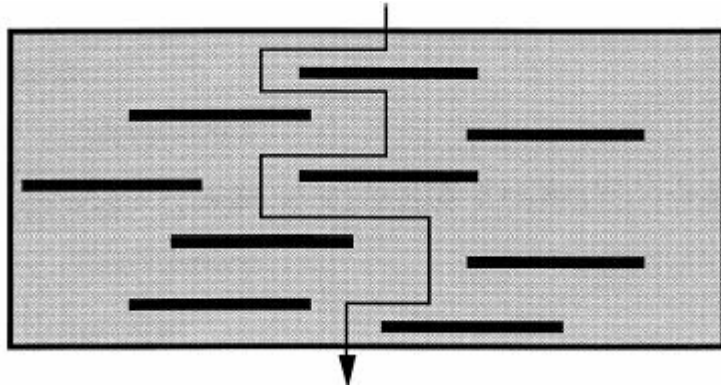


**Figure 1.9** The proposed model of torturous zigzag diffusion path in an exfoliated polymer – clay nanocomposite when used as a gas barrier [9]

Although the maximum enhancement in material properties is still not as high as the fiber reinforced composites (Figure 1.10), when clay/polymer nanocomposites and fiber reinforced composites are compared in the low filler range, nanocomposites exhibit better reinforcement than conventional fiber composites (Figure 1.11) [12].

Also, since polymer-clay nanocomposites achieve composite properties at a lower volume fraction of reinforcement, costly fabrication techniques common to conventional fiber or mineral-reinforced polymers can be avoided.

A partial list of polymer products and areas of property enhancement are listed in Table 1.2.

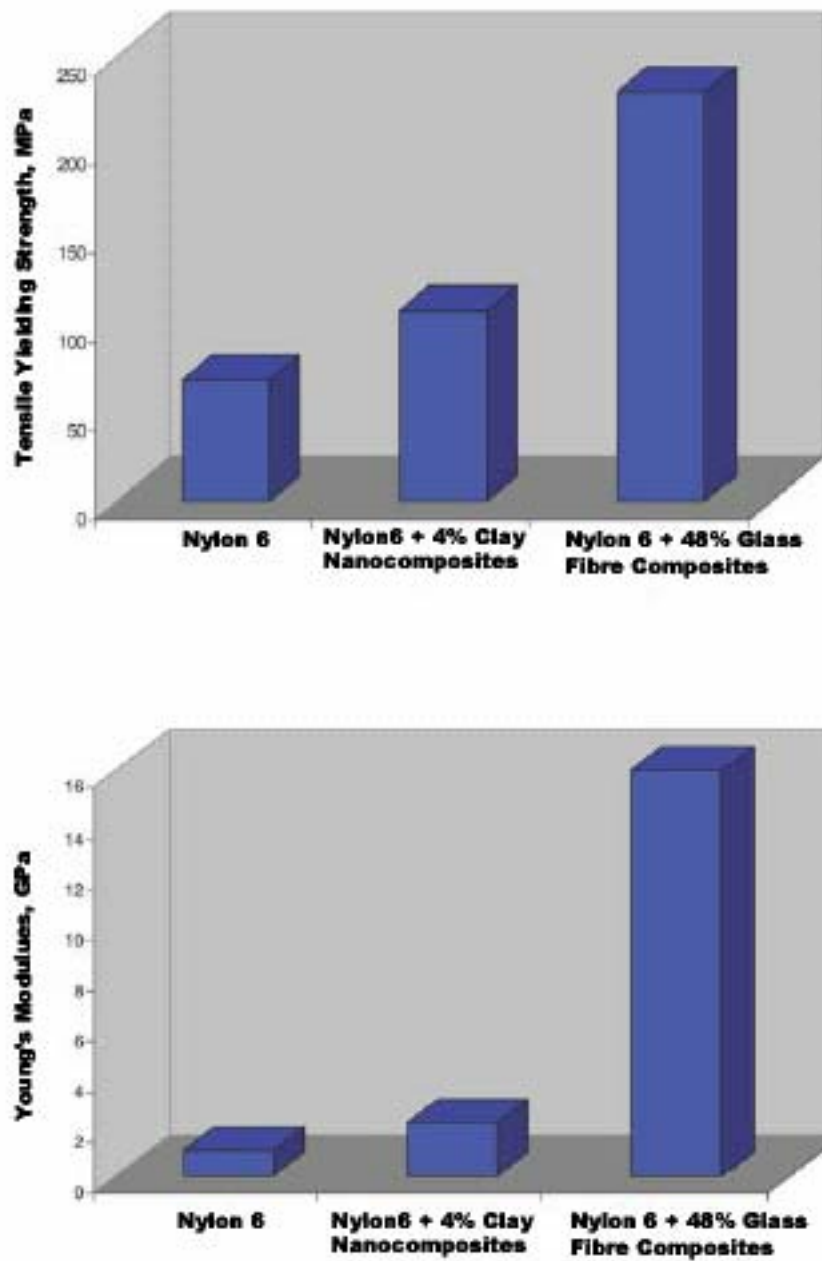


**Figure 1.10** Comparison of the tensile strength and modulus of the best clay/nylon-6 nanocomposites and a glass fiber reinforced nylon-6 composite with 48 wt% fiber content. The properties of the original nylon-6 are also shown [12].

### 1.2.6 Application Fields of P/LS Nanocomposites

The large array of improved mechanical and thermal properties attained at very low filler content (5wt.% or less) together with ease of production through simple

processes such as melt intercalation make layered silicate-based nanocomposites a very promising new class of materials.

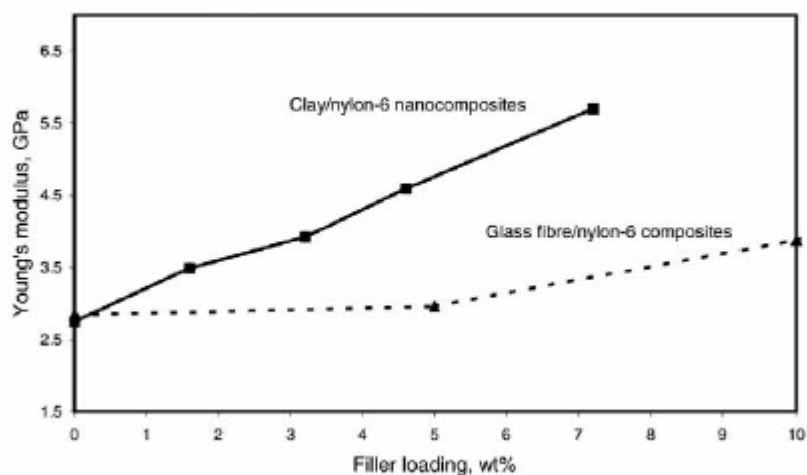


**Figure 1.11** Comparison of the Young's modulus of clay/nylon-6 nanocomposites and glass reinforced nylon-6 composites with low filler loading [12].

The first commercial application of these materials was the use of clay/nylon-6 nanocomposites as timing belt covers for Toyota cars, in collaboration with Ube in 1991. Shortly after this, Unitika introduced nylon-6 nanocomposites for engine covers on Mitsubishi's GDI engines. In August 2001, General Motors and Basell announced the application of clay / polyolefin nanocomposites as a step assistant component for GMC Safari and Chevrolet Astro vans [12]. This was followed by the application of these nanocomposites in the doors of Chevrolet Impalas. More recently, Noble Polymers has developed clay/polypropylene nanocomposites for

structural seat backs in the Honda Acura, while Ube is developing clay/nylon-12 nanocomposites for automotive fuel lines and fuel system components.

**Table 1.2** Property enhancements of different polymer matrices [28]

<b>Nylon 6 Films and Bottles</b>	<b>PET Multilayer Films and Bottles</b>
Oxygen and CO <sub>2</sub> barrier Water vapor barrier UV transmission Thermal stability Stiffness Down-gauging Clarity Anti-tack	Oxygen and CO <sub>2</sub> barrier
	<b>Polyolefin Films and Bottles</b>
	Oxygen and CO <sub>2</sub> barrier Thermal stability Stiffness Down-gauging Melt fracture reduction
<b>Nylon 6 Injection Mold</b>	<b>Polyolefin Injection Mold</b>
Thermal stability Shrinkage / warpage reduction Stiffness Solvent / chemical resistance Fuel barrier Flame resistance Weight reduction Fiberglass reduction Thin-walling Sink reduction Anti-bloom	Thermal stability Shrinkage / warpage reduction Stiffness Solvent / chemical resistance Flame resistance Weight reduction Fiberglass reduction Thin-walling Anti-bloom
<b>EVA</b>	<b>TPE</b>
Stiffness Oxygen barrier Thermal stability Flame resistance Solvent / chemical resistance Anti-bloom	Oxygen and CO <sub>2</sub> barrier Water vapor barrier Stiffness Flame resistance Anti-bloom
<b>Epoxy</b>	<b>UPE</b>
Higher T <sub>g</sub> Stiffness Solvent / chemical resistance Flame resistance Rheology control Scratch and mar Anti-bloom	Higher T <sub>g</sub> Stiffness Solvent / chemical resistance Flame resistance Sag control Scratch and mar

In addition to automotive applications, clay/polymer nanocomposites have been used to improve barrier resistance in beverage applications. Alcoa CSI has applied multilayer clay/polymer nanocomposites as barrier liner materials for enclosure applications. Honeywell has developed commercial clay/nylon-6 nanocomposite products, Aegis TM NC resin, for drink packaging applications. More recently, Mitsubishi Gas Chemical and Nanocor have codeveloped Nylon-MXD6 nanocomposites for multilayered polyethylene terephthalate (PET) bottle applications [12].

### **1.3 Previous Works on P / LS Nanocomposites**

#### **1.3.1 Milestone Studies on P / LS Nanocomposites**

Although the intercalation chemistry of polymers when mixed with appropriately modified layered silicate and synthetic layered silicates have long been known, the field of polymer layered silicate nanocomposites has gained momentum recently. Two major findings have stimulated the revival of interest in these materials: first the studies of the Toyota research group on Nylon-6 / montmorillonite nanocomposites [15], for which very small amounts of layered silicate loadings resulted in pronounced improvements of thermal and mechanical properties; and second, the observation of Vaia *et al.* [29] that it is possible to melt-mix polymers with layered silicates, without the use of organic solvents. Today efforts are being conducted globally, using almost all types of polymer matrices [12].

### 1.3.2 Studies on P/ LS Nanocomposites with Phenolic Matrices

Choi *et al.* [23] carried out the first study on organoclay reinforced phenolic resin nanocomposites; using novalac type phenolic resins. They investigated the effect of modifiers of organosilicate on the curing behavior and final morphology of phenolic resin-layered silicate nanocomposites prepared by melt intercalation. They have shown that:

- Intercalation of the polymer into the clay galleries occurs during mixing, but there is always the possibility of de-intercalation.
- The clay modifier material should always be chosen such that it is either an initiator of the polymerization reaction or some material that reacts with the polymer itself.
- Phenolic resins have a 3-D network structure even before cure. This makes intercalation very difficult for this kind of polymers.
- The structural affinities between the modifier and the polymer; such as benzene rings, have proven to have a good effect on the intercalation.
- Intercalation kinetics are very fast when compared to curing rates; the average intercalation duration was examined to be 5 minutes. If occurs, delamination also is as fast.

Choi *et al.* [24] also published the mechanical properties and thermal stabilities of the nanocomposites they produced earlier [23]. Their results have shown that the mechanical properties of the produced nanocomposites change with the achieved degree of intercalation and exfoliation, whereas the thermal properties are not affected much from the addition of clay. Their specimens showed increases in tensile strength (32%), tensile modulus (37%), toughness (73%), and elongation at break (45%).

Byun *et al.* [30] carried out the first study concentrating on producing nanocomposites from resol type phenolic resins. They prepared resol type phenolic resin/layered silicate nanocomposites using various layered silicates by melt intercalation. They have concluded that;

- Exfoliation is expected to be more difficult with resol type phenolic resins than novalac type phenolic resins, since these resins have a more 3D structure even prior to curing. This 3D structure is due to the polyfunctionality of phenol and the excess formaldehyde available during the production of the resins, as the structure tends to become 3D and bulky when there are more than one reaction sites.
- The influence of the molecular weight of the polymer is a critical parameter for intercalation; since degree of intercalation increases with increasing molecular weight.
- Hydrophilicity decreased as chain length of modifier increased. Therefore, molecular weight of resol should be as small as possible whereas the molecular weight of modifier should be as high as possible.
- Rate of intercalation should always be faster than the rate of the curing reaction; but this is nearly always the case as intercalation kinetics are very fast with this system.
- It is very critical to modify the clay with a suitable modifier. If the clay is modified to be highly hydrophobic than intercalation does not occur efficiently at the beginning of the curing reaction, as the resin is hydrophilic before curing, due to the methylol groups in its structure. If the clay is not modified and left hydrophilic, then deintercalation occurs when the resin loses its methylol groups and becomes hydrophobic near the end of the curing reaction. Therefore, the modification treatment should be carried out so that sufficient intercalation occurs at the beginning and minimum deintercalation occurs at the end of the curing reaction.

- As the amount of clay decreases, the enhancement of the properties is more easily achieved. This is mainly due to the defects of stacked silicates and dangling chain formations.
- The toughness is increased due to the plasticizing effect of the organic modifier and conformational effect of polymer at the P/LS interface.

Wang *et al.* [21] synthesized novalac/layered silicate nanocomposites by condensation polymerization of phenol and formaldehyde catalyzed by H-montmorillonite. They found out that the reactants entered the interlayer galleries easily when the condensation polymerization of phenol and formaldehyde is carried out in the presence of montmorillonite. H-montmorillonite, which is actually hydrochloric acid modified montmorillonite, worked as the catalyst for the reaction.

Wang *et al.* [31] also prepared resol/layered silicate nanocomposite by the intercalative polymerization of phenol and formaldehyde in the presence of acid-modified montmorillonite. They have seen complete exfoliation on some of their specimens with a clay content below 5%. This increase has shown to have a positive effect on  $T_g$  and impact strength (53%) values of the produced specimens.

Wu *et al.* [22] prepared phenolic resin/clay nanocomposites using a suspension condensation polymerization method that was suitable to both novalac and resole type phenolic resins. X-ray diffraction and transmission electron microscopy analysis revealed that the clay exfoliation or intercalation in novalac is easier than in resole. They also found out that the modifier with the benzene ring was more compatible with novalac or resole than the aliphatic type modifier; they also proposed an exfoliation-adsorption and an in situ condensation mechanism on the formation of nanocomposites.



## **1.4 Important Parameters in Property Enhancement of Phenolic Resin/Organoclay Nanocomposites**

The main aim in mixing the modified clay phase and the phenolic resin is to obtain a structure in which clay layers are distributed separately from each other and homogeneously in the polymer matrix. There are several factors that affect the degree of achievement of this task; such as the microstructure and molecular weight of the resin, cation exchange capacity (CEC) of the clay, intergallery distance between the clay layers, choice of modifier material, etc. In order to achieve intercalation or exfoliation, a perfect combination of these parameters should be arranged.

### **1.4.1 Microstructure of the Polymer**

Resol type phenolic resins are one of the most rarely studied resins in P/LS nanocomposites literature, which is mainly due to the 3D network structure of the resin, existing even before cure. This network is a result of the polyfunctionality of phenol, i.e. having more than one reactive site for aromatic substitution reaction and an excess of formaldehyde. These structural peculiarities may cause resins to be too bulky to synthesize a nanocomposite, especially compared to other thermosetting resins such as widely studied epoxy or even novalac type phenolic resins, which are rather linear and easier to intercalate (Figure 1.12)

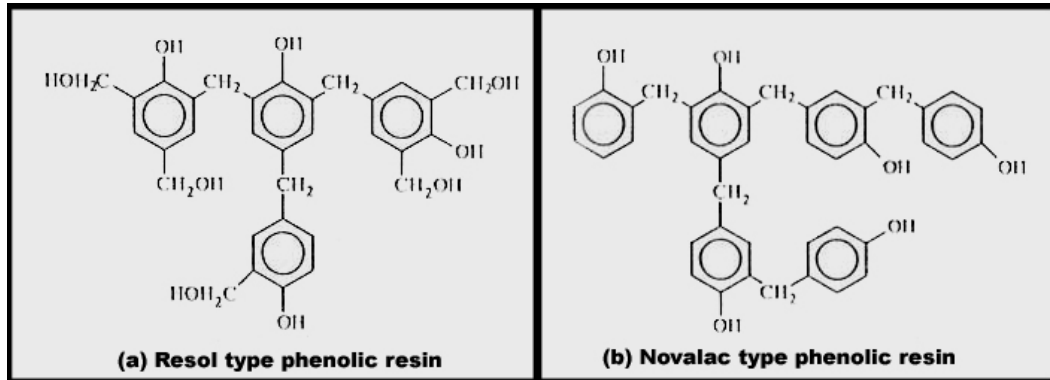


**Figure 1.12** Molecular structures of resol and novalac type phenolic resins [32].

### 1.4.2 Molecular Weight of the Polymer

As the cure of the resol type phenolic resin commences by heating or acidification, molecular weight advancement occurs, leading to an insoluble, chemically stable, mechanically rigid, and crosslinked structure. Consequently, the molecular weight of resol type phenolic resin could be an important factor to synthesize resol type phenolic resin /layered silicate nanocomposites. The lower the molecular weight of the resin, the easier it penetrates through the silicate gallery.

### 1.4.3 Rate of Curing Reaction

To fabricate resol type phenolic resin / layered silicate nanocomposites successfully, the reaction rate should be sufficiently low in order that low molecular prepolymers of phenolic resin have enough time to be intercalated into the silicate galleries. After vitrification, the mobility of the polymer chains is abruptly reduced and the reaction becomes diffusion controlled.

### 1.4.4 Degree of Crosslinking

An interesting phenomenon is seen with the resol type phenolic resins. Due to the high number of methylol groups, these polymers are actually hydrophilic before

the beginning of the crosslinking reaction; this in turn causes a high degree of polymer intercalation into the galleries of the clay. However, as the cure treatment commences, most of the methylol groups are lost, which causes the polymer to show a more hydrophobic behaviour. This change in the degree of hydrophilicity may cause intercalated polymer chains to deintercalate out of the clay galleries.

#### **1.4.5 Clay Type**

Smectite clays and especially the widely used montmorillonite clay, have a cation poor layer surface leading to easy layer separation for polymer intercalation or exfoliation. That is why montmorillonite is the most effective type of clay used in polymer/layered silicate nanocomposites.

#### **1.4.6 Clay Source**

The source of the montmorillonite clay is also important, not only because the aspect ratio of the layers that form the clay may change from source to source, but also because the cation-exchange capacity (CEC), which is the capability of the clay to exchange ions, is highly dependent on the nature of the isomorphous substitutions in the tetrahedral and octahedral sheets and therefore on the nature of the soil where the clay was formed. This explains why montmorillonites from different origins show differences in CEC [33, 34].

#### **1.4.7 Interlayer Spacing of the Clay**

One of the most critical parameters, which affects the degree of polymer intercalation into the clay galleries and/or clay layer exfoliation, is the interlayer spacing of the clays. The larger the gallery space the easier the polymer will get between the layers and exfoliate them. This spacing can be increased by modification of the clay.

#### **1.4.8 Modifier of the Clay**

Alkylammonium or alkylphosphonium cations lower the surface energy of the inorganic host and improve the wetting characteristics of the polymer matrix and result in a larger interlayer spacing. Additionally, they can provide functional groups that can react with the polymer matrix, or in some cases initiate the polymerization of monomers to improve the strength of the interface between the inorganic and the polymer matrix [27].

#### **1.4.9 CEC of the Clay**

The CEC is critical because it controls the space available for diffusion of modifier molecules during mixing of the organoclay with the polymer resin. The highest CEC provides the minimum space, as bulky alkylammonium ions take the available space themselves.

#### **1.5 Aim of the Study**

The main objective of this thesis is to build up and optimize a process to produce resol type phenolic resin/layered silicate nanocomposites. As shown earlier, there are several studies on this topic, in which the solid resol resin is hot pressed with the clay; however none of these studies involved production of the composites by mixing the clay with the liquid resin. There exist several parameters that have an effect on the final chemical and physical condition of the composite material to be produced; such as the types of resin and clay, the amount of clay or the curing method. The final morphology and mechanical and thermal properties of the nanocomposites will be investigated in order to develop an optimum processing flow sheet. For the characterization of the nanocomposite materials produced; X-ray diffraction analysis, scanning and transmission electron microscopy, mechanical tests and thermal tests will be carried out.

## CHAPTER 2

### EXPERIMENTAL WORK

#### 2.1 Materials

##### 2.1.1 The Matrix; Phenol Formaldehyde Resin

The matrix materials chosen for the production of nanocomposites are resol type phenol-formaldehyde resins **PF76** and **PF76TD**, both of which were kindly provided by POLISAN (Turkey). PF76 is neat water based phenolic resin whereas PF76TD has additions of monoethyleneglycol (**MEG**) and diethyleneglycol (**DEG**). Product data for both are given in Table 2.1.

**Table 2.1** Product Data of Polisan Phenolic Resins

PROPERTIES	PF76	PF76TD
Appearance	Red-brown liquid	Red-brown liquid
Solid Mass (wt%)	76±1	76±1
Viscosity (cPs, 20°C)	800-1100	800-1100
pH (20°C)	7.5 - 8.5	7.5 - 8.5
Density (g/cm <sup>3</sup> )	1.215 - 1.230	1.210 - 1.225
Unreacted Formaldehyde (%)	Max. 3	Max. 2
Unreacted Phenol (%)	Max. 5	Max. 3
Water Tolerance	1/1.5 - 1/2.5	1/1.5 - 1/3.0

##### 2.1.2 The Curing Agent; Methyl-4-Toluenesulfonate

Resol type phenolic resins can be cured by heat only, or by using a curing agent. The curing agent used in this study is **methyl-4-toluenesulfonate**, which is purchased from MERCK (Germany). The product data are given in Table 2.2.

**Table 2.2** Product Data of Curing Agent

<b>PROPERTY</b>	<b>METHYL 4-TOLUENESULFONATE</b>
<b>Formula</b>	C <sub>8</sub> H <sub>10</sub> O <sub>3</sub> S
<b>Molar Mass (g/mol)</b>	186.23
<b>Density (g/cm<sup>3</sup>, 20°C)</b>	1.23
<b>Melting Point (°C)</b>	24 – 27
<b>Boiling Point (°C)</b>	292
<b>Flash Point (°C)</b>	130
<b>Solubility in Water</b>	Insoluble

### **2.1.3 The Reinforcement; Layered Silicates (Na-Montmorillonite)**

In this study, Na-montmorillonite was chosen as the layered silicate reinforcement. The nine different montmorillonite clays that were used were obtained from three different sources; (i) Cloisite (Southern Clay- USA), (ii) Rheospan (Nanocor- USA) and (iii) Resadiye (Karakaya- Turkey)

The first group of clays, the Cloisite montmorillonite clays, were purchased from Southern Clay Products in pure unmodified condition (Cloisite Na+) and as organoclays (Cloisite 10A, Cloisite 15A, Cloisite 20A, Cloisite 25A, Cloisite 30B and Cloisite 93A) treated by six different chemical modifiers. Product data of Cloisite clays are given in Table 2.3 and information on modifiers in Table 2.5.

The second Na-montmorillonite clay **Rheospan** (Nanomer I.33M) which is chemically modified by alkyl dimethyl benzyl ammonium, was purchased from Nanocor Inc.(USA) and its product data is given in Table 2.4.

**Table 2.3** Product Data of Cloisite Clays

CLAY	CEC (meq/100g clay)	DENSITY (g/cc)	MOISTURE (%)	SIZE		
				10%	50%	90%
Cloisite Na+	92.6	2.86	< 2%	<2 $\mu$	<6 $\mu$	<13 $\mu$
Cloisite 10A	125	1.90	< 2%	<2 $\mu$	<6 $\mu$	<13 $\mu$
Cloisite 15A	125	1.66	< 2%	<2 $\mu$	<6 $\mu$	<13 $\mu$
Cloisite 20A	95	1.77	< 2%	<2 $\mu$	<6 $\mu$	<13 $\mu$
Cloisite 25A	95	1.87	< 2%	<2 $\mu$	<6 $\mu$	<13 $\mu$
Cloisite 30B	90	1.98	< 2%	<2 $\mu$	<6 $\mu$	<13 $\mu$
Cloisite 93A	90	1.88	< 2%	<2 $\mu$	<6 $\mu$	<13 $\mu$

**Table 2.4** Product Data of Rheospan (Nanomer I.33M) Clay

PROPERTIES	RHEOSPAN
Appearance	Off white powder
Mean dry particle size (microns)	14-16
Specific gravity (gm/cc)	1.9
Moisture (%)	3 max
Mineral purity (%min)	98

**Table 2.5** Modifiers of Cloisite Clays

CLAY	CHEMICAL NAME	ANION	STRUCTURE
Cloisite 10A	Dimethyl, benzyl, hydrogenated tallow*, quaternary ammonium	Chloride	$\begin{array}{c} \text{CH}_3 \\   \\ \text{CH}_3 - \text{N}^+ - \text{CH}_2 - \text{C}_6\text{H}_5 \\   \\ \text{HT} \end{array}$
Cloisite 15A	Dimethyl, Dehydrogenated tallow, quaternary ammonium	Chloride	$\begin{array}{c} \text{CH}_3 \\   \\ \text{CH}_3 - \text{N}^+ - \text{HT} \\   \\ \text{HT} \end{array}$
Cloisite 20A	Dimethyl, Dehydrogenated tallow, quaternary ammonium	Chloride	$\begin{array}{c} \text{CH}_3 \\   \\ \text{CH}_3 - \text{N}^+ - \text{HT} \\   \\ \text{HT} \end{array}$
Cloisite 25A	Dimethyl, hydrogenated tallow, 2ethylhexyl quaternary ammonium	Methyl sulfate	$\begin{array}{c} \text{CH}_3 \\   \\ \text{CH}_3 - \text{N}^+ - \text{CH}_2\text{CH}(\text{CH}_2\text{CH}_2\text{CH}_2\text{CH}_2\text{CH}_3) \\   \quad \quad \quad   \\ \text{HT} \quad \quad \quad \text{CH}_3 \end{array}$
Cloisite 30B	Methyl, tallow, bis-2-hydroxyethyl, quaternary ammonium	Chloride	$\begin{array}{c} \text{CH}_2\text{CH}_2\text{OH} \\   \\ \text{CH}_3 - \text{N}^+ - \text{T} \\   \\ \text{CH}_2\text{CH}_2\text{OH} \end{array}$
Cloisite 93A	Methyl, Dehydrogenated tallow ammonium	HSO <sub>4</sub>	$\begin{array}{c} \text{H} \\   \\ \text{CH}_3 - \text{N}^+ - \text{HT} \\   \\ \text{HT} \end{array}$

\*Hydrogenated Tallow = (~65% C18; ~30% C16; ~5% C14)

The third clay **Resadiye** which is natural Na-montmorillonite from Tokat region has been kindly provided by Karakaya Bentonit (Turkey). In order to increase the purity of this clay, certain purification procedures were conducted and the clay



minerals were separated from other minerals by decantation. The procedure is shown in Figure 2.1

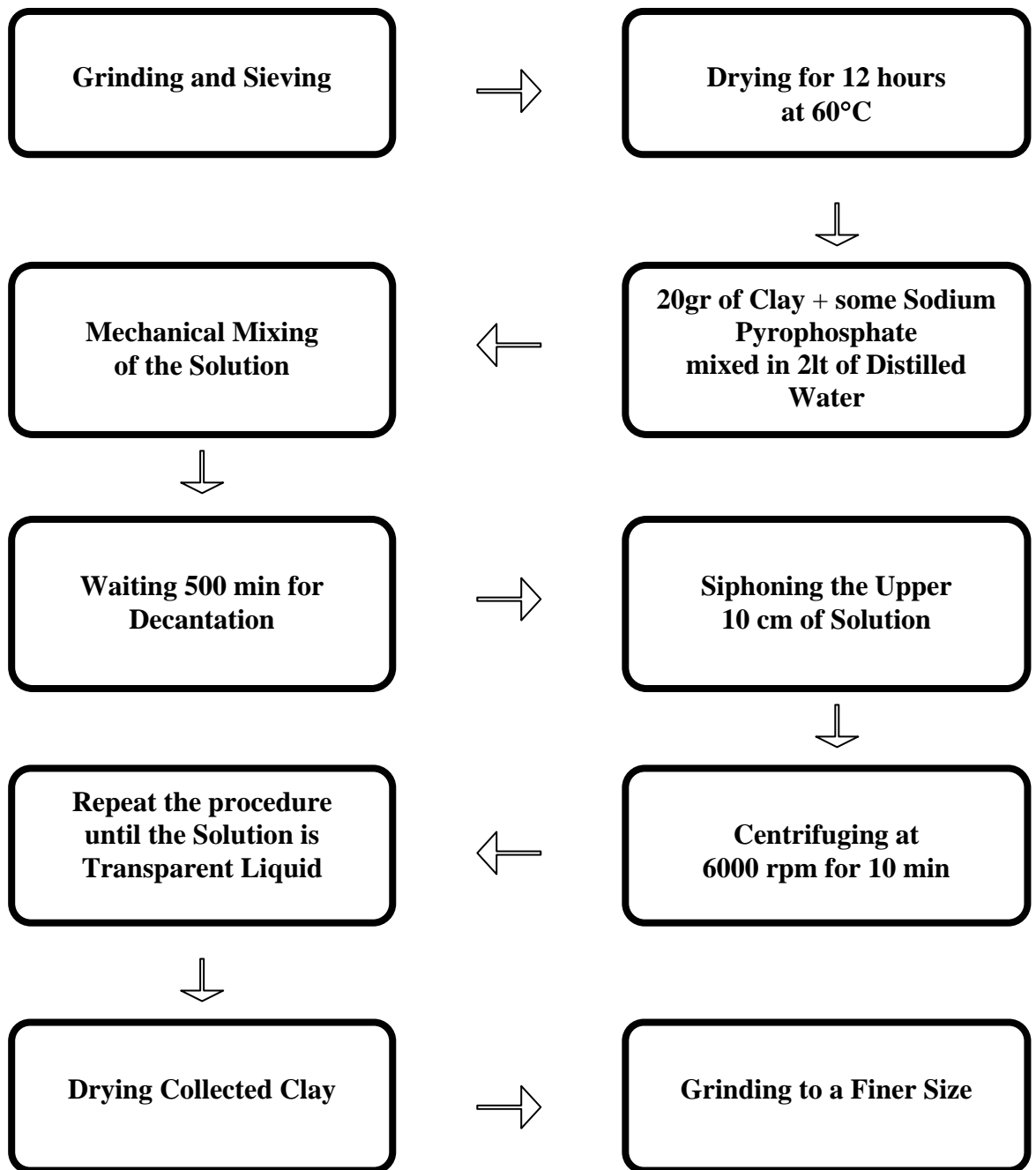


**Figure 2.1** Flowchart of the Purification Procedure of Resadiye Clay

This procedure relies mainly on Stoke's Law. According to this law, the non-clay minerals will settle down 5 cm during each period of 250 min while bringing the

clay minerals away. Therefore, the clay minerals can be separated by centrifuging the suspension that is taken from the upper 10 cm at the end of the 500 minutes period.

## **2.2 Production of the Nanocomposite Specimens**

One of the main goals of this study was to investigate the production of intercalated or exfoliated phenolic resin / layered silicate nanocomposites. As this study is the only one in literature involving liquid phase mixing of the phenolic resin and organoclay, several attempts were carried out. After so many trials to find the optimum way to produce the nanocomposite specimens, two routes were developed using the ability of resol type phenolic resins to be cured either with the application of heat only or with the addition of a curing agent.

The first route, named as the “**heat cure route**”, started with the mixing of the desired amount of organoclay with the phenolic resin, for 1 hour at 55°C in the mechanical mixer. The rate of mixing is initially held at 50 rpm and then increased to 100 rpm and then finally to 150 rpm. Following mechanical mixing, the mixture was further mixed in an ultrasonic bath operating at 35 Hz, for 30 minutes at 55°C. The homogeneous mixture is poured into PTFE molds and placed in the curing oven. The curing schedule developed was as follows: 60°C for 24 hours, and then 80°C for 12 hours, then 100°C for 10 hours and finally 130°C for 1 hour. After curing, specimens were removed from the molds for characterization.

The second route, named as the “**acid cure route**”, started with the mechanical mixing of the desired amount of organoclay with the phenolic resin, for 30 minutes at 55°C. Following that, the mixture was mixed in the ultrasonic bath for 30 minutes at 55°C. Then, the required amount of methyl-4-toluenesulfonate is added and the resin-clay mixture is mixed in the mechanical mixture for another 1.5 hours. Then the mixture is poured into the molds and placed in the curing oven for 3.5 hours at 70°C and then 1 hour at 130°C. The flow charts of both routes are given in Figure 2.2.

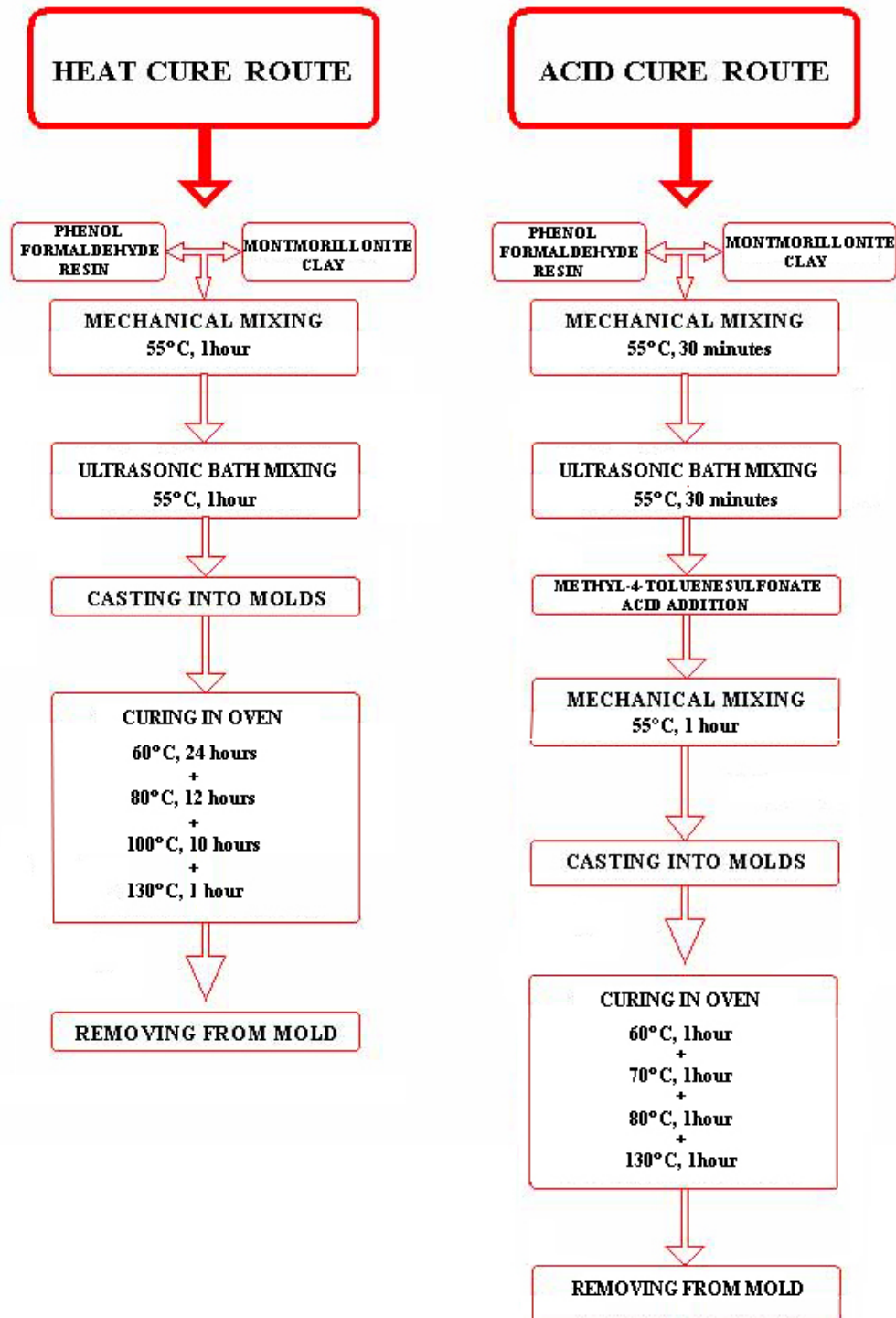


**Figure 2.2** Flowcharts of the Heat Cure and Acid Cure Routes of the Nanocomposite Specimen Production

## **2.3 Specimen Characterization**

### **2.3.1 X-ray Analysis**

XRD is a critical tool in polymer / layered silicate research; especially in measuring the d-spacings of the layered clays. In this study, XRD analysis of the specimens was carried in three different places.

The X-ray analysis of Resadiye clay was carried out in MTA laboratories, using a Rigaku Geigerflex D-Maxll TC model X-ray diffractometer, scanning a  $2\theta$  range of  $2^\circ$ - $70^\circ$ .

The X-ray diffractogram of the neat resins, clays and the produced specimens were carried out at METU Chemistry Department, using a Rigaku diffractometer, with  $\text{CuK}\alpha$  radiation, at a general voltage of 30kV and a general current of 15mA. Scanning was in continuous steps at a speed of 5  $^\circ$ /min, scanning a  $2\theta$  range of  $2^\circ$ -  $20^\circ$  for clays and  $2^\circ$ -  $10^\circ$  for the nanocomposite specimens.

The specimens having clay percentage over 3% were analyzed at METU Metallurgical and Materials Engineering Department, using a 100 kV Philips twin tube X-ray diffractometer (PW/1050), with  $\text{CoK}\alpha$  radiation, at a general voltage of 30 kV and a general current of 8 mA. Scanning was in continuous steps at a speed of 1  $^\circ$ /min, scanning a  $2\theta$  range of  $6^\circ$ -  $50^\circ$ .

Specimens were put into XRD in both powder and bulk form.

### **2.3.2 SEM Analysis**

Fractured surfaces of the nanocomposites were examined at METU Metallurgical and Materials Engineering Department; using Jeol JSM-6400 Scanning Electron Microscope. The surfaces were coated with gold to obtain a conductive surface. Microstructural analysis were carried out to investigate the degree of clay agglomeration and the distribution of clay particles in the specimens.

### **2.3.3 TEM Analysis**

TEM analysis, along with X-ray diffraction, is one of the most widely used characterization methods for the polymer / layered silicate nanocomposites. It is the only characterization tool which provides a means to visualize the amount of increase in the gallery space of the clay layers. TEM analysis was carried out at Kirikkale University Physics Department, using a 300 kV JEOL3010 Transmission Electron Microscope.

Specimens were prepared in the Department of Histology – Embriology at Ankara University. To prepare ultrathin sections, the specimens were first trimmed using a Leica EMTRIM machine. Then, TEM specimens were cut from the nanocomposite block using an ultramicrotome, Leica Ultracut R, equipped with glass and diamond knives. Thin specimens of (200 nm-300 nm) were cut using a glass knife and much thinner specimens of (~70 nm) were cut using the diamond knife. The cut specimens were collected in a trough filled with water and placed on a 300 mesh copper grid, on which they are placed in TEM specimen holders.

### **2.3.4 DSC Analysis**

Differential Scanning Calorimetry tests were carried out at METU Metallurgical and Materials Engineering Department; using Setaram DSC 131 to record the thermal behavior of specimens between 20°C-300°C, at a rate of 10°C/min, in Argon atmosphere.

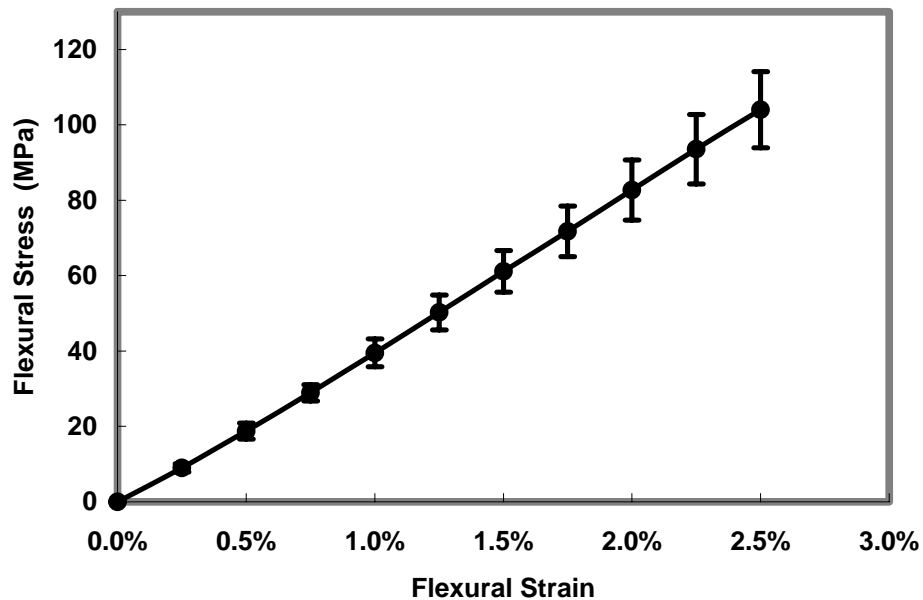
### **2.3.5 Mechanical Testing**

All mechanical tests were performed at room temperature and according to the requirements of related ISO standards. At least five specimens were tested for all different conditions.

### 2.3.5.1 Flexural Tests

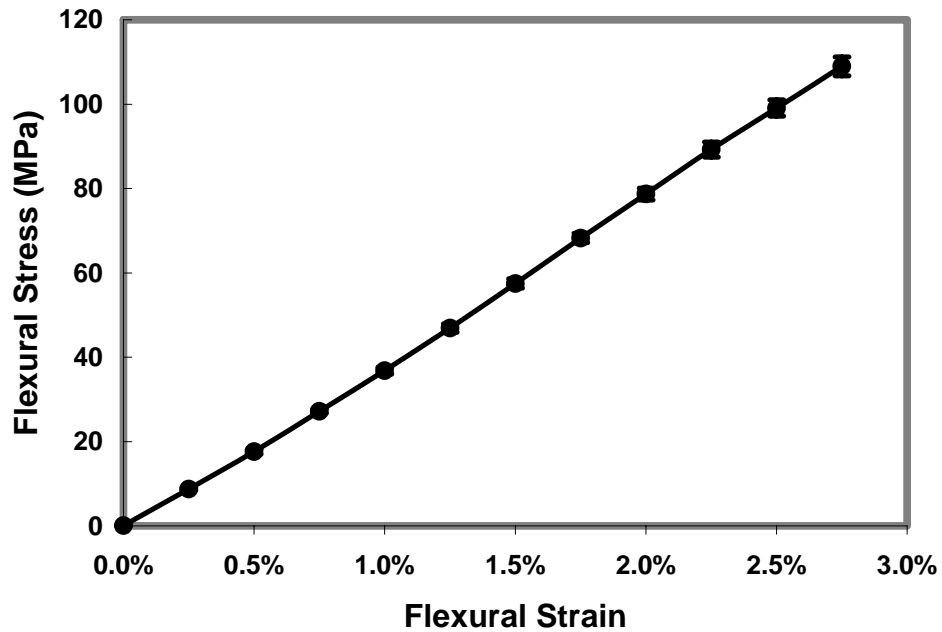
Three point bending tests were carried out at METU Metallurgical and Materials Engineering Department; using a 10 kN Shimadzu AGS-J machine according to ISO 178 standard, for the specimen size of 80x10x4 mm.

Five specimens were tested for each type of nanocomposite produced. Flexural strength, flexural modulus and flexural strain-at-break of the nanocomposite specimens were measured by finding the mean curve from the five curves obtained; via calculation of the average flexural stress values at fixed flexural strain points. Standard deviations at these chosen flexural strain values are also calculated and placed on the curves obtained, to achieve a better understanding of the possible amounts of error in these mechanical tests. Two of the curves obtained by using this procedure are shown in Figure 2.3.



(a)

**Figure 2.3** Two examples of the Mean Curves determined by the procedure used; (a) PF76 and (b) PF76TD neat resin specimens



(b)

Figure 2.3 (cont.)

### 2.3.5.2 Charpy Impact Tests

Notched Charpy impact tests were carried out at METU Chemistry Department; using a Coesfeld Material Test Unit according to ISO 179-1 standard for the single-edge-notched specimens of 80x100x4 mm.

### 2.3.5.3 Fracture Toughness Tests

Plane Strain Fracture Toughness Tests were carried out at the Department of Metallurgical and Materials Engineering, at METU; using Shimadzu AGS-J machine according to ISO 13586 standard, for the single-edge-notched-bending specimens of 80x10x4mm.

## CHAPTER 3

### RESULTS AND DISCUSSION

The fundamental goal in this study was to obtain an efficient and reproducible way to process phenolic resin / organoclay nanocomposites. For this purpose, different phenolic resins, different clays, different clay modifiers and different clay contents have been tried in order to find the most suitable conditions. Since resol type phenolics have complex 3D structures even prior to cure, preventing them from intercalating into narrow clay galleries and exfoliating the clay layers; the number of studies on these resins are very limited compared with other thermosetting resins such as epoxy and unsaturated polyester. There is almost no work in the literature so far investigating liquid phenolic resins; as all the groups working on this type of phenolics produced their samples by hot pressing solid resins. It is because of this lack of knowledge on this topic that a new route was to be developed to produce these nanocomposites.

#### **3.1 Production of the Specimens**

The first task to be accomplished in this study was to determine a certain curing heat treatment schedule to produce proper specimens. It was already known that resol type phenolic resins had the ability to cure either by heating only or by the use of a curing agent. Both methods are used in this study.

##### **(i) Heat Cure Cycle**

Since the phenolic resins used were water based and since upon the condensation polymerization reaction occurring during curing also produces some water; the biggest problem to be overcome on this task, was the elimination of these water vapor bubbles which get trapped in the specimen when the rate of curing reaction was higher than that of the water evaporation.



In order to solve this problem, the first approach was to heat cure the specimens in a vacuum oven. However, this approach created some other problems, such as foaming at the surface of the specimens. Upon several trials it was observed that vacuuming was actually not necessary if the heat cure treatment allows release of the water vapor before the start of intensive crosslinking in the resin structure. For this condition, gel time should be kept long enough for the slow water vapor release leading to no bubble formation. This approach required very long heating schedules (as long as 3 days). Similarly, water formed during condensation reaction was also slowly given out by keeping the rate of crosslinking as low as possible. It should be stated that PF76 was much more difficult to cure; not only was the cure cycle much longer but also the possibility of void formation was observed to be more likely; and whatsmore when formed, these voids were observed to be larger in size compared to those formed in PF76TD.

The heat cure cycles given in Table 3.1 for each resin were determined after comparing the flexural strength values of the specimens produced by so many different heat cure schedules.

**Table 3.1** The Heat Cure Cycle for the phenolics resins of PF76 and PF76TD

<b>Resin Type</b>	<b>Heat Cure Cycles</b>
<b>PF76</b>	<b>12h @40°C + 24h @60°C + 24h @80°C + 10h @100°C + 1h @130°C</b>
<b>PF76TD</b>	<b>24h @60°C + 12h @80°C + 10h @100°C + 1h @130°C</b>

The heat cure cycle of PF76 started with successive incremental steps of 12 hours at 40°C and then 24 hours at 60°C and then another 24 hours at 80°C for the very long gel time period, and then 10 hours at 100°C for curing, and finally 1 hour at 130°C for post-curing.

The heat cure cycle of PF76TD was similar to that of PF76's, however the gelation time was held much shorter as it required no 12 hour-step at 40°C and it was held just for 12 hours at 80°C.

Once the heat cure cycles were determined for the neat resins, the method of mixing the clay with the resins was investigated. Several durations, temperatures and speeds of consecutive mechanical mixing steps were tried. It was concluded that mechanical mixing should be carried out at an optimum speed of around 100 rpm; since slower rates caused insufficient clay mixing and faster rates caused foaming at the resin surface and also excessive amounts of air getting trapped inside the resin. It was also observed that dividing the mechanical mixing into three steps of increasing rates, i.e. first step at 50 rpm and then at 100 rpm and finally at 150 rpm, gave the best results in terms of homogeneous mixing of the clay.

The optimum temperature for mechanical mixing was observed to be around 55°C and the duration of mechanical mixing was limited to 1 hour only. Longer mixing durations were also tried (up to 5 hours), but not used in specimen production; as the mechanical tests showed that the duration of mixing did not have any positive effects on the mechanical properties, and whatsmore, longer mixing durations increased the amount of air bubbles getting trapped inside the resin.

Another method which proved to be ineffective in the final morphology and mechanical properties of the specimens was mechanical mixing under vacuum. It was proposed that higher rates of mechanical mixing rates could be obtained if air bubbles getting trapped inside the resin could simultaneously be removed from the surface of the resin by the help of a vacuum pump. For this purpose, two different vacuum pumps were tried, one with an attainable vacuum of -400 mmHg, the other with -600 mmHg. However, due to the high viscosity of the

PF76 and PF76TD resins (~1000 cPs), neither of the vacuum pumps could show any effect on the trapped air bubbles.

The duration and temperature of the ultrasonic mixing step were also investigated by macroscopic examinations and mechanical tests; and it was concluded that, following the mechanical mixing step, a short duration ultrasonic mixing step of at most 1 hour at 55°C was enough for agglomerated clay particles to divide into smaller particles. Longer ultrasonic mixing durations did not show any observable change in the produced specimens.

As a result of all specimen production trials, keeping the mechanical test results and the specimen structures in mind, the best procedure for producing heat cured resol type phenolic resin / layered silicate nanocomposites was defined as shown in Figure 2.2.

#### **(ii) Acid Cure Cycle**

After successfully producing phenolic composites by heat curing, acid curing was tried. For this purpose, methyl-4-toluenesulfonate was used as a curing agent. In this method crosslinking can happen much quicker, preventing the agglomeration or precipitation of the clay phase, sorting out the most serious problem faced in the heat cure cycle. To achieve this goal, two parameters were investigated; temperature and the amount of curing agent added. It was observed that high temperatures (above 100°C), or very high amounts of curing agent addition (over 7%) resulted in foaming of the resin. Optimum values were found for both of these parameters, which shortened the curing cycle by more than 48 hours, i.e. decreasing 3 days of heat cure cycle to only one day. The optimum acid cure cycle for neat resins are given in Table 3.2. The optimum amount for curing agent was observed to be 5%.

For the mixing stage, as shown in Figure 2.2, the clay and the polymer was first mechanically mixed for 30 minutes, then ultrasonically mixed for the same

amount of time. Following the curing agent addition, another mechanical mixing stage of 1 hour was carried out to ensure that the curing agent is mixed homogeneously with the resin.

All the specimens produced for evaluation in this study are tabulated in Table 3.3. Since acid cure cycle was much shorter and the specimens produced with this method had a more homogeneous clay distribution; the majority of the specimens were produced using the acid cure cycle. Similarly, PF76TD was used with the majority of the specimens as it had much lower void formation compared to PF76. Specimens without clay loadings were produced as control experiments, specimens with Rheospan clay were produced to observe the effect of clay concentration, specimens with different Cloisite clays were produced to observe the effect of different clay modification and specimens with Resadiye clay were produced to see the effect of clay source by comparing with the other unmodified Na-montmorillonite clay, Cloisite Na+.

**Table 3.2** The Acid Cure Cycle for the phenolic resins of PF76 and PF76TD

<b>Resin Type</b>	<b>Acid Cure Cycles</b>
<b>PF76</b>	<b>3.5h @60°C + 1h @130°C</b>
<b>PF76TD</b>	<b>1h @60°C + 1h @70°C + 1h @80°C + 1h @130°C</b>

## **3.2 Characterization of the Specimens**

### **3.2.1 Morphological Analysis**

The characteristics of materials are strongly related to their microstructures, as it is the features of these microstructures that determine the behaviour of a material against the stimuli. Therefore, it is scientifically meaningless to analyze results and come to conclusions without examining and understanding microstructure of any materials. The situation is very much the same, if not more critical, with the P/LS nanocomposites. As the word “nano” implies, very small structures are involved in these materials (Figure 3.1); which in turn necessitate the use of very precise and delicate instruments in analyzing these materials.

The critical question with the specimens produced in this study was whether the polymer, that is the resol type phenol formaldehyde resin, intercalated into the layers of silicate, exfoliating the silicate layers homogeneously into the polymer matrix. To come up with an answer, XRD, SEM and TEM analysis were carried out. Then, to evaluate the behaviour of the specimens mechanical and thermal tests were performed.

#### **3.2.1.1 XRD Analysis**

XRD is the most widely used technique in studying polymer/layered silicate nanocomposites. It is the most convenient technique to measure the *d*-spacing of any crystalline layer such as silicate layers. The interpretation of the XRD patterns of polymer/layered silicate materials is as given in Figure 3.2.

**Table 3.3** All the specimens produced for evaluation in this study

<b>Experiment no</b>	<b>Resin type</b>	<b>Clay type</b>	<b>Clay content (%)</b>	<b>Cure cycle type</b>
1	PF76	-	-	ACID
2	PF76TD	-	-	ACID
3	PF76TD	RHEOSPAN	0.5	ACID
4	PF76TD	RHEOSPAN	1	ACID
5	PF76TD	RHEOSPAN	1.5	ACID
6	PF76TD	CLOISITE 10A	0.5	HEAT
7	PF76TD	CLOISITE 10A	0.5	ACID
8	PF76TD	CLOISITE 15A	0.5	ACID
9	PF76TD	CLOISITE 20A	0.5	ACID
10	PF76TD	CLOISITE 25A	0.5	ACID
11	PF76TD	CLOISITE 30B	0.5	ACID
12	PF76TD	CLOISITE 93A	0.5	ACID
13	PF76TD	CLOISITE Na+	0.5	ACID
14	PF76TD	REŞADIYE	0.5	ACID

**(a) XRD of the Clays**

The XRD diffractograms of the clays used in this study are given in Appendix A. These diffractograms were evaluated especially to determine the interlayer distance ( $d$ ) of the silicates by using the Bragg's Law. Table 3.4 gives these  $d$  values and other data obtained

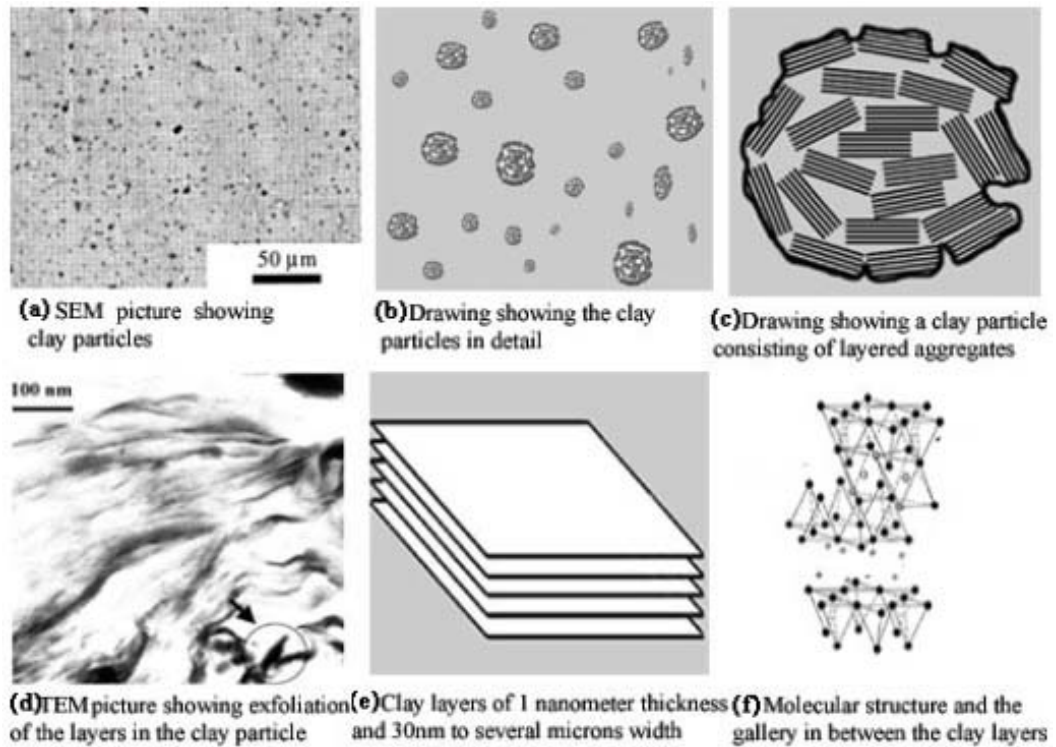


**Figure 3.1** Polymer – clay microstructures, starting from a low magnification SEM picture in (a) to the atomic structures shown in (f). ((a)[35], (d)[8] )

It is seen that unmodified clays (Resadiye, Cloisite Na<sup>+</sup>) have *d*-spacings of 11-12 nm, while chemical modification of the clays increases the *d*-value to 25 nm (e.g. in Rheospan) or as much as 30 nm (e.g. in Cloisite 15A).

It is seen in Table 3.4 that there is a slight difference between the measured values of the interlayer distance of the Cloisite clays and the values provided by the producer Southern Clay Products. This may be due to clay humidity or it may also be the effect of impurities that somehow mixed into the samples

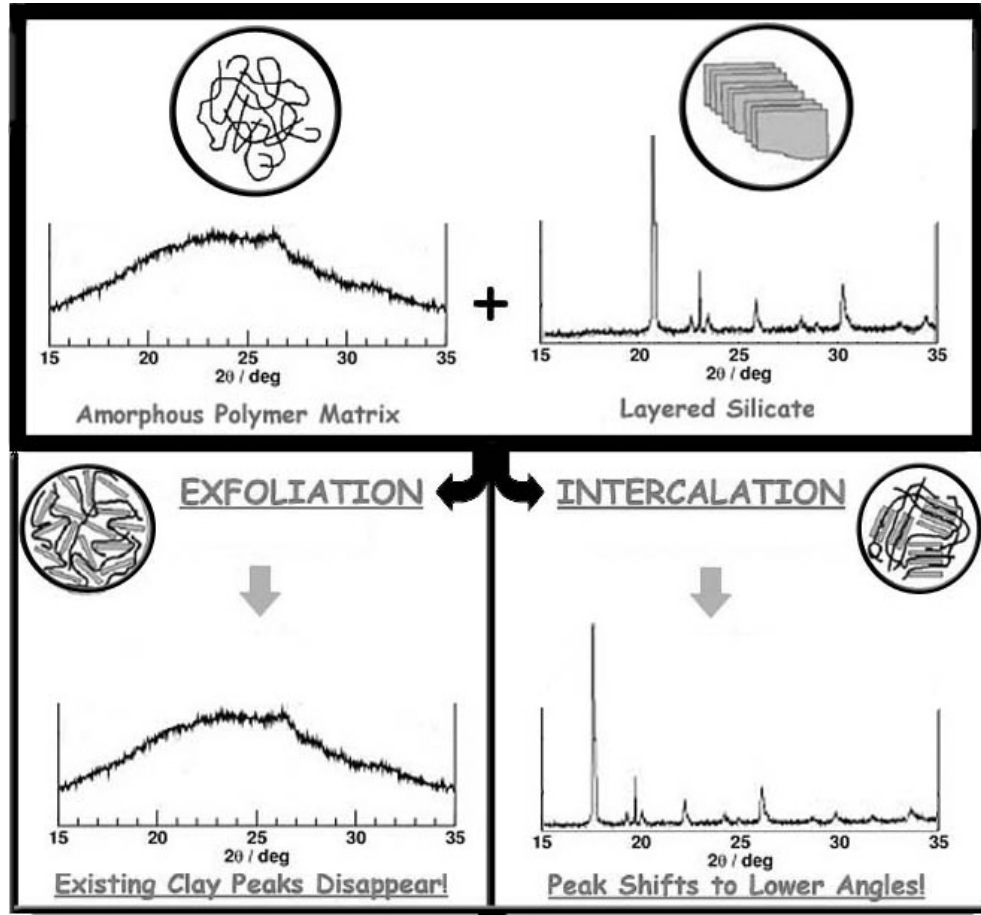


**Figure 3.2** Interpretation of XRD analysis of polymer/layered silicate nanocomposites

**Table 3.4** X-ray analysis data and  $d$ -spacings of the clays used

	$2\theta$ (°)	$\text{Sin}\theta$	$d_{\text{measured}}$ (nm)	$d_{\text{given}}$ (nm)*
<b>Rheospan</b>	3.4	0.030	26.0	-
<b>Cloisite Na+</b>	7.8	0.068	11.3	11.7
<b>Cloisite 10A</b>	4.7	0.041	18.8	19.2
<b>Cloisite 15A</b>	2.9	0.025	30.5	31.5
<b>Cloisite 20A</b>	3.4	0.030	26.0	24.2
<b>Cloisite 25A</b>	4.4	0.038	20.1	18.6
<b>Cloisite 30B</b>	4.8	0.04	18.4	18.5
<b>Cloisite 93A</b>	3.6	0.03	24.5	23.6
<b>Reşadiye</b>	-	-	12.6	-

\*Data provided by SCP



## (b) XRD of the Specimens

As stated earlier, X-ray diffraction analysis governs several problems and is not a stand-alone technique in the characterization of layered silicate nanocomposites. In this study, all the produced samples have been put into XRD in both the bulk form and the powder form (diffractograms are given in Appendix B) in order to investigate the effects of clay content, clay modifier type and XRD specimen size.

### (i) Effect of Clay Content

In order to illustrate the influences of clay content in the specimens, diffractograms of neat clay (Rheospan), and the composite specimens with different clay contents (0.5%, 1%, 1.5%) are evaluated in Figure 3.3.

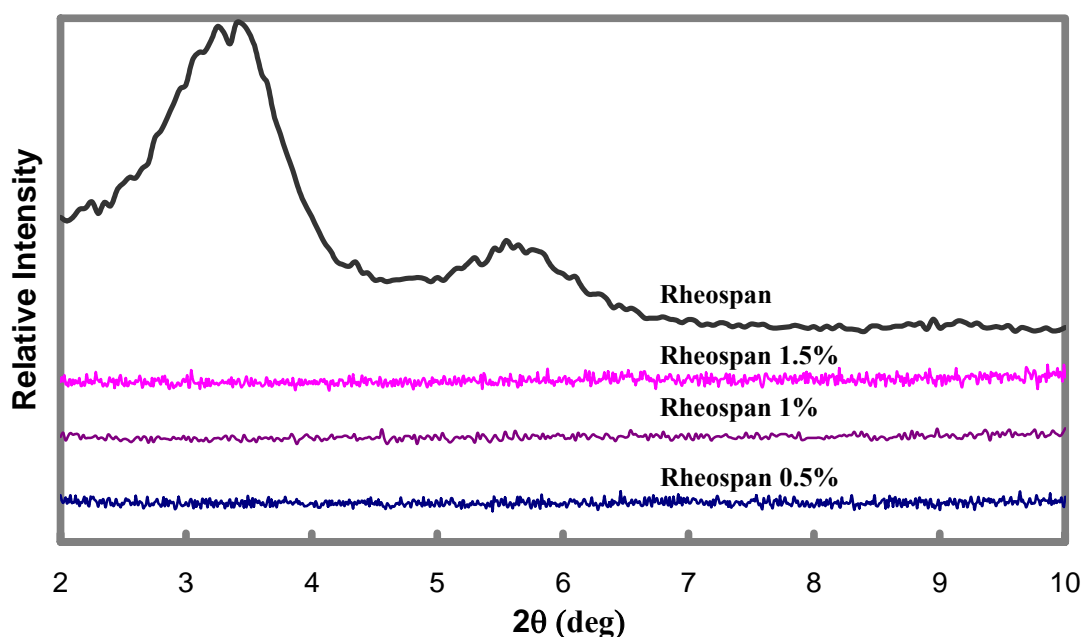


**Figure 3.3** XRD diffractograms of Rheospan clay and the composite specimens with different Rheospan clay contents (1.5%, 1%, 0.5%)

It is seen that the crystalline morphology of the layered Rheospan clay, which is the uppermost curve in the figure, has been dismantled and the peak at around

$2\theta=3.4^\circ$  has been lost when it is used in the composites specimens. This means that no regular “intercalation” of the silicate layers occurred in the specimens. However, the loss of the diffraction peaks in these specimens might also be due to the irregular “exfoliation” of the silicate layers; since normally when a peak is completely wiped out from the diagram it means that exfoliation took place [36].

Figure 3.3 also shows that there is no difference in the diffractograms of the specimens with different clay contents (0.5%, 1% and 1.5%). However, mechanical tests (see Section 3.3) indicated that strength and toughness values of the specimen with 0.5% Rheospan clay were considerably increased compared to neat resin and other specimens with 1% and 1.5% Rheospan clay. Therefore, the rest of the study continued only using 0.5% of other clays (Cloisites and Resadiye).

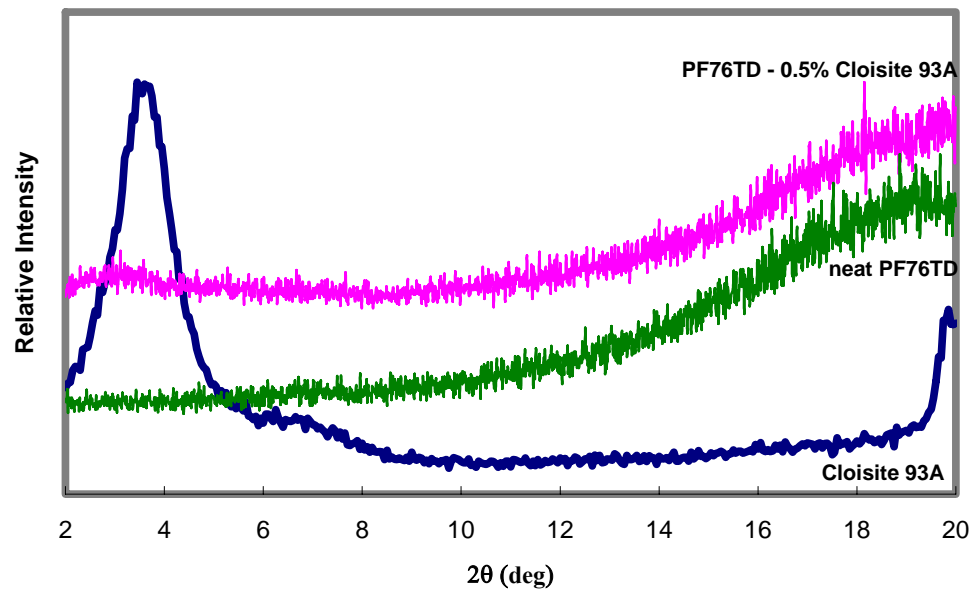
#### **(ii) Effect of Clay Modifiers**

XRD diffractograms of the composite specimens given in Appendix B indicate that use of six different cloisite organoclays resulted in no apparent diffraction peaks, but some very low intensity peaks. This might be interpreted as the occurrence of irregular “exfoliation” or very limited level of “intercalation”.

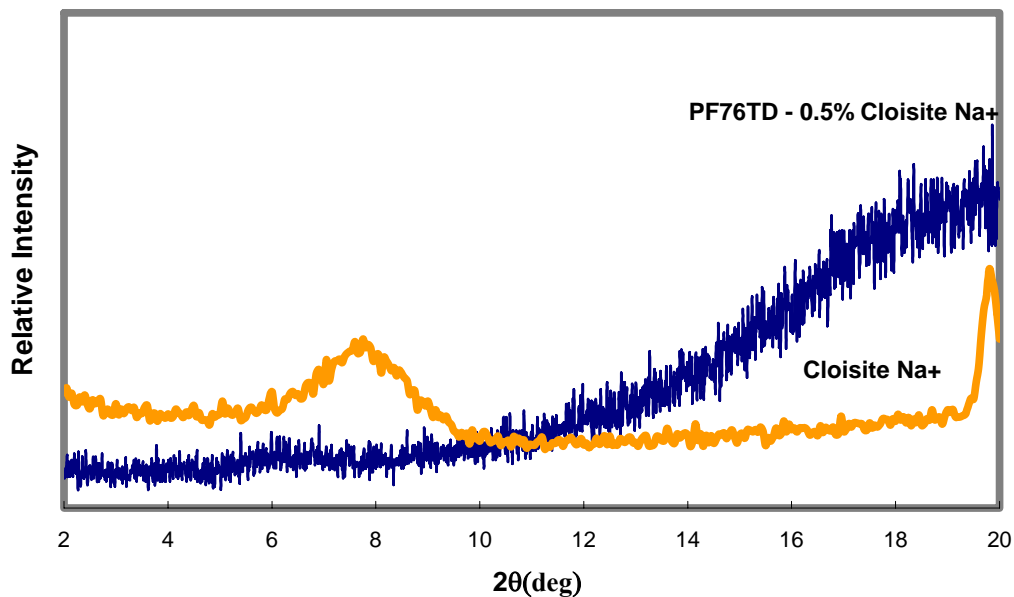
For instance, although mechanical test results of it were poor compared to the other Cloisite clays, Cloisite 93A seems to be somewhat compatible with the resol type phenolic resin PF76TD. As seen in Figure 3.4(a), there is a slight shift from the original peak at  $3.6^\circ$  to  $3.1^\circ$ ; which means that the interlayer spacing has increased from 24.53 nm to 28.49 nm due to some limited level of intercalation.

Another interesting result showing some limited level of intercalation was obtained for the specimen reinforced with unmodified montmorillonite (Cloisite Na<sup>+</sup>). As given in Figure 3.4(b), the peak shifted from  $7.9^\circ$  to  $6.1^\circ$ ; indicating an increase in the interlayer distance. This result was probably due to the initial

compatibility between the relatively more hydrophilic clay (Cloisite Na<sup>+</sup>) and the hydrophilic nature of the resol type phenolic resin (PF76TD) prior to cure.



(a)



(b)

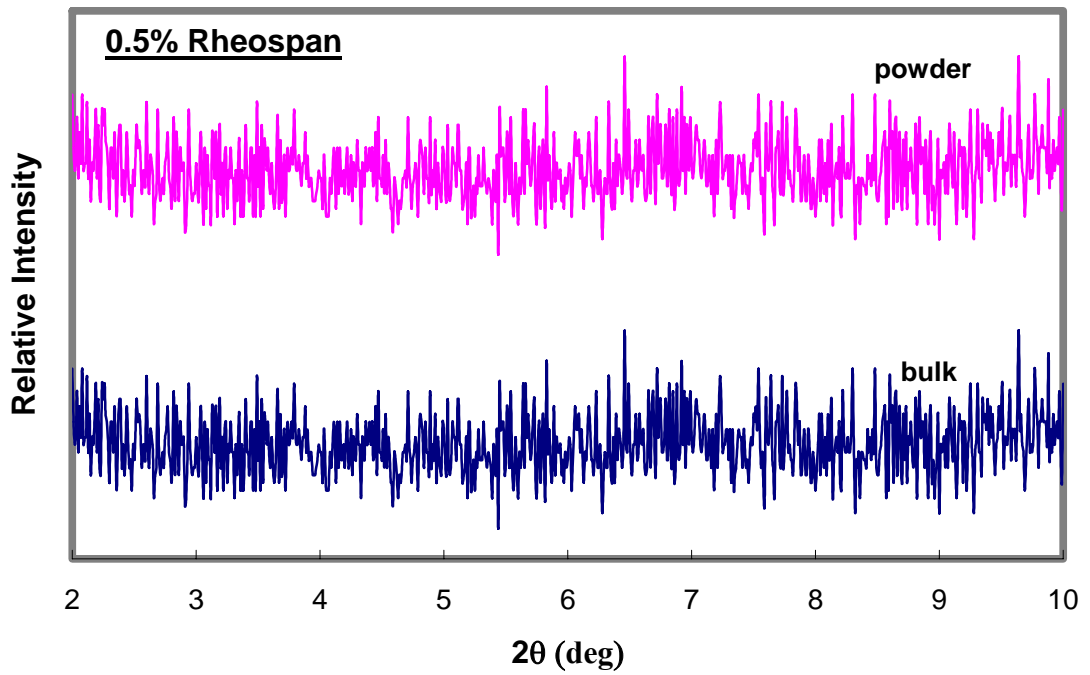
**Figure 3.4** XRD diffractograms of neat PF76TD resin, Cloisite clay and composite specimens with 0.5% Cloisite clay; for (a) Organoclay Cloisite 93A and (b) Unmodified Cloisite Na<sup>+</sup>

### **(iii) Effect of XRD Specimen Size**

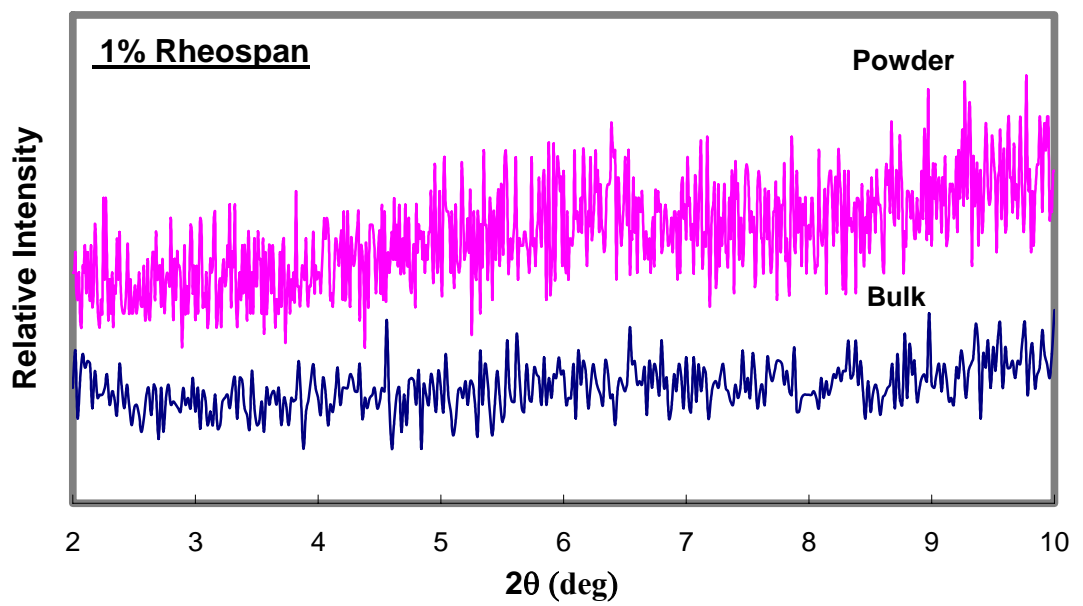
To check whether the specimens being in bulk or powder form had any effect on the XRD diffractograms, specimens were ground into powder form and XRD analysis were carried out again. Three different comparison of the diffractograms of these two specimen forms are given in Figure 3.5, for the composite specimen containing three different amounts of Rheospan clay.

It is seen in Figure 3.5(a) that there is no difference when the clay content is 0.5%. However, Figures 3.5(b) and 3.5(c) show that, although the bulk form did not show any peak at any point, a very low intensity and broad peak at around  $2\theta=6^\circ$  could be seen in 1% Rheospan and 1.5% Rheospan specimens in the powder form.

This observation may mean that some peaks might be skipped when X-ray analysis was carried out on bulk specimens, and a more satisfying X-ray spectrum could be obtained from the powder form of the specimens. This could be interpreted as follows; when the powder size gets smaller, the possibility of seeing all the peaks in the diffractograms increases. However, the deformation applied during grinding operation to obtain powder form may also affect the results of the XRD analysis significantly, leading to false results and conclusions.

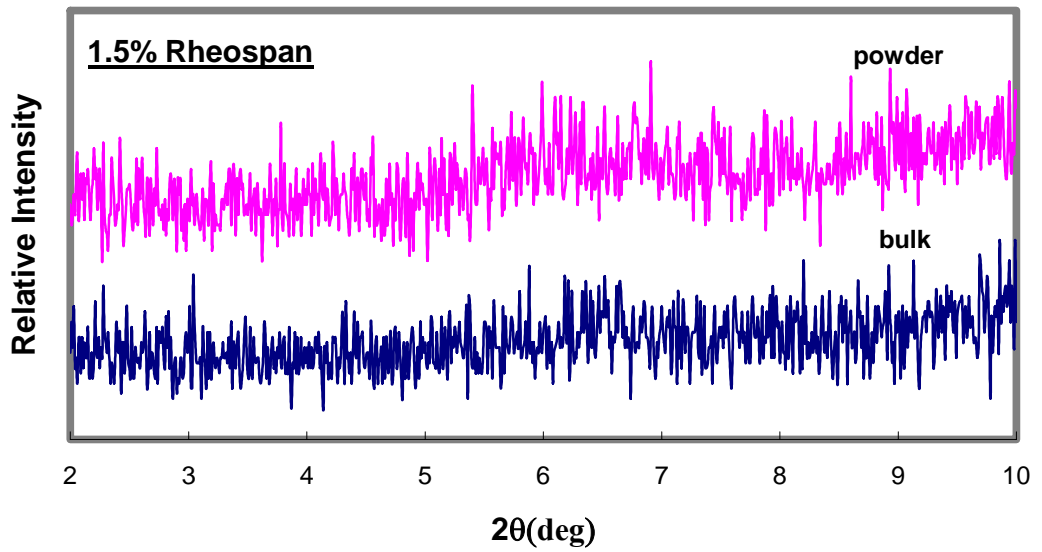


(a)



(b)

**Figure 3.5** XRD diffractograms of composite specimens in the form of powder and bulk; for three different Rheospan clay contents (a) 0.5% , (b) 1% , (c) 1.5%



(c)

Figure 3.5 (cont.)

#### (iv) Effect of High Clay Content

The lack of peaks could also be due to the low concentration of the clay phase in these specimens, since the intensity of diffraction peaks of a second phase in a matrix will be depended on the concentration of that particular phase [37]. For this purpose, two extra specimens were produced by acid curing, having a concentration of 3% and 10% Rheospan clay, and their XRD diffractograms are given in Figure 3.6.

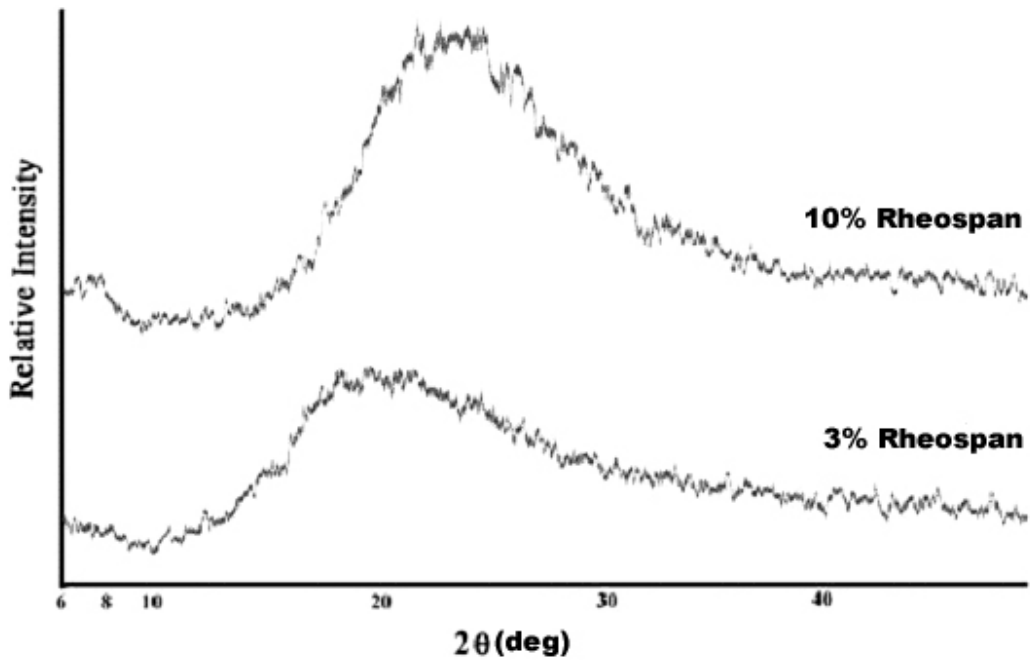


**Figure 3.6** XRD diffractograms of composite specimens with high clay contents; 3% and 10%

This figure shows that, the peak which was observed at  $2\theta=6^\circ$  in the X-ray spectra of the powder specimens at lower clay loadings is now much more obvious with the increased clay content. Furthermore, it has moved to a slightly higher theta value of  $7^\circ$ . This means that the layer distance between the clay layers has decreased as clay amount increased, which is in harmony with the fact stated in several studies that amount of clay loading above a certain point decreases mechanical properties.

### 3.2.1.2 SEM Analysis

In order to observe the morphology of the matrix and the reinforcement and the interaction at their interface on a microscopic level, surfaces of the Charpy Impact Test specimens were examined under the scanning electron microscope (Figures 3.7 to 3.15).

In Figure 3.7, morphology of the two resins; resol type phenol formaldehyde resin PF76 and its ethylene-glycol modified counterpart PF76TD are compared. In these SEM fractographs of neat resin specimens, microvoids of different sizes can be seen. These voids are formed as a result of water vapor, which is the by-product of the polymerization reaction, getting trapped inside the specimen during curing. The effect of ethylene-glycol on the microstructure can be observed clearly when these micrographs, which are of the same magnification (850X), are compared. In neat PF76 specimen (Figure 3.7(a)) microvoids are relatively larger and their concentration is higher when compared to those in neat PF76TD specimen (Figure 3.7(b)). Furthermore, it is observed that microvoids in PF76 are empty; indicating the ease of fracture which had proceeded in a brittle manner. However, in PF76TD, as shown in the magnified insert image in Figure 3.7(b), many of the voids are filled with deformed polymer; indicating the plasticizer effect of mono and diethylene glycol.

Effects of clay addition into the resin matrix can be observed in Figure 3.8. As shown in Figure 3.8(b), when 1% Rheospan clay were added the number of microvoids in PF76TD resin (Figure 3.8(a)) had decreased. There might be two reasons for this difference; first, as clays are very hydrophilic in nature they may have taken the water molecules formed during curing, and secondly, the extra time elapsed for the mixing stage of composite specimen production might have reduced the amount of water molecules left in the specimen.



Another effect of clay addition is the fracture surface roughness of the specimens (Figure 3.8). Neat PF76TD resin specimen has rather smooth fracture surface (Figure 3.8(a)) indicating its brittleness, while 1% Rheospan clay composite specimen has large numbers of deformation lines, i.e. rivermarkings. Rivermarkings are elongated markings, often branching at narrow angles, present on a fracture surface and resulting from the fracture crack propagating along a parallel array of cleavage planes at different levels [38]. The existence of such features on a rough fracture surface shows that a higher amount of energy absorption occurred during cracking and fracturing.

In Figure 3.9, SEM fractographs of heat and acid cured PF76TD resins are shown. As explained in Section 3.1 in detail, the heat curing route of this phenolic resin provides a relatively void-free microstructure (Figure 3.9(a)), which was mainly due to the very long curing schedule giving sufficient time for the by-product water to be released out of the resin before curing was over. However, in the acid curing route, the crosslinking rate was much faster than the water vapor release rate and gelation occurred before completion of water vapor release, which resulted in formation of several microvoids (Figure 3.9(b)).

Although the heat curing route of this resin type phenolic resin provides less microvoids, it caused significant problems during the production of the composite specimens. The main problem was the formation of two different layers, as shown in Figure 3.10(a), for the heat cured PF76TD-0.5% Cloisite10A specimen. This layered structure forms due to the very long curing schedule providing enough time for the clay and polymer phases to get separated due to their density difference. The high-density clay particles settle to the lower regions of the specimen (Figure 3.10(b)) before the resin gets intensively crosslinked, leading to a non-homogeneous final structure and poor mechanical properties.

Interfacial attraction between the resin matrix and the clay particles is very crucial in terms of the mechanical properties of the composite specimens. In Figure 3.11, some incompatible polymer – clay interfaces are shown. Figure 3.11(a) shows a Cloisite 10A clay tactoid of approximately 10  $\mu\text{m}$  radius. It is observed that this clay particle remained as a tactoid in the polymer microstructure, without getting into much interaction with the polymer. The incompatibility between the clay and the polymer caused debonding to occur at the interface upon application of stress. In Figure 11(b), similar incompatibility is also observed for the Cloisite 30B clay.

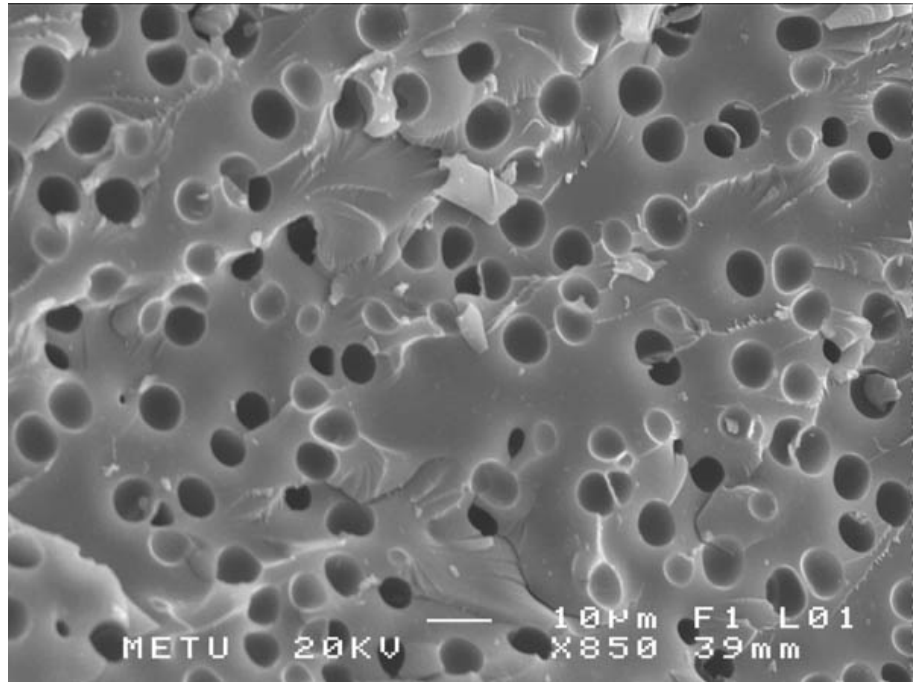
When the clays are organically modified with suitable modifiers, then the interaction between the resin matrix and the organoclays would be sufficient to lead to intercalation and/or exfoliation. In Figure 3.12, such compatible polymer-clay systems are shown. In both PF76TD-0.5% Rheospan (Figure 3.12 (a)) and PF76TD-0.5% Cloisite 15A (Figure 3.12 (b)) fractographs, it is seen that the two phases are well intercalated into each other and no distinct interface and no debonding can be observed. These differences in the structures, observed in Figure 3.12 (a,b) prove that modification of the Rheospan and Cloisite 15A clays were very helpful in obtaining a well intercalated nanocomposite material.

As explained earlier, the roughness of the fracture surfaces may give a general idea on the toughness of the produced specimens. As the fracture surface changes from a rather smooth and featureless surface, which is an indication of brittle fracture, to a highly deformed rough surface, it can be concluded that the amount of energy absorbed for the crack growth during fracture increases; which in turn increases the toughness. This was already shown in Figure 3.8, referring to the change in the morphology of the rivermarkings with the increase of clay content in the polymer. Such an effect can also be observed in Figure 3.13. The fracture surface of the phenolic resin reinforced with more compatible Rheospan clay (Figure 3.13(b)) is

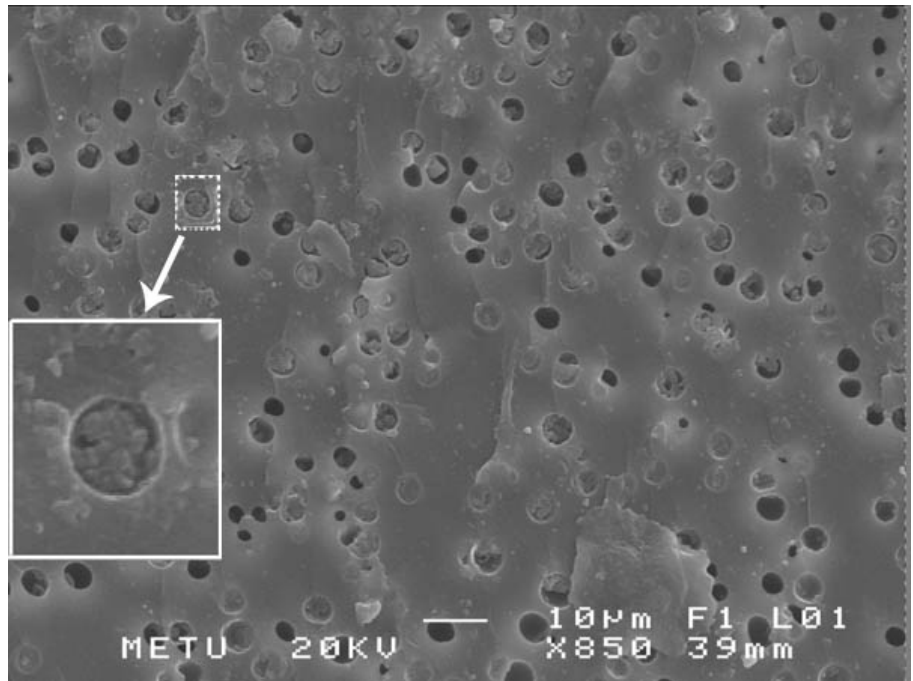
relatively much more deformed than the less compatible Cloisite 10A clay (Figure 3.13(a)). It can also be seen from the results of the mechanical tests that the fracture toughness of PF76TD-0.5% Rheospan specimen is much higher than that of PF76TD-0.5% Cloisite 10A specimen.

There are several toughening mechanisms for the particulate reinforced polymers, such as crack tip blunting, crack pinning or crack deflection at the particulate interface; but actually all of these mechanisms stand on the same principle: to decrease the propagation rate of cracks. If there is proper interface between the matrix and the particle, then these toughening mechanisms would be very effective, as shown in Figure 3.14 for the PF76TD resin with tactoids of Rheospan organoclay.

However, these toughening mechanisms would not be very operative for the rather incompatible matrix-reinforcement systems, as shown in Figure 3.15 for the tactoid of unmodified Resadiye clay in PF76TD resin matrix. Here, the propagating crack was not pinned or deflected, but resulted in large amount of debonding and particle cracking.

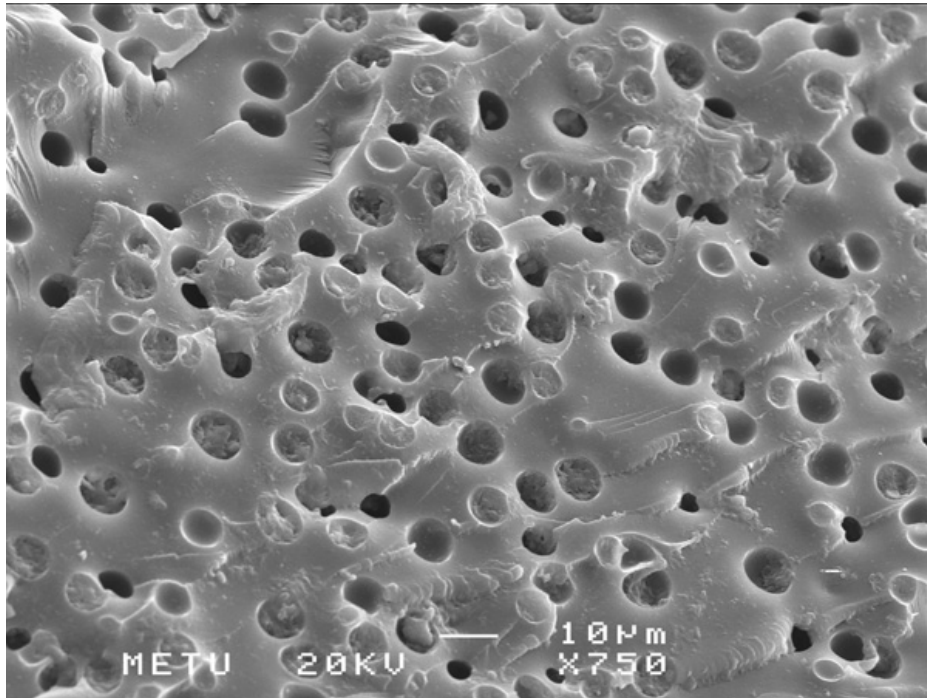


(a)

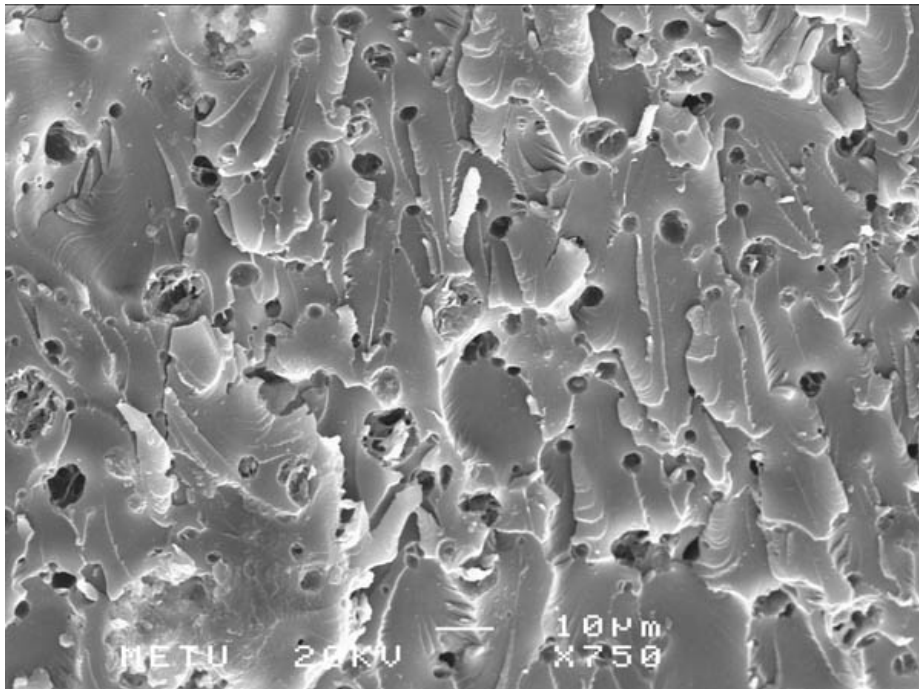


(b)

**Figure 3.7** Comparison of the void formation for the two different neat resin specimens (a) PF76, and (b) PF76TD

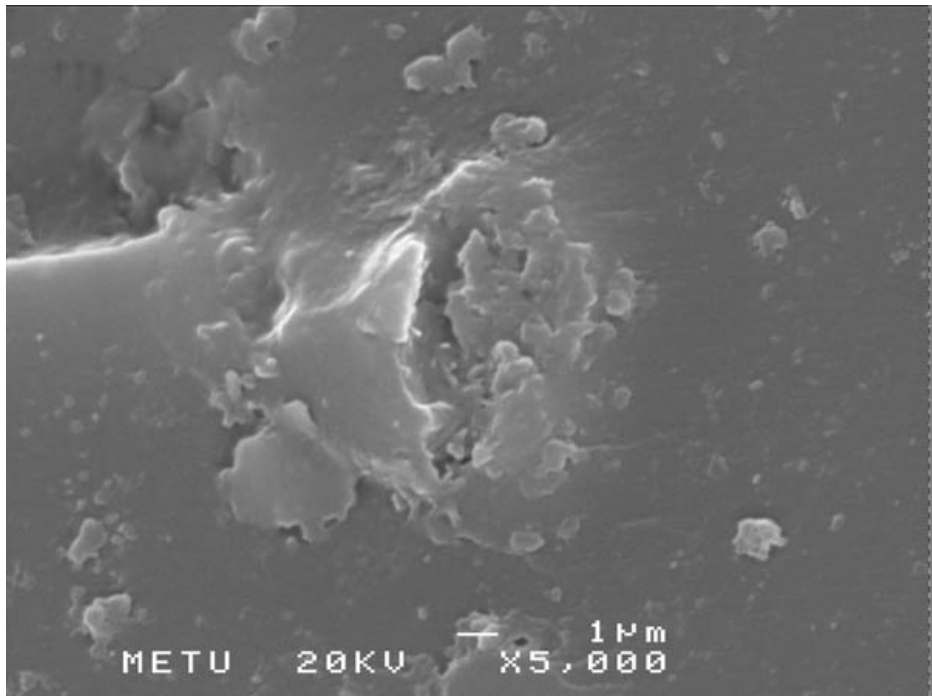


(a)

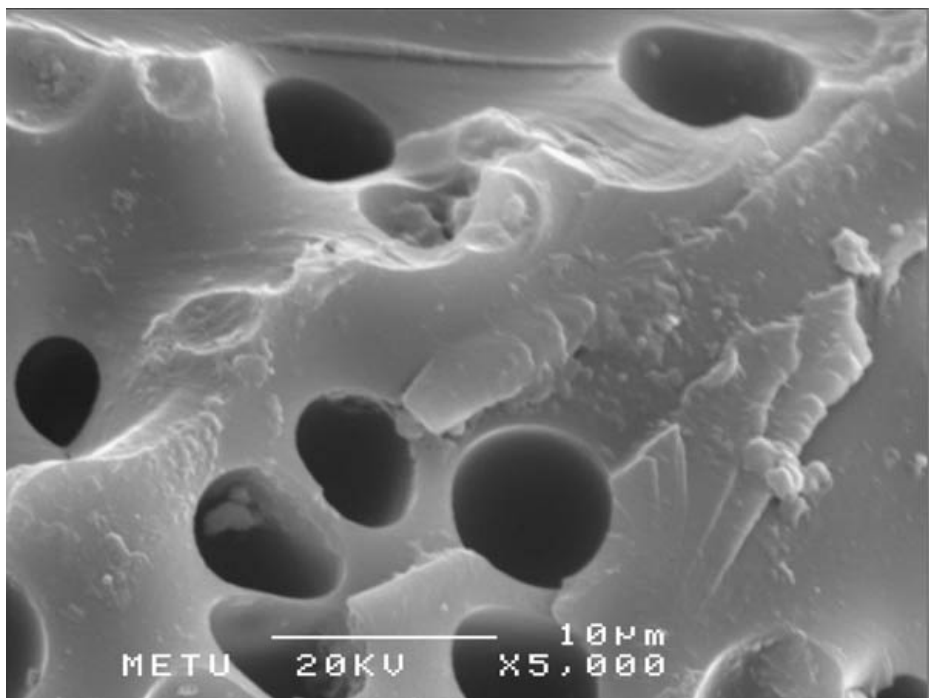


(b)

**Figure 3.8** Comparison of the void formation and fracture surface roughness for the specimens of (a) neat PF76TD resin and (b) 1% Rheospan clay composite

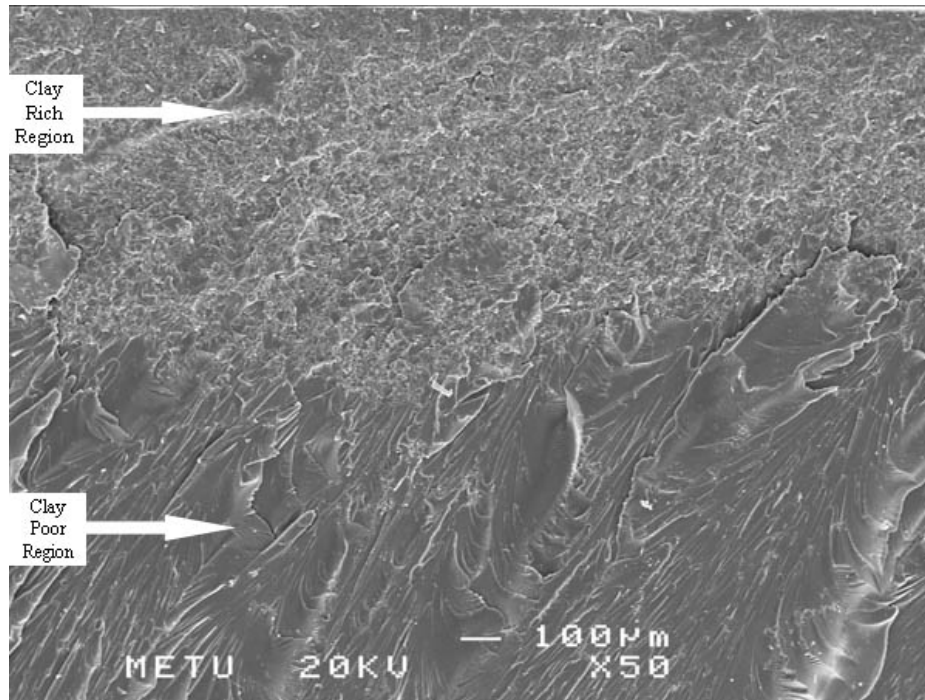


(a)

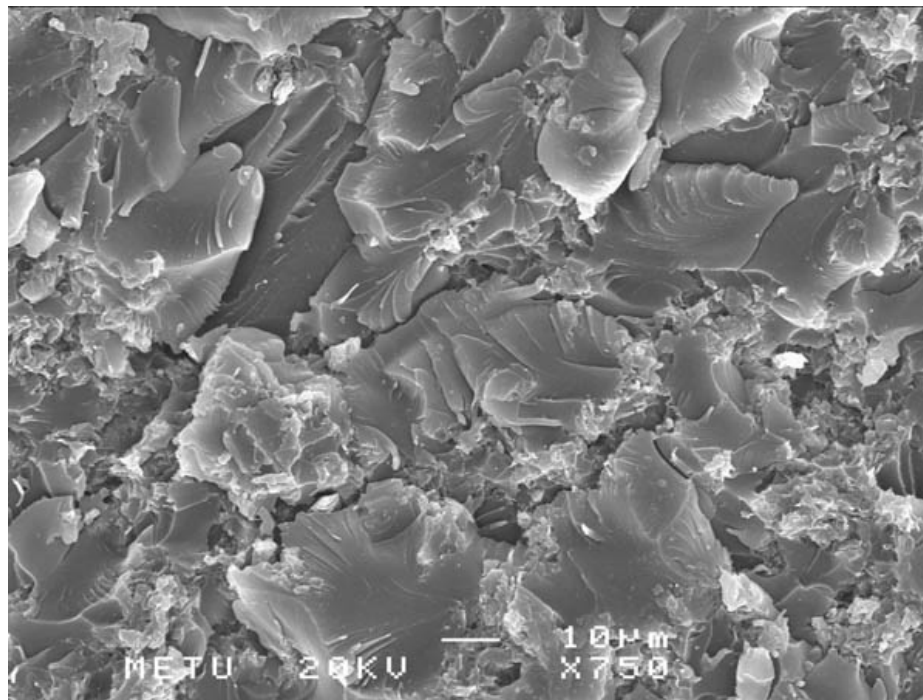


(b)

**Figure 3.9** Comparison of the two different curing routes used for the PF76TD resin, (a) Heat Cure and (b) Acid Cure

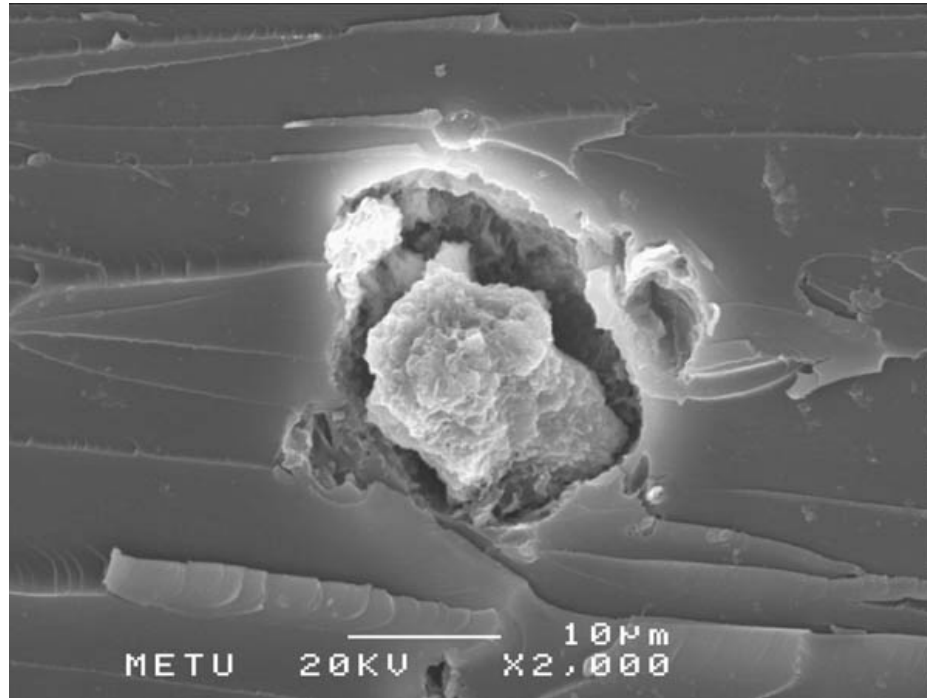


(a)

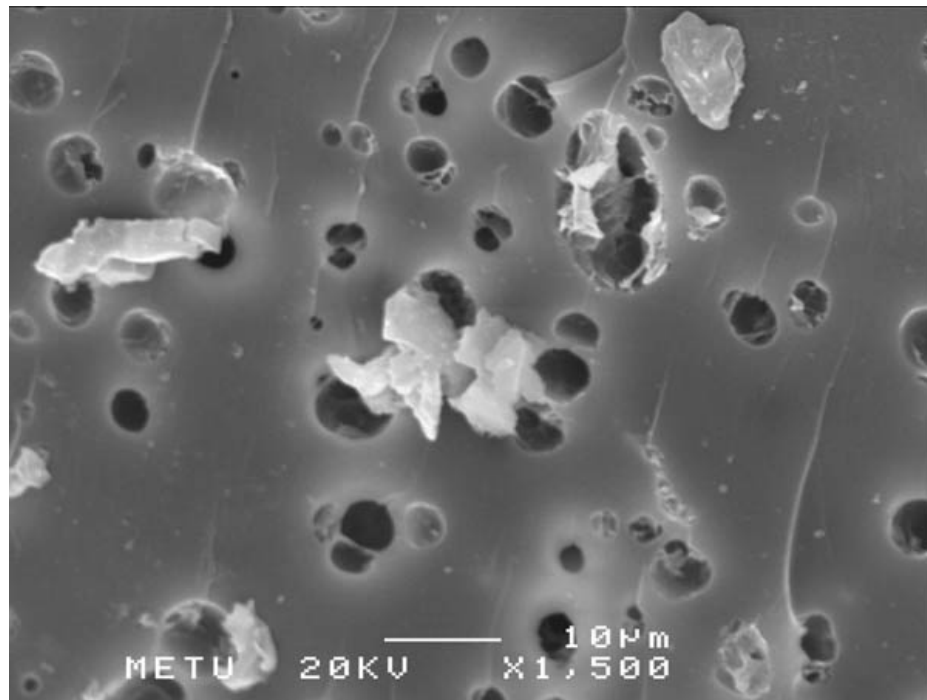


(b)

**Figure 3.10** (a) Layer formation in Heat Cured PF76TD-0.5% Cloisite 10A and (b) Closer View of this Clay Rich Region



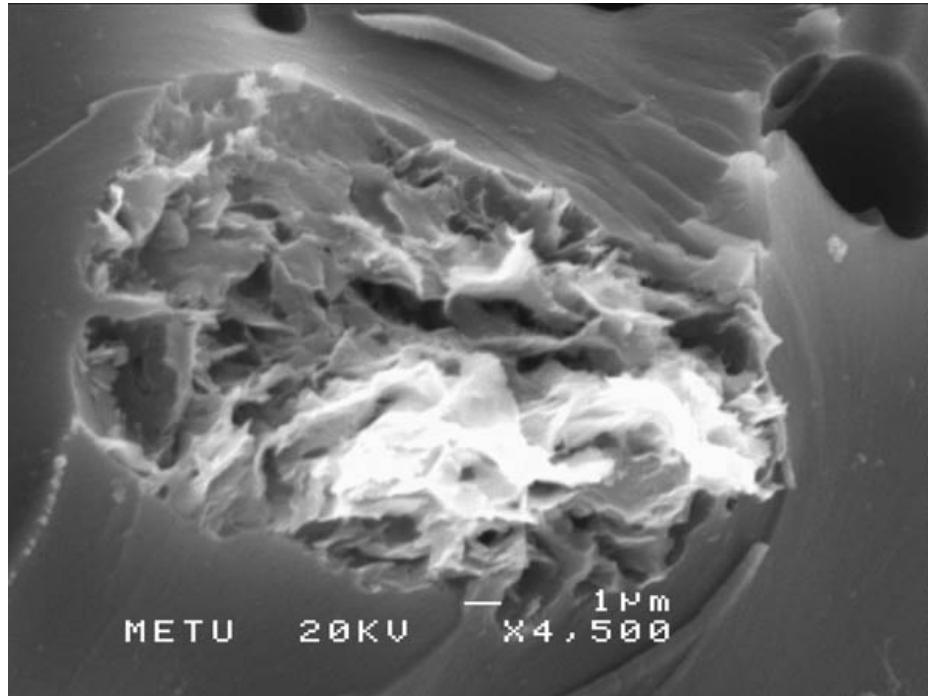
(a)



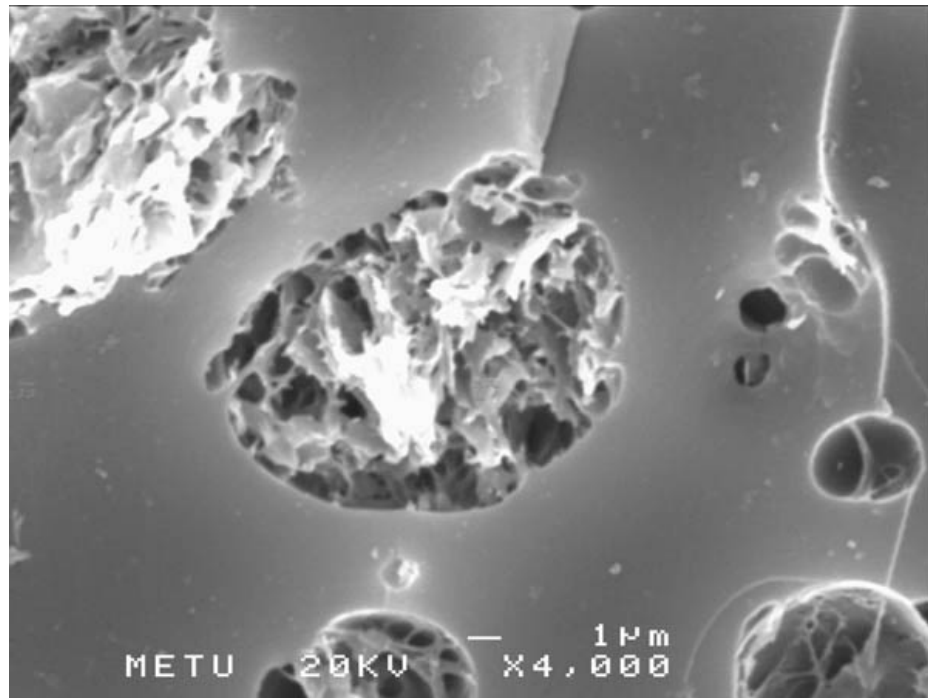
(b)

**Figure 3.11** Weak interfacial adhesion between PF76TD resin and tactoids of (a) Cloisite 10A and (b) Cloisite 30B clays



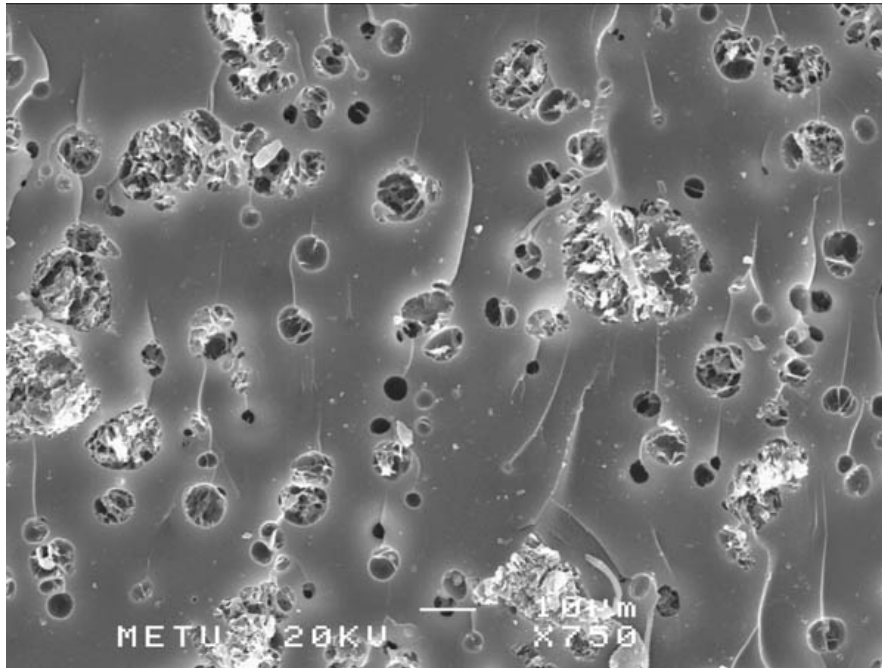


(a)

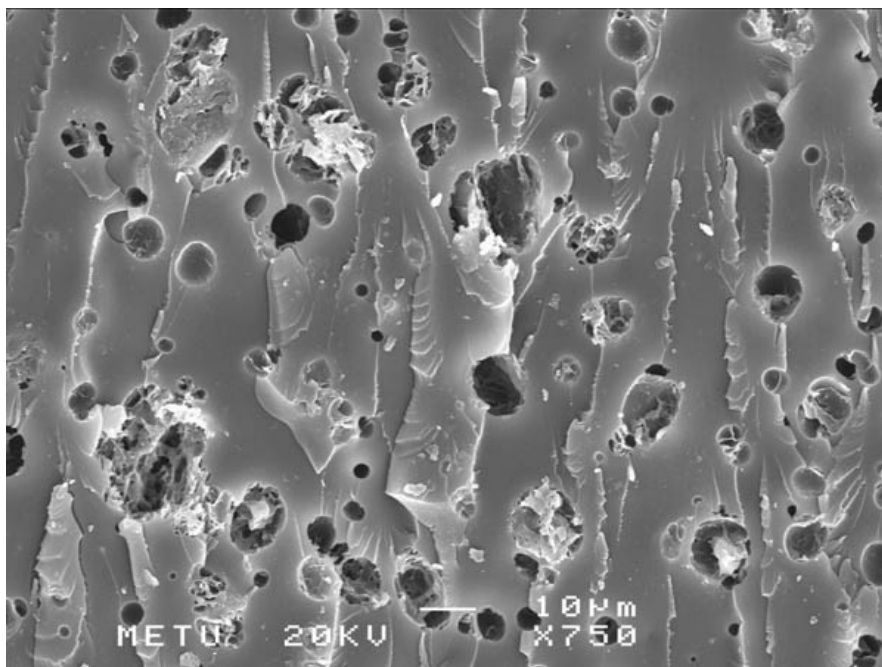


(b)

**Figure 3.12** Proper interfacial adhesion between PF76TD resin and (a) Rheospan  
(b) Cloisite 15A clays

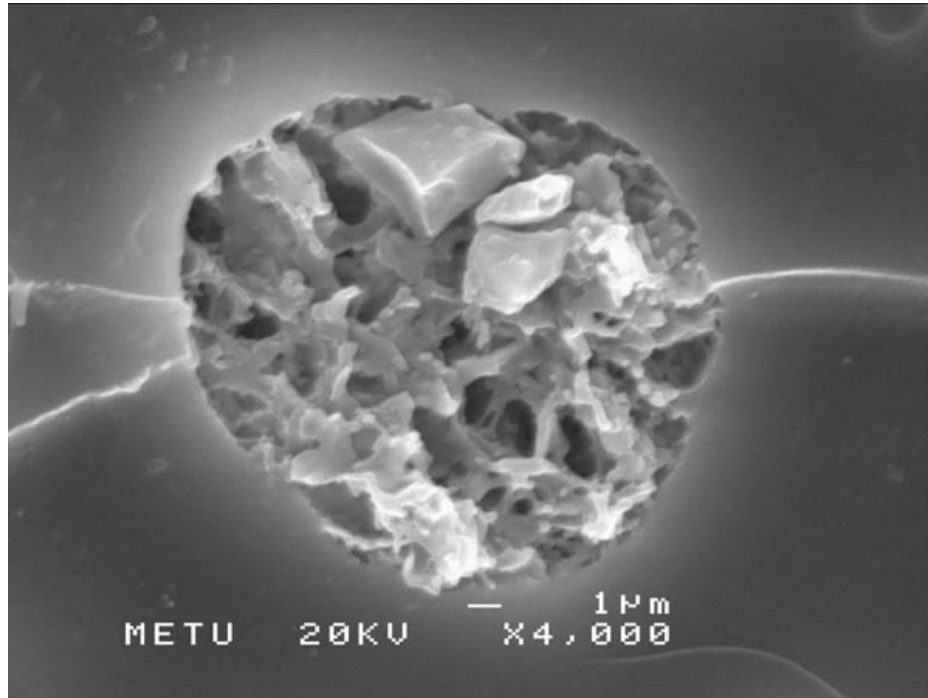


(a)

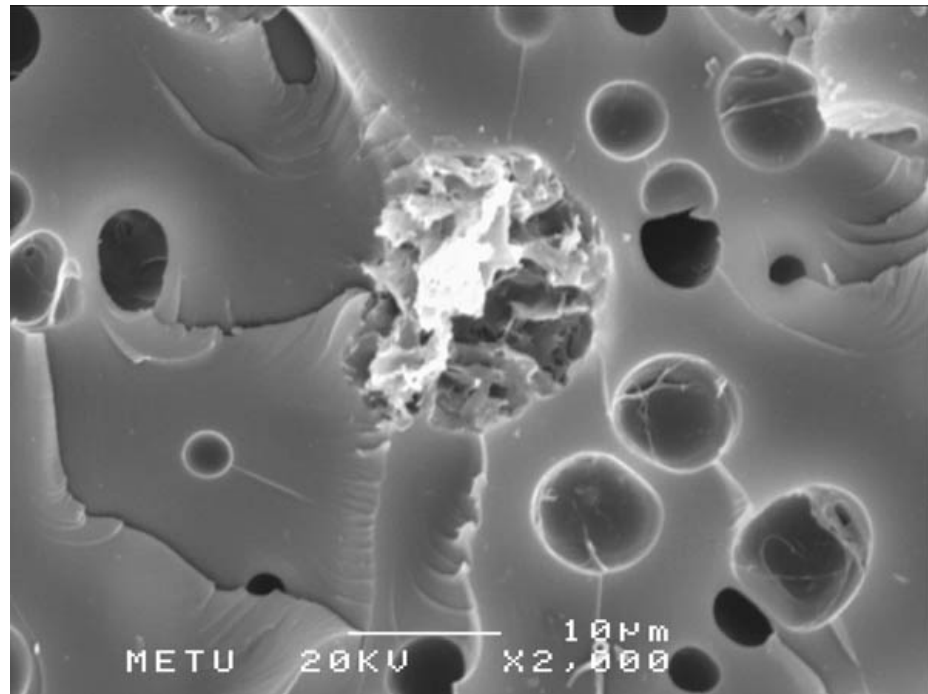


(b)

**Figure 3.13** Comparison of the fracture surface roughness of the PF76RD resin specimens reinforced with (a) less compatible Cloisite 10A and (b) more compatible Rheospan clays



(a)



(b)

**Figure 3.14** (a) and (b) Crack Pinning or crack deflection at the tactoids of Rheospan organoclay in PF76TD resin

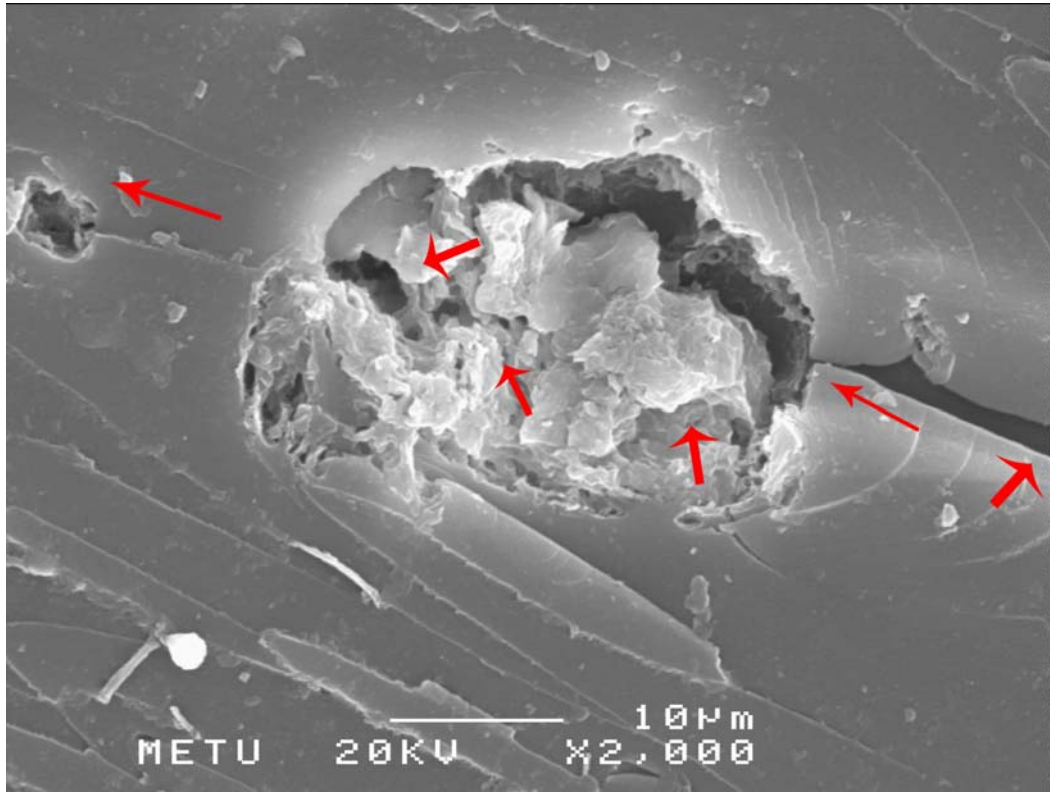


**Figure 3.15** Large amount of debonding and particle cracking at a Resadiye clay tactoid in PF76TD matrix

### 3.2.1.3 TEM Analysis

SEM analysis is generally useful in understanding the distribution of clay particles in the polymer matrix; however it may give only a brief idea about the degree of intercalation of the clay layers. This is due to the relatively low-resolution capacity of SEM, which is not sufficient to observe the changes in the clay layer galleries, which are in the orders of nanometers. However, the enhancements in the material properties of polymer/layered silicate nanocomposites depend highly on the degree of intercalation and/or exfoliation of the clay layers that is why it is very important to conduct TEM analysis.

In this study, XRD data, SEM fractographs and mechanical tests showed that Rheospan is the most compatible clay to resol type phenol formaldehyde resin PF76TD; and a partially intercalated morphology may have occurred at especially very low clay concentrations. Therefore, for TEM analysis only the specimens of PF76TD resin with 0.5% Rheospan clay were chosen.

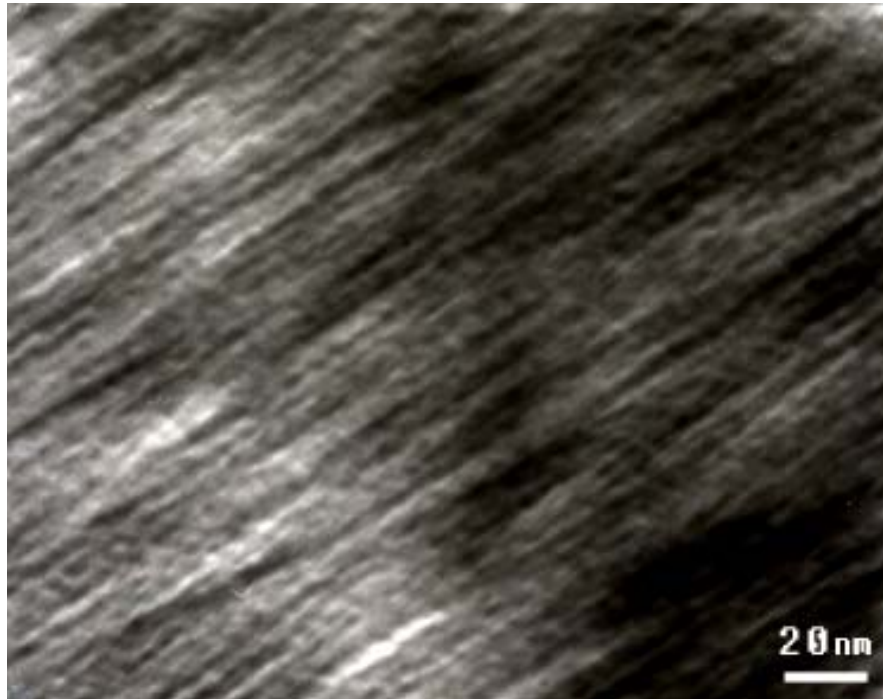
During TEM analysis, three different layered morphologies, at three different magnification levels were observed.

The first type of layered morphology (Figure 3.16) was observed at very high magnification levels (600 000 – 1 000 000 X). Layered structures seen in these TEM micrographs should be the galleries of Rheospan clay where the layer thicknesses are in the order of a few nanometers.

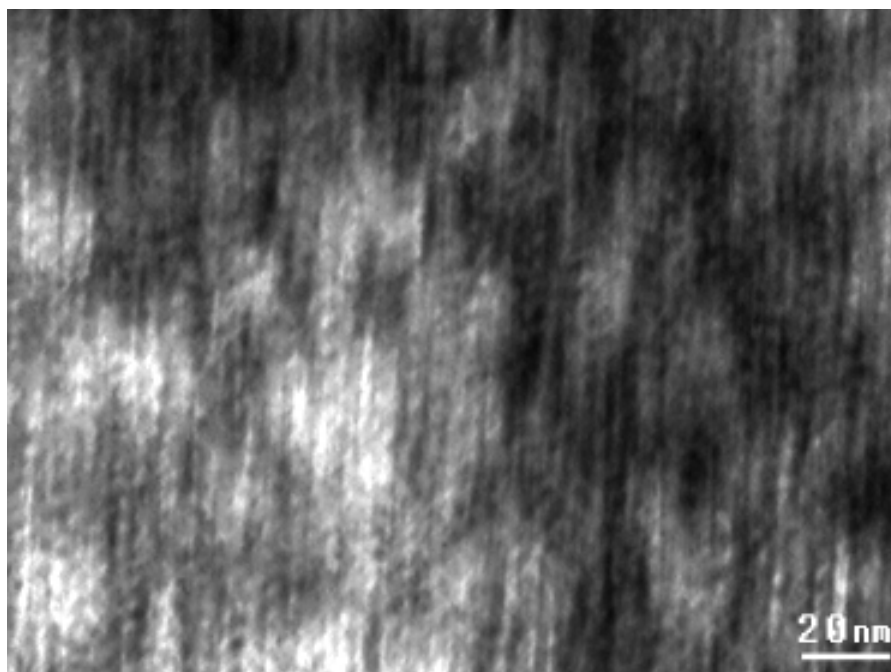
The second type of layered morphology (Figure 3.17) observed was at a magnification level of 400 000X. Layered structures seen in these TEM micrographs have this time widened interlayer galleries in the range of 40-80 nm. The interlayer distance determined for Rheospan clay by XRD was 26 nm. Therefore, these wide galleries should be showing the possibility of a certain level of intercalation and/or exfoliation of the Rheospan clay.

The last type of layered morphology (Figure 3.18) was at relatively lower magnification levels (25 000 – 40 000 X). The thickness of the layered silicate structures seen in these TEM micrographs are in the range of 40 - 60 nm, while the interlayer galleries have widths ranging from 100 nm to 200 nm. Normally the thickness of smectite clay layers are in the order of 1 nanometer and the interlayer galleries may range from tens of nanometers to microns, depending on the level of intercalation.

Therefore, it is difficult to consider these layers as intercalated Rheospan clay. In order to clarify this statement, TEM diffraction patterns of these structures were taken. Figure 3.19 shows that somekind of crystallinity is existing in these layered structures. Thus, it could be interpreted that, these layers may represent not single clay layers, but the possibility of a collection of these layers.

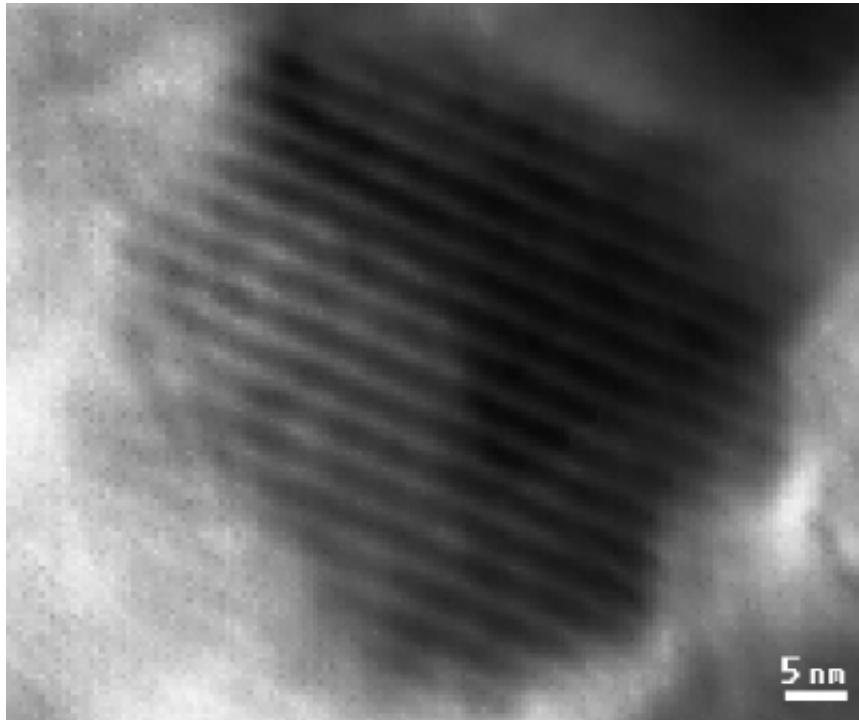


(a)

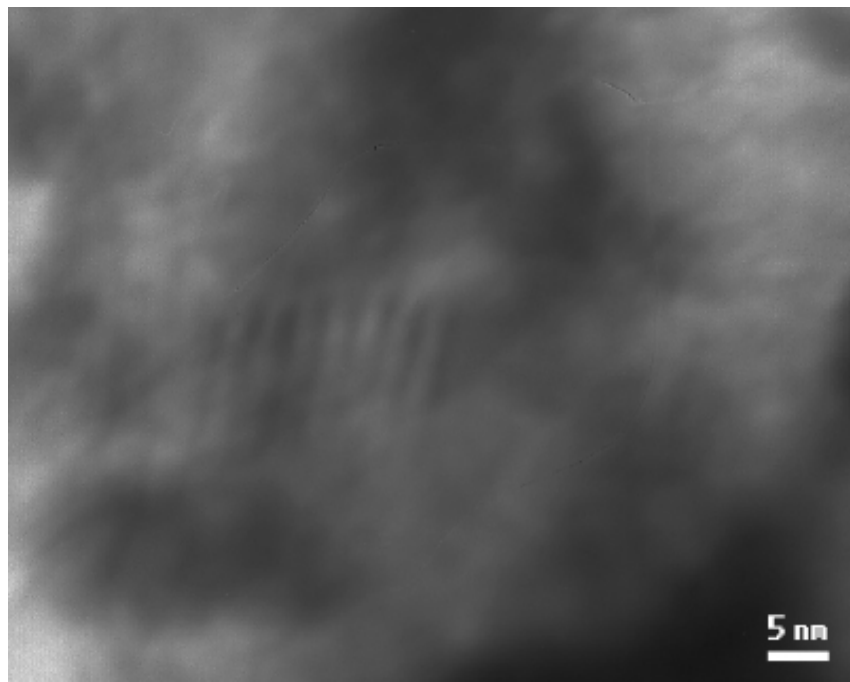


(b)

**Figure 3.16** TEM micrographs of the layered structure of Rheospan clay, (a) and (b) general views, (c) and (d) closer views.



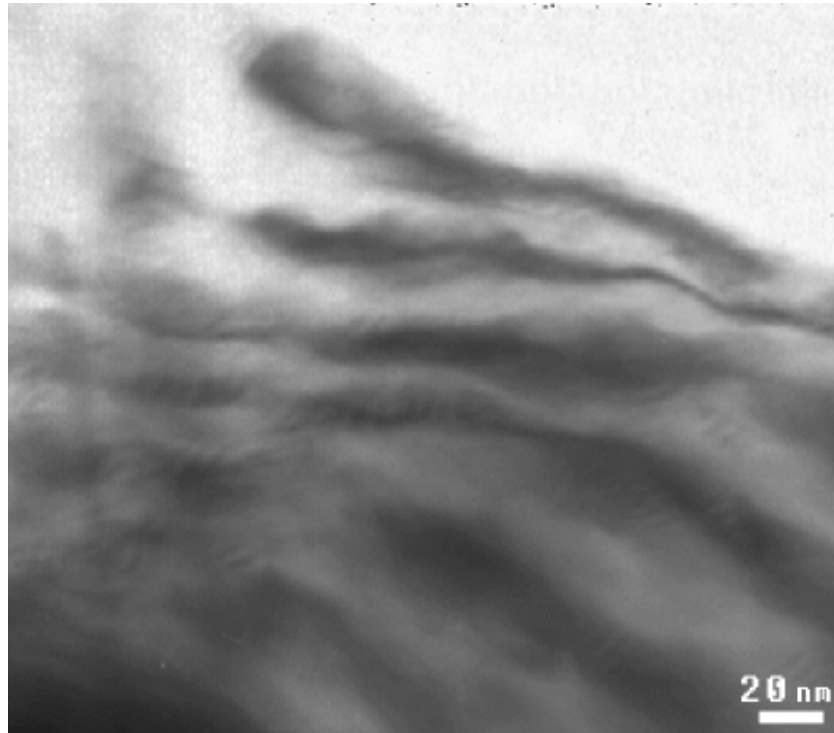
(c)



(d)

**Figure 3.16** (cont.)



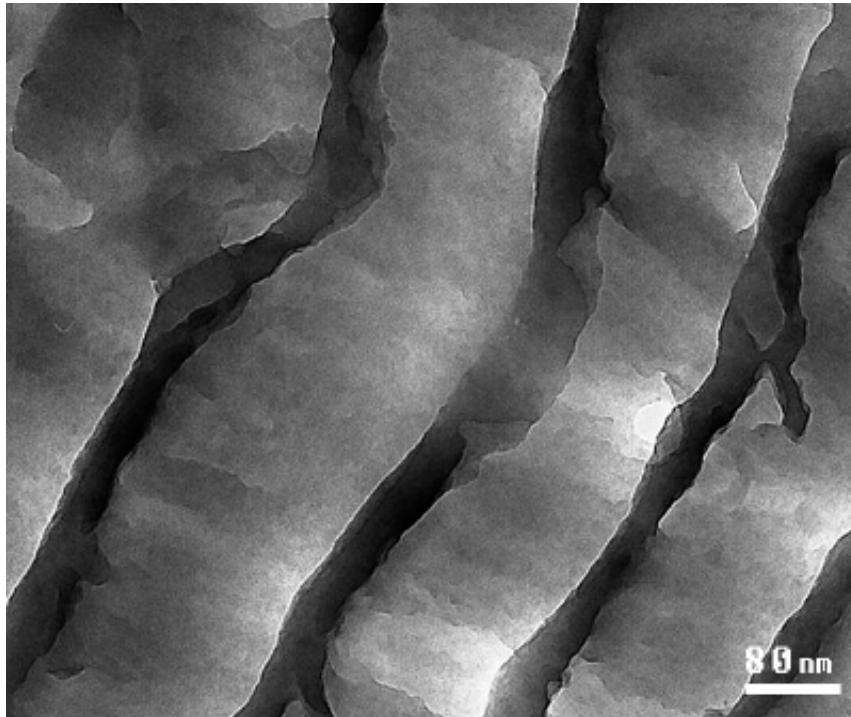


(a)

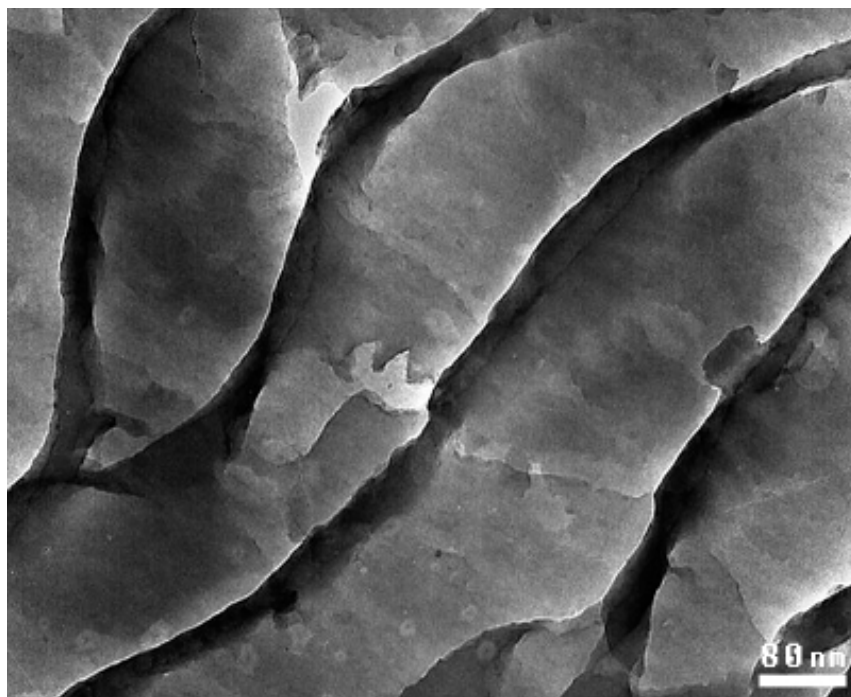


(b)

**Figure 3.17 (a) and (b)** TEM micrographs of the intercalated and/or exfoliated Rheospan clay.

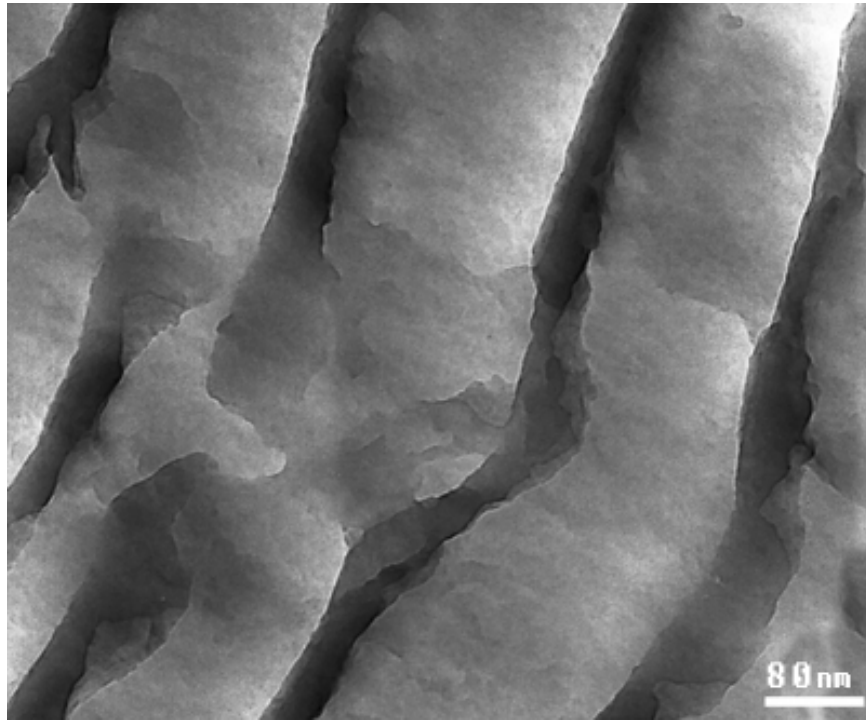


(a)

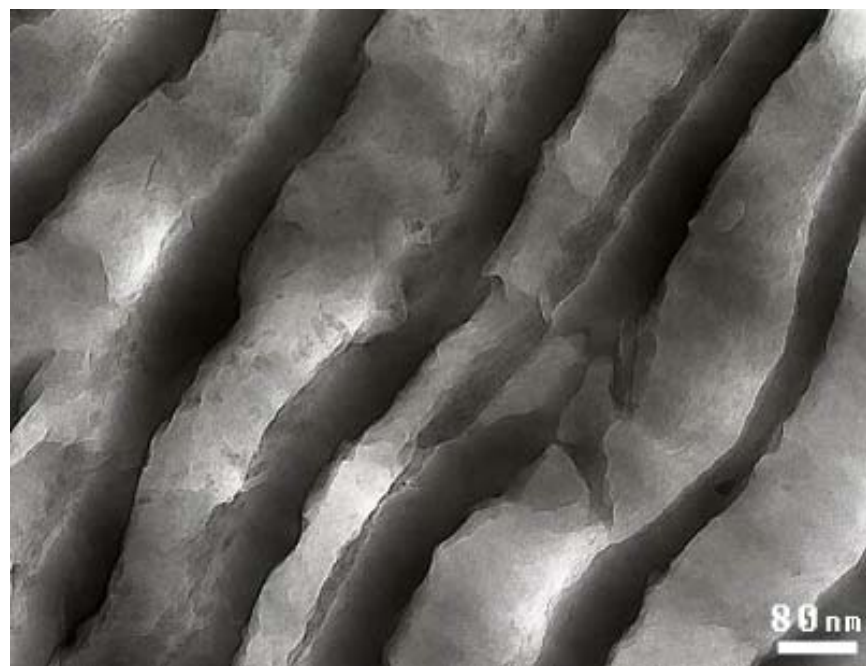


(b)

**Figure 3.18 (a), (b), (c) and (d)** TEM micrographs showing large scale layered structure morphology



(c)



(d)

**Figure 3.18** (cont.)

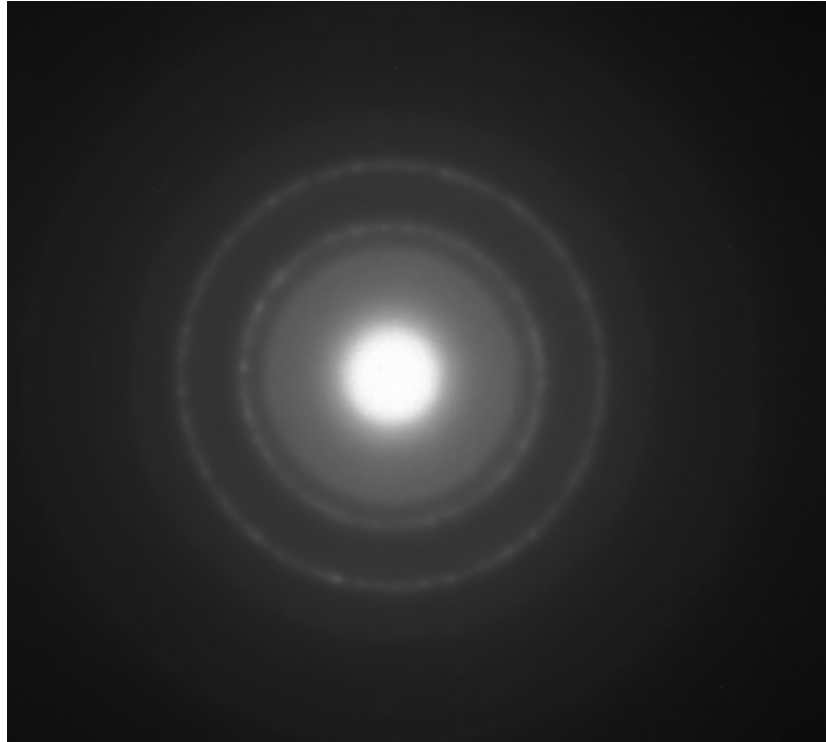


**Figure 3.19** TEM Diffraction patterns of the large scale layered structures shown in Figure 3.18.

### **3.2.2 Mechanical Testing**

Three types of mechanical tests; Flexural (3-point bending), Charpy Impact and Plane Strain Fracture Toughness tests were carried out for 14 different types of specimens. For each condition five specimens were tested and then their standard deviations were calculated.

Flexural test data were first evaluated to obtain Flexural Stress vs Flexural Strain curves as shown in Appendix C. Then, these curves are used to determine Flexural Strength, Flexural Strain at Break and Flexural Modulus of the specimens.

Energy data obtained in the Charpy Impact tests were evaluated per unit area of the fractured surface.

In the Fracture Toughness tests, first Load vs Deflection curves were determined (see Appendix D) and then  $P_Q$  values of these curves were used to calculate the Fracture Toughness ( $K_{IC}$ ) of the specimens.

Mechanical properties of 14 different specimen groups determined by these tests were first given in Table 3.5, and then these data were evaluated to investigate different production parameters in the following subsections.

#### **3.2.2.1 Effect of Resin Type**

Two types of water-based resol type phenolic resins provided from Polisan Co. required different curing schedules, as explained earlier. This difference consequently led to different mechanical properties. Flexural stress-strain curves of their 3-point bending tests are given in Figure 3.20. The mean curves shown in this figure were obtained by the method described in Section 2.3.5.1. All the mechanical properties of both resins are then tabulated in Table 3.6.

**Table 3.5** Mechanical properties of 14 different specimen groups produced

Specimen Group	Resin Type	Clay Type	Clay Content (%)	Cure Type	Flexural Strength (MPa)	Flexural Modulus (GPa)	Flexural Strain at Break (%)	Fracture Toughness (MPa√m)	Charpy Impact Strength (kJ/m <sup>2</sup> )
1	PF76	-	-	ACID	101 ± 7	4.4 ± 0.3	2.38 ± 0.75	0.87 ± 0.10	0.93 ± 0.10
2	PF76TD	-	-	ACID	105 ± 7	4.2 ± 0.1	2.78 ± 0.40	0.92 ± 0.02	1.08 ± 0.14
3	PF76TD	RHEOSPAN	0.5	ACID	111 ± 2	3.7 ± 0.1	3.08 ± 0.44	1.53 ± 0.29	1.08 ± 0.06
4	PF76TD	RHEOSPAN	1	ACID	108 ± 7	3.6 ± 0.2	3.04 ± 0.16	0.73 ± 0.05	1.02 ± 0.16
5	PF76TD	RHEOSPAN	1.5	ACID	95 ± 4	3.5 ± 0.1	2.80 ± 0.23	0.76 ± 0.19	1.12 ± 0.15
6	PF76TD	CLOISITE 10A	0.5	HEAT	51 ± 6	2.8 ± 0.3	2.24 ± 0.42	0.57 ± 0.11	0.89 ± 0.03
7	PF76TD	CLOISITE 10A	0.5	ACID	68 ± 6	3.9 ± 0.1	1.95 ± 0.21	0.67 ± 0.05	0.83 ± 0.07
8	PF76TD	CLOISITE 15A	0.5	ACID	98 ± 5	4.5 ± 0.5	2.23 ± 0.55	1.08 ± 0.26	0.80 ± 0.06
9	PF76TD	CLOISITE 20A	0.5	ACID	92 ± 8	3.6 ± 0.3	2.66 ± 0.52	1.00 ± 0.07	0.73 ± 0.05
10	PF76TD	CLOISITE 25A	0.5	ACID	92 ± 12	3.4 ± 0.1	2.89 ± 0.81	0.79 ± 0.14	0.70 ± 0.03
11	PF76TD	CLOISITE 30B	0.5	ACID	67 ± 8	3.3 ± 0.4	2.01 ± 0.11	0.98 ± 0.02	0.93 ± 0.05
12	PF76TD	CLOISITE 93A	0.5	ACID	85 ± 8	3.4 ± 0.1	2.57 ± 0.34	0.67 ± 0.01	0.85 ± 0.07
13	PF76TD	CLOISITE Na+	0.5	ACID	101 ± 7	3.5 ± 0.2	3.02 ± 0.21	0.85 ± 0.02	0.91 ± 0.07
14	PF76TD	RESADIYE	0.5	ACID	94 ± 3	3.5 ± 0.2	2.75 ± 0.37	0.77 ± 0.03	0.89 ± 0.04

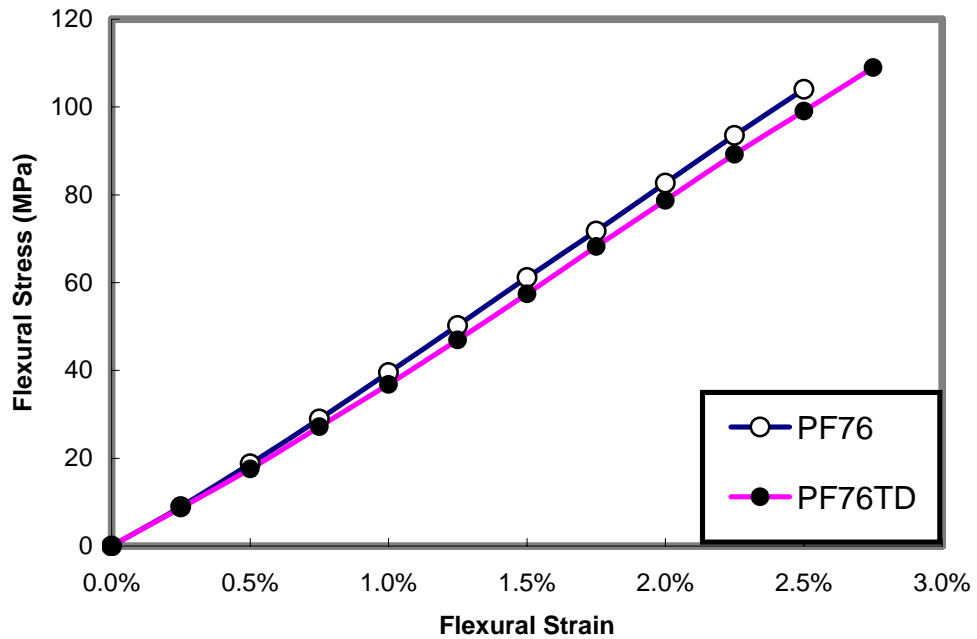


**Figure 3.20** Flexural stress-strain curves of PF76 and PF76TD neat resin specimens produced with acid curing route

As seen in Table 3.6, neat PF76TD, which is the phenolic resin containing ethylene glycol, had higher mechanical properties than PF76 neat resin.

One of the biggest problems of water based phenolic resins is the formation of micro voids of 8-10  $\mu\text{m}$  size during curing of the resin, due to the evaporation of the initially existing water and also the water formed as a by-product of the curing reaction. It is known that these micro voids affect the microstructure of the resins in a negative way.

**Table 3.6** Mechanical properties of the two resol type phenol formaldehyde neat resin specimens produced with acid curing route

<b>Resin Type</b>	<b>Flexural Strength (MPa)</b>	<b>Flexural Modulus (GPa)</b>	<b>Flexural Strain at Break (%)</b>	<b>Charpy Impact Strength (kJ/m<sup>2</sup>)</b>	<b>Fracture Toughness (MPa√m)</b>
PF76	101 ± 7	4.4 ± 0.3	2.38 ± 0.75	0.93 ± 0.10	0.87 ± 0.10
PF76TD	105 ± 7	4.2 ± 0.1	2.78 ± 0.40	1.08 ± 0.14	0.92 ± 0.02

Other than the toughening effect, the addition of MEG and DEG has been reported as a good additive for their behavior as replacement diluents on water loss, which affects micro void formation, distribution and consequently, the mechanical properties. A decrease in void content and increase in density along with a significant improvement in flexural strength and fracture toughness have been observed upon replacement of water with ethylene glycol [39].

These property enhancements, caused by ethylene glycol, are also observed for PF76TD as seen in Table 3.6, and also from SEM fractograph given in Figure 3.7. Furthermore, as stated earlier, curing treatment of PF76TD was also much shorter and easier than it was for PF76. Due to all these reasons, PF76TD was chosen as the matrix resin to be used for the specimen production.

### **3.2.2.2 Effect of Cure Method**

Resol type phenolic resins can be cured by using heat or acid curing agent. As mentioned earlier, whether crosslinking is carried out with or without an agent has an important effect on the properties of the polymer – clay composites. In order to compare mechanical properties of the specimens cured by heat only and by using an acid, one specimen group was tested and evaluated. Flexural stress-strain curves and all mechanical properties of this group (PF76TD resin with 0.5% Cloisite 10A) are given in Table 3.7 and Figure 3.21, respectively.



**Table 3.7** Mechanical properties of heat and acid cured PF76TD resin with 0.5% Cloisite 10A specimens

Cure Type	Flexural Strength (MPa)	Flexural Modulus (GPa)	Flexural Strain at Break (%)	Charpy Impact Strength (kJ/m <sup>2</sup> )	Fracture Toughness (MPa√m)
HEAT	51 ± 6	2.8 ± 0.3	2.24 ± 0.42	0.89 ± 0.03	0.57 ± 0.11
ACID	68 ± 6	3.9 ± 0.1	1.95 ± 0.21	0.83 ± 0.07	0.67 ± 0.05

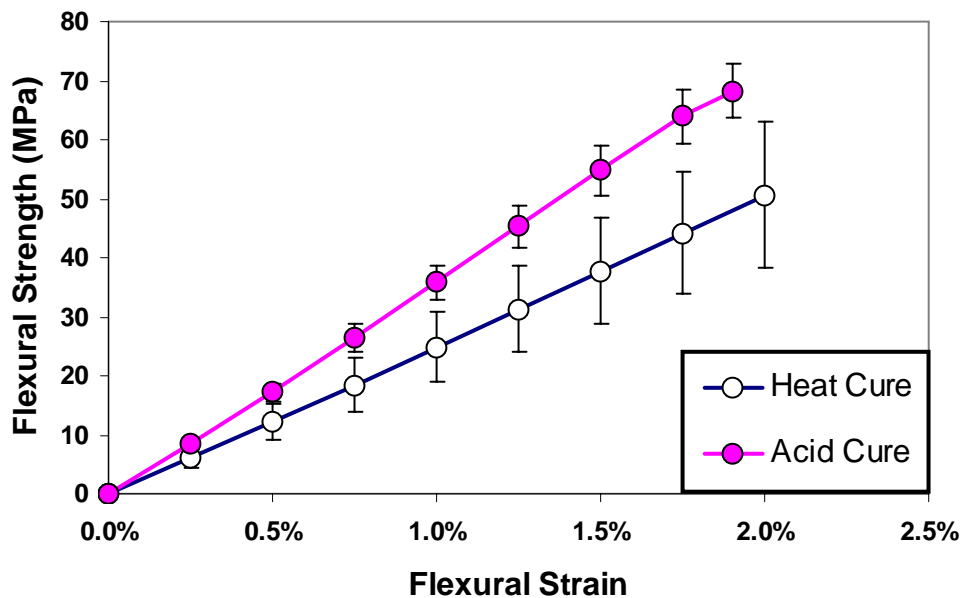


**Figure 3.21** Flexural stress-strain curves of heat and acid cured PF76TD resin with 0.5% Cloisite 10A specimens

When Figure 3.21 is examined, it is seen that the mechanical properties of the acid cured specimens are much better than that of the heat cured ones. This was an expected result, since the prolonged heat treatment schedule of the heat cure route (nearly 3 days), resulted in formation of two different layers on a macroscale, where the clay particles collected at the top layer of the specimen due to their density difference (Figure 3.10(a)). Although the sufficiently long curing

schedule of this route allowed easy water vapor release preventing void formation, non-homogeneous behavior of the layered structure destroyed this advantage. Therefore, acid cured specimens had higher mechanical properties than the heat cured ones.

### 3.2.2.3 Effect of Clay Source

In order to investigate the influences of the clay source, two unmodified montmorillonite clays from two different sources; Wyoming-USA (Cloisite Na+) and Tokat-Turkey (Resadiye) were used. Flexural stress-strain curves of the specimens produced by using 0.5% Cloisite Na+ and Resadiye clays in PF76TD resin are given in Figure 3.22, and all mechanical properties are given in Table 3.8.

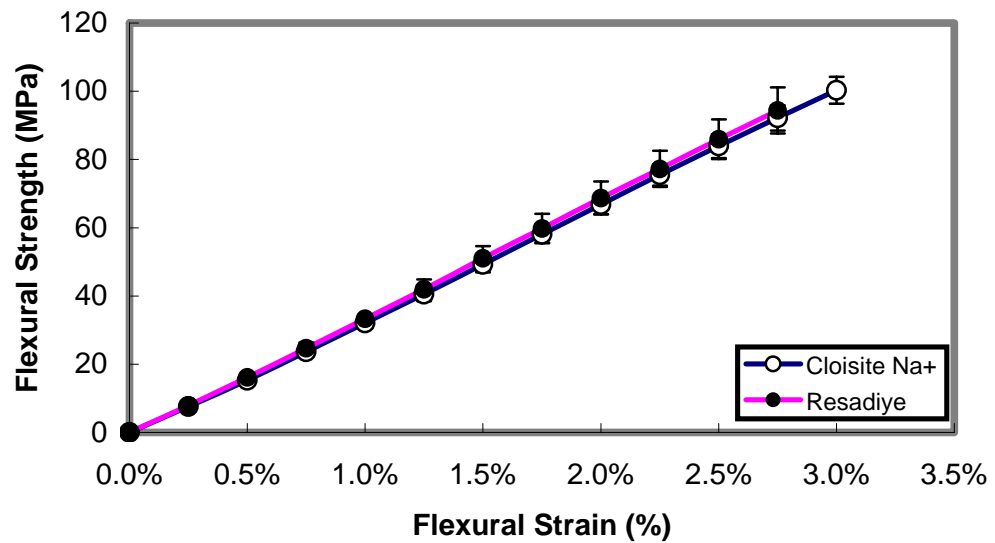


**Figure 3.22** Flexural stress-strain curves of PF76TD resin with 0.5% unmodified Cloisite Na+ and Resadiye clays

**Table 3.8** Mechanical properties of PF76TD resin with 0.5% unmodified Cloisite Na<sup>+</sup> and Resadiye clays

Clay Source	CEC	<i>D</i> (Å°)	Flexural Strength (MPa)	Flexural Modulus (GPa)	Flexural Strain at Break (%)	Charpy Impact Strength (kJ/m <sup>2</sup> )	Fracture Toughness (MPa√m)
CloisiteNa <sup>+</sup> (Wyoming)	92.6	11.7	101 ± 7	3.5 ± 0.2	3.02 ± 0.21	0.91 ± 0.07	0.85 ± 0.02
Resadiye (Tokat)	80	12.6	94 ± 3	3.5 ± 0.2	2.75 ± 0.37	0.89 ± 0.04	0.77 ± 0.03

Clays from different sources, even in cases where they are the same mineral, may have dissimilar properties. This also affects the properties of the clay reinforced composite materials that are produced. The level and distribution of cationic exchange sites, the average size of the platelet stacks and of the individual platelets that comprise them, and the purity level of the clay are among many structural variables that may affect the extent of clay dispersion and the final particle size. Montmorillonites from different origins may especially show significant differences in their CEC's. This is because CEC is highly dependent on the nature of the isomorphous substitutions in the tetrahedral and octahedral layers and therefore on the nature of the soil where the clay was formed [33, 34].

The CEC values of clays influence the behavior of these clays during their modification treatment. Therefore, the difference in CEC values of the Wyoming clay (Cloisite Na<sup>+</sup>) and Tokat-Resadiye clay should not have any significant effect on mechanical properties.

Table 3.8 shows that specimens with Cloisite Na<sup>+</sup> clays had slightly higher mechanical properties than those of specimens with Resadiye clay. These slight differences in flexural strength, flexural strain-at-break, fracture toughness and charpy impact strength may be attributed to the difference in individual clay layer dimensions.

### 3.2.2.4 Effect of Clay Concentration

In order to observe the effects of using different clay concentrations on the behavior of the composite specimens, Rheospan clay was chosen. Specimens with three different clay contents; 0.5, 1 and 1.5wt% were compared with the neat resin specimen designated as 0% clay content. Flexural stress-strain curves and all mechanical properties of those specimens produced by acid curing route of PF76TD resin are given in Figure 3.23 and Table 3.9, respectively. Then, Flexural Strength, Flexural Modulus, Flexural Strain at Break, Charpy Impact Strength and Fracture Toughness of these specimens were discussed in detail in Figure 3.24(a) through 3.24(e).

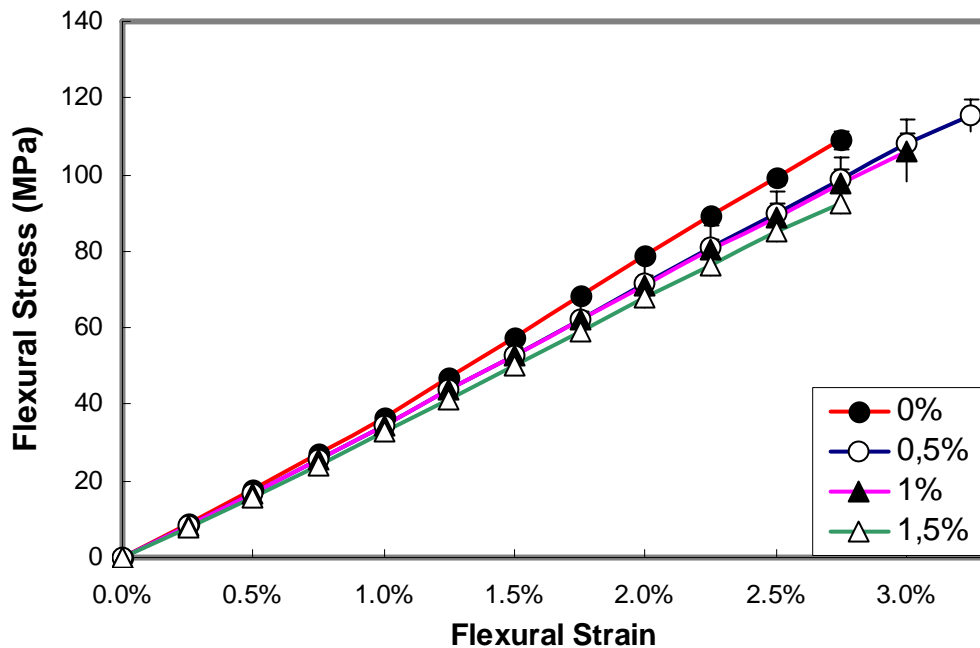


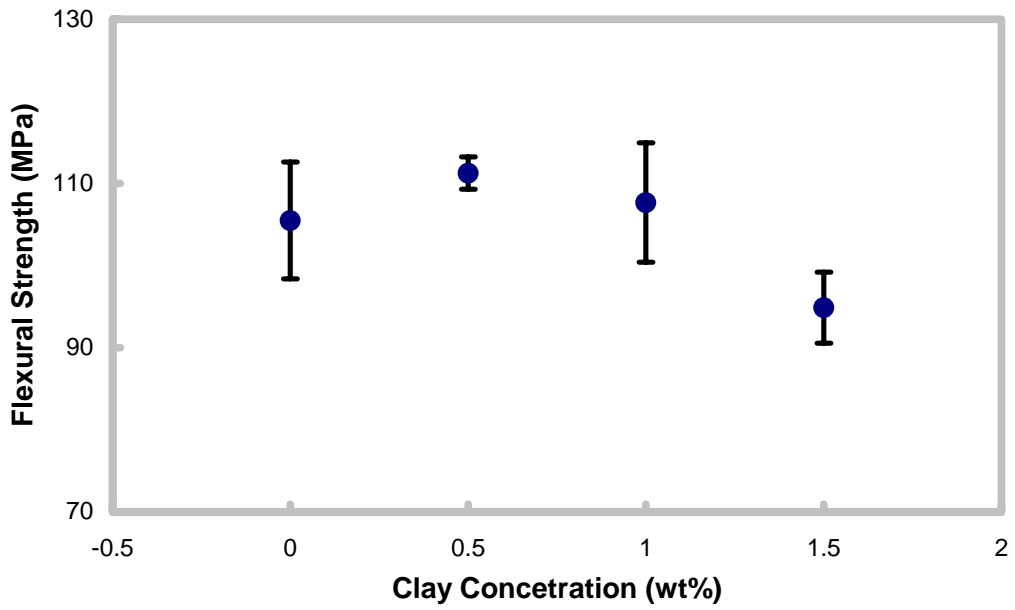
**Figure 3.23** Flexural stress-strain curves of PF76TD resin with 0%, 0.5%, 1% and 1.5% Rheospan clay produced by acid cure route.

**Table 3.9** Mechanical properties of PF76TD resin with 0%, 0.5%, 1% and 1.5% Rheospan clay produced by acid cure route

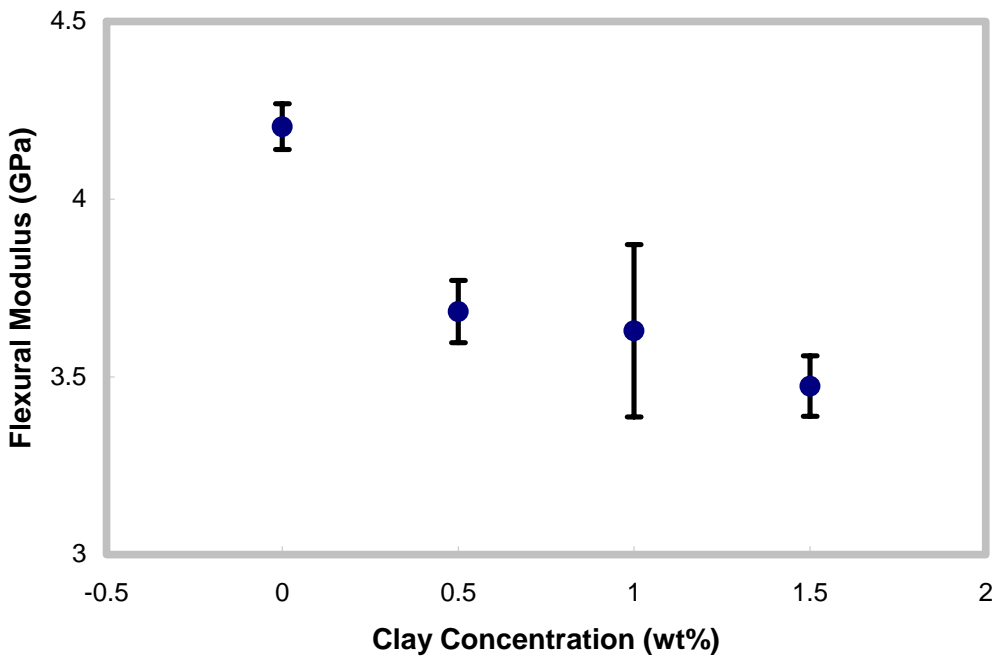
Clay Content (%)	Flexural Strength (MPa)	Flexural Modulus (GPa)	Flexural Strain at Break (%)	Charpy Impact Strength (kJ/m <sup>2</sup> )	Fracture Toughness (MPa√m)
0	105 ± 7	4.2 ± 0.1	2.78 ± 0.40	1.08 ± 0.14	0.92 ± 0.02
0.5	111 ± 2	3.7 ± 0.1	3.08 ± 0.44	1.08 ± 0.06	1.53 ± 0.29
1	108 ± 7	3.6 ± 0.2	3.04 ± 0.16	1.02 ± 0.16	0.73 ± 0.05
1.5	95 ± 4	3.5 ± 0.1	2.80 ± 0.23	1.12 ± 0.15	0.76 ± 0.19

#### (i) Flexural Strength

It is seen from Figure 3.24(a) that flexural strength of the neat resin specimen increases with the use of 0.5% and 1% Rheospan clay where this increase is approximately 6% in the specimen with 0.5% clay, which may be regarded as a limiting value. However, flexural strength decreases for the 1.5% clay specimens. The reason for this behavior may be attributed to the degree of intercalation of the clay layers by the phenolic resin. With low amounts of clay loadings these tasks are more readily achieved, but as clay amount increases, clay layers tend to form tactoids as seen in the SEM fractographs (Figure 3.14 (a, b)). These tactoids, due to their larger size compared to a few nanometers thick clay layers, would act as stress concentration points decreasing the strength of the specimens produced.

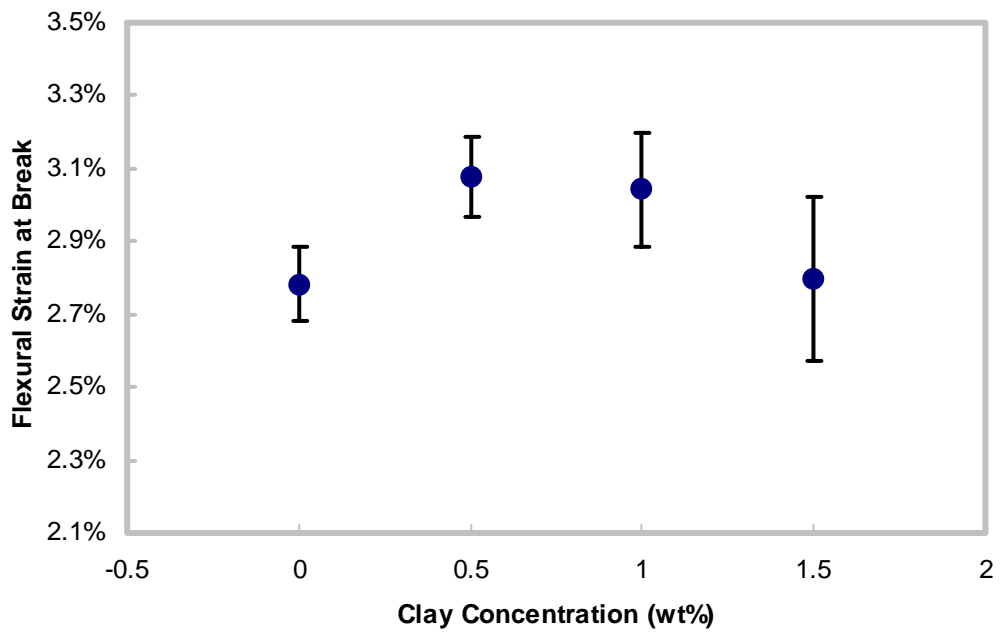


(a)

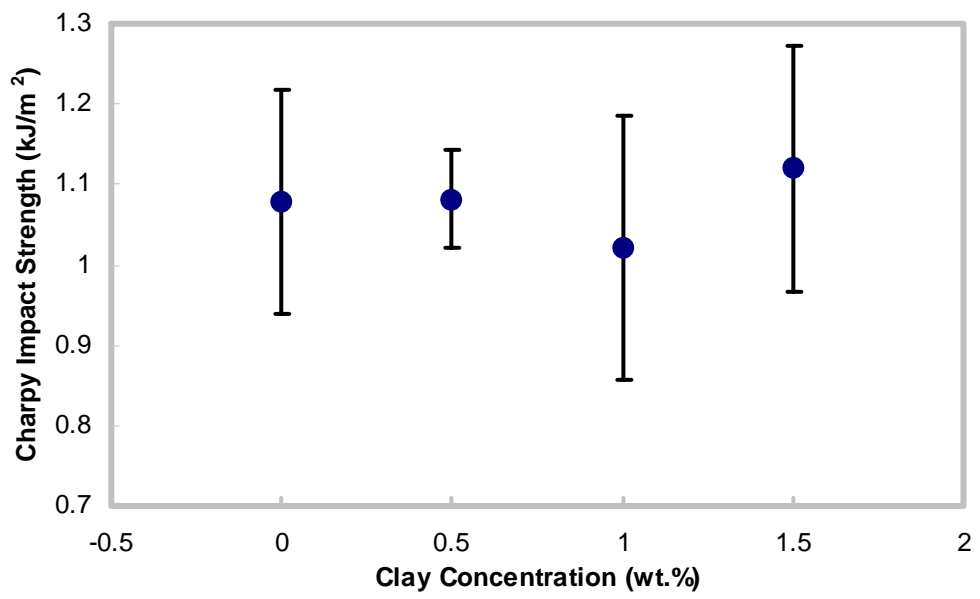


(b)

**Figure 3.24** Effects of Clay (Rheospan) concentration on the mechanical properties of PF76TD resin specimens produced with acid curing route; (a) Flexural Strength, (b) Flexural Modulus, (c) Flexural Strain at Break, (d) Charpy Impact Strength, and (e) Fracture Toughness



(c)



(d)

Figure 3.24 (cont.)

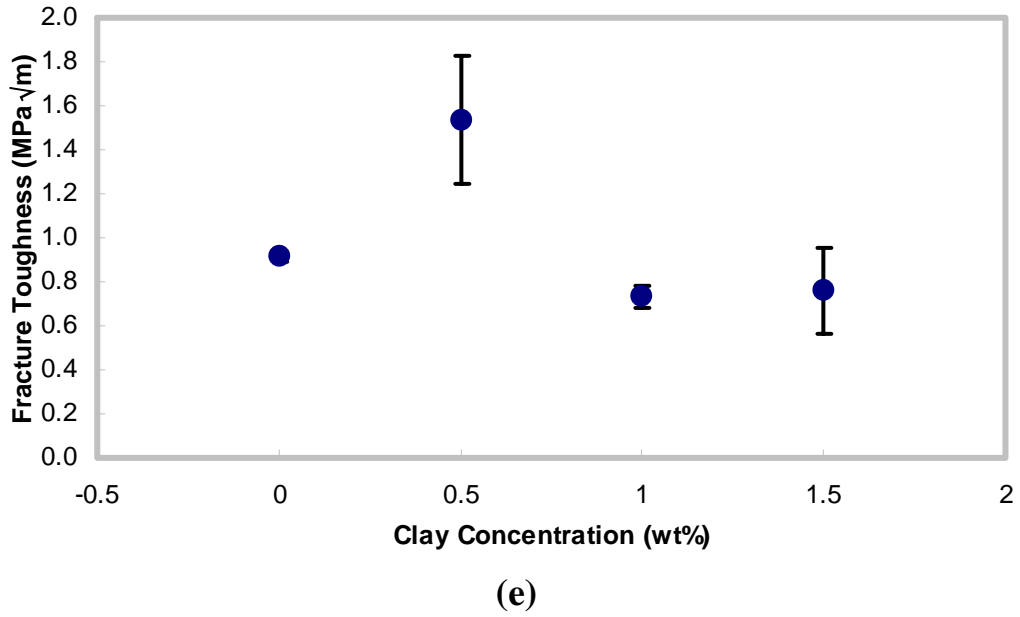


**Figure 3.24** (cont.)

**(ii) Flexural Modulus**

When Figure 3.24 (b) is examined, it is seen that the Flexural Modulus of the specimens decreased slightly with increasing clay content. It is thought that this slight decrease could be due to the toughening mechanisms observed, which will be explained in the subsections below. Clay insertion in the resin caused some stiffness to be sacrificed, but only in expense of higher strength and toughness.

**(iii) Flexural Strain at Break**

The effect of clay concentration on the Flexural Strain at Break values of the specimens is shown in Figure 3.24 (c). It is seen that, flexural strain at break values of the specimens had similar behavior as flexural strength data, having a highest value at 0.5% clay content and then a decreasing trend with the increase of clay content.



#### **(iv) Charpy Impact Strength**

The effect of clay concentration on Charpy Impact Strength is shown in Figure 3.24 (d). Generally, impact tests produce large scattered data compared to other tests. Therefore, it is seen that clay concentration resulted in no significant decreases or increases when their comparably higher standard deviation values are considered.

#### **(v) Fracture Toughness**

Figure 3.24(e) shows that 0.5% Rheospan clay increases the fracture toughness of the neat resin specimen as much as 66%. This increase is the highest improvement achieved in this study, compared to other mechanical properties. Higher clay contents (1% and 1.5%) decreased the fracture toughness values.

For the particulate reinforced composites, there are two basic toughening mechanisms; one is *crack pinning* (in the form of crack bowing or crack deflection) and the other is *crack tip blunting* (in the form of interface debonding and/or particle cracking). It is assumed that propagating cracks can be impeded by rigid, impenetrable and well bonded particles. When a propagating crack encounters such obstacles, it becomes temporarily pinned and tends to bow out between the particles, forming secondary cracks. Thus, it results in increased energy absorption due to not only the creation of the new fracture surface, but also to the formation of the new non-linear crack front. On the other hand, crack tip blunting can take place due to localized shear yielding and damage zones such as debonding of the particle/matrix interface and fracture of particles both leading to large amounts of energy absorption.

At low clay loading (0.5%), mechanical mixing was much more effective for the homogeneous dispersion of the clay particles in the polymer matrix. Consequently, it was easier to intercalate and/or exfoliate the clay layers, which makes the toughening mechanism mentioned above, much more operative.

As the amount of clay increased (1 and 1.5%), due to the homogeneous mixing problems, intercalation and/or exfoliation of the polymer into the clay galleries became much more difficult, leading to a structure with clay tactoids and voids. Therefore, these larger defects acted as stress concentration points rather than crack pinning or blunting sites; resulting in low fracture toughness values.

### **Use of High Clay Concentrations**

In order to observe effects of clay concentration higher than 1.5 wt%, specimens having 3 and 10 wt% were also produced. However, their mechanical properties were not tabulated and not included in the discussions above. The reason is that these specimens had significant problems during their production stage. As it is stated earlier, when clay concentration increases, it is very difficult to prevent clay particles forming agglomerates; especially when the specimens are produced via casting and mechanical mixing methods. Specimens having 3% clay had the problem of clay agglomeration and the specimens having 10% clay had high amounts of void formation and the structure resembled foam.

In literature it is indicated that clay insertion into the polymer matrices have been most effective with very low filler amounts; and to produce phenolic resin/clay nanocomposites having higher clay concentrations, a different production method which involves hot pressing of solid resin particles together with clays has been used [30, 31].

### 3.2.2.5 Effect of Clay Modification

Modification of clay minerals for the purpose of achieving better compatibility at the clay-polymer surfaces is a very frequently applied method in the polymer / layered silicate studies in literature. For the polymer to have the ability to wet the clay layers, the surfaces of both of these components should be chemically compatible with each other. This compatibility depends highly on the polarities of the two components. Clays are normally polar structures; i.e. their structure has two poles or electrostatically opposite regions. Isomorphous substitution within the layers provide negative charges ( $\text{Al}^{+3}$  replaced by  $\text{Mg}^{+2}$  or by  $\text{Fe}^{+2}$ , or  $\text{Mg}^{+4}$  replaced by  $\text{Li}^{+}$ ) and the cations in the interlayers ( $\text{Na}^{+}$  or  $\text{Ca}^{+2}$ ) provide the positive charges. A solvent with a similar polar structure is water. It is due to this reason that the clay is compatible with water; or in other words, water can dissolve clay in it. That is why clay is accepted as a **hydrophilic** material.

Normally, most of the polymers are hydrophobic, i.e. they do not have polar structures, and thus they lead to incompatibility with the hydrophilic clays. That is why clays are modified to make them more hydrophobic, with less polar structures, by taking away the positive ions in the clay galleries and replacing them with bulky alkylammoniums. This modification treatment may have three different positive effects on the polymer – clay interaction. It may influence the compatibility by:

- i) Changing the hydrophobicity of the clay, causing the clay layers to have similar polarities with the matrix polymer
- ii) Increasing the interlayer distance ( $d$ ) of the clay layers, which provides a larger space for the polymer to intercalate into
- iii) Providing functional groups that may either react with the polymer matrix or facilitate the polymerization reaction.

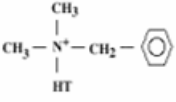
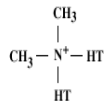
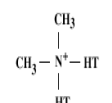
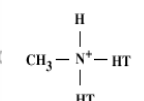
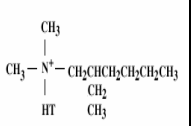
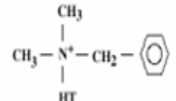
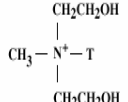
In order to observe the effects of using different modifiers on the behavior of the phenol formaldehyde / Na-montmorillonite composite specimens of PF76TD

resin with 0.5 wt% of two different unmodified clays (Resadiye and Cloisite Na+) and seven different organoclays (Rheospan and Cloisite 10A, 15A, 20A, 25A, 30B, 93A) were produced and tested. All the mechanical properties determined for these specimens, together with interlayer spacing and modifier type of the clays used are given in Table 3.10. In the following sections, three effects of the clay modification mentioned above will be discussed according to these data.

### **(i) Effect of Clay Surface Hydrophobicity**

As explained earlier, for the polymer and the clay to be compatible, their hydrophobicity level should be similar. Relative surface hydrophobicity levels of the Cloisite clays are given in Figure 3.25. According to this data, which is provided from the producer *Southern Clay Products*, unmodified Na-montmorillonite clay Cloisite Na+ has the lowest hydrophobicity level and quarternary ammonium modified Cloisite 15A has the lowest hydrophilicity level. For the levels of hydrophobicities of Resadiye and Rheospan clays, due to the lack of product data, only estimated levels were tabulated on the same diagram; taking especially their *d*-spacing values as a reference. The effect of clay surface hydrophobicity on mechanical properties of the produced specimens is given in Figure 3.26. For comparison, values for the neat PF76TD resin are also indicated in the inset of these figures.

**Table 3.10** Interlayer spacing and modifier types of the clays used together with the mechanical properties of PF76TD resin reinforced with 0.5wt% of these clays

Clay	Interlayer Distance (nm)	Modifier Type	Flexural Strength (MPa)	Flexural Modulus (GPa)	Flexural Strain at Break (%)	Fracture Toughness (MPa√m)	Charpy Impact Strength (kJ/m <sup>2</sup> )
Resadiye	12.6	-	94 ± 3	3.5 ± 0.2	2.75 ± 0.37	0.77 ± 0.03	0.89 ± 0.04
Cloisite Na+	11.7	-	101 ± 7	3.5 ± 0.2	3.02 ± 0.21	0.85 ± 0.02	0.91 ± 0.07
Rheospan	26.0		111 ± 2	3.7 ± 0.1	3.08 ± 0.44	1.53 ± 0.29	1.08 ± 0.06
Cloisite 15A	31.5		98 ± 5	4.5 ± 0.5	2.23 ± 0.55	1.08 ± 0.26	0.80 ± 0.06
Cloisite 20A	24.2		92 ± 8	3.6 ± 0.3	2.66 ± 0.52	1.00 ± 0.07	0.73 ± 0.05
Cloisite 93A	23.6		85 ± 8	3.4 ± 0.1	2.57 ± 0.34	0.67 ± 0.01	0.85 ± 0.07
Cloisite 25A	20.6		92 ± 12	3.4 ± 0.1	2.89 ± 0.81	0.79 ± 0.14	0.70 ± 0.03
Cloisite 10A	19.2		68 ± 6	3.9 ± 0.1	1.95 ± 0.21	0.67 ± 0.05	0.83 ± 0.07
Cloisite 30B	18.5		67 ± 8	3.3 ± 0.4	2.01 ± 0.11	0.98 ± 0.02	0.93 ± 0.05

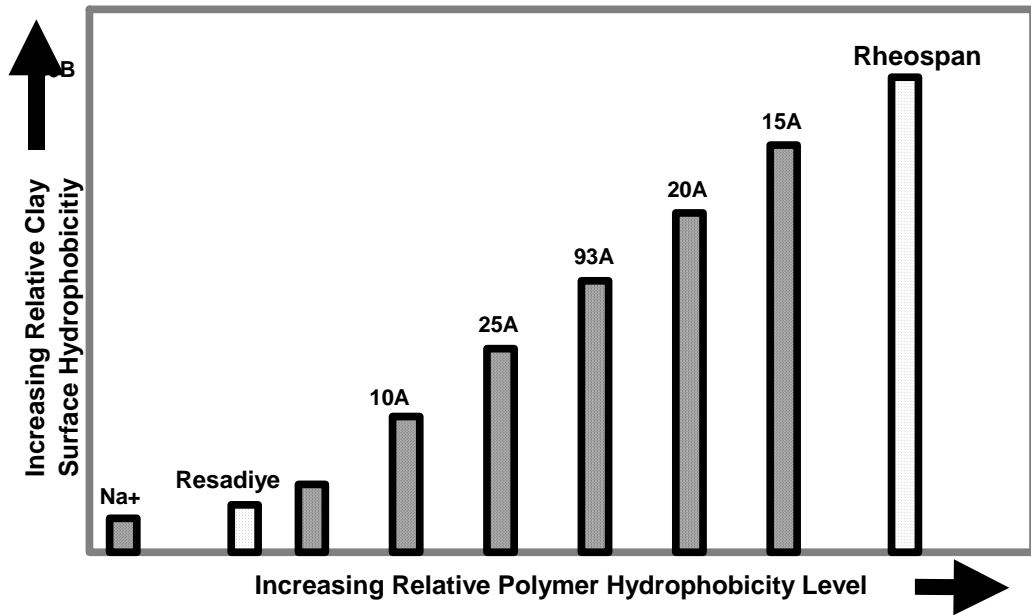
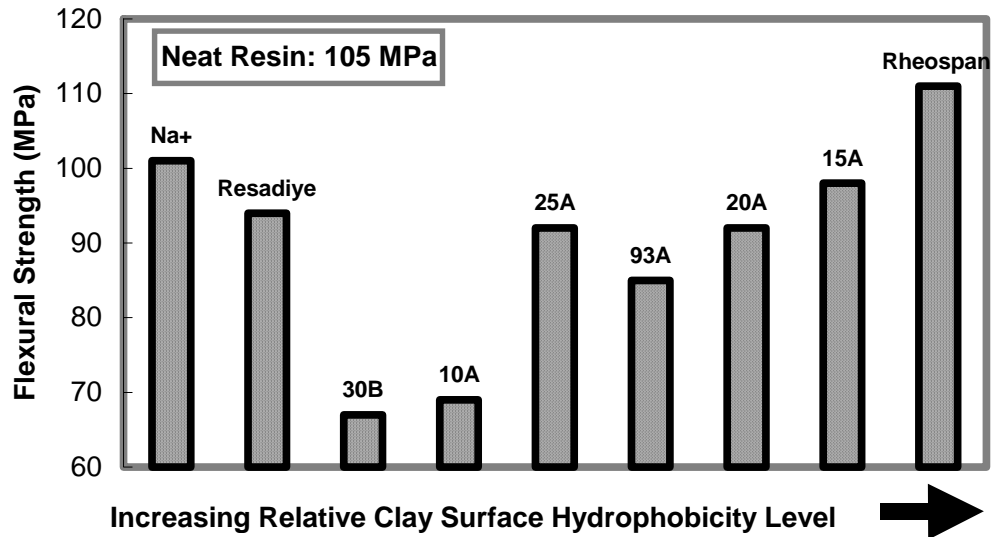
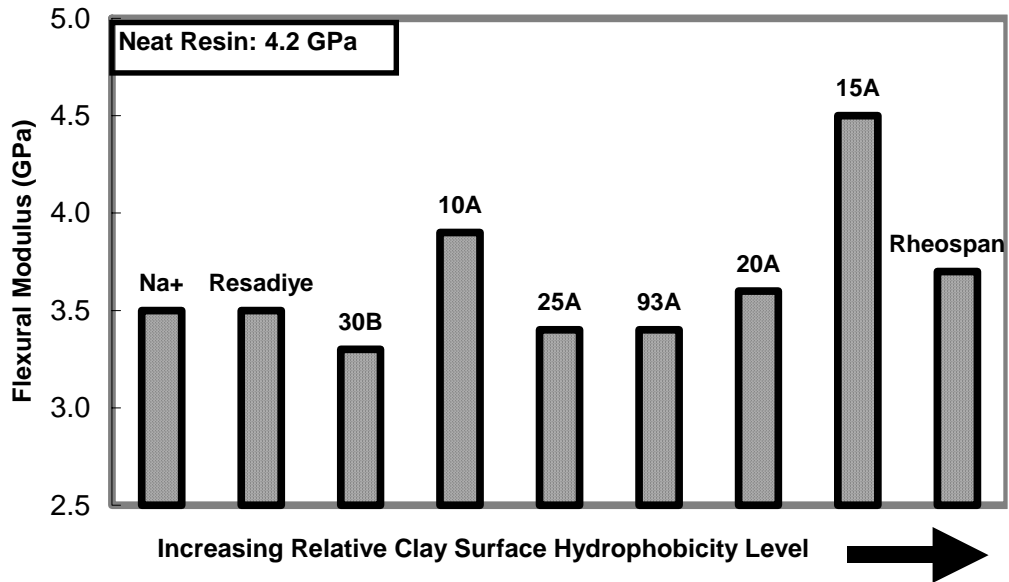


**Figure 3.25** Relative hydrophobicity levels of the Cloisite clays (provided by SCP), and the estimated levels for Resadiye and Rheospan clays.

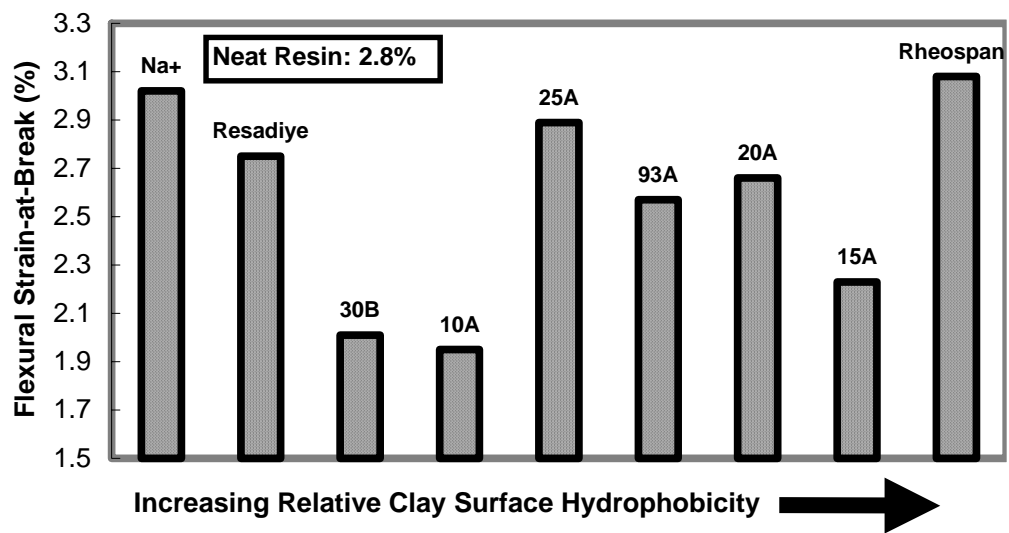


(a)

**Figure 3.26** Effect of increasing relative clay surface hydrophobicity level on (a) Flexural Strength, (b) Flexural Modulus, (c) Flexural Strain-at-Break, (d) Fracture Toughness, (e) Impact Toughness of the composite specimens. Note that the values in the insets are for the neat PF76TD resin.

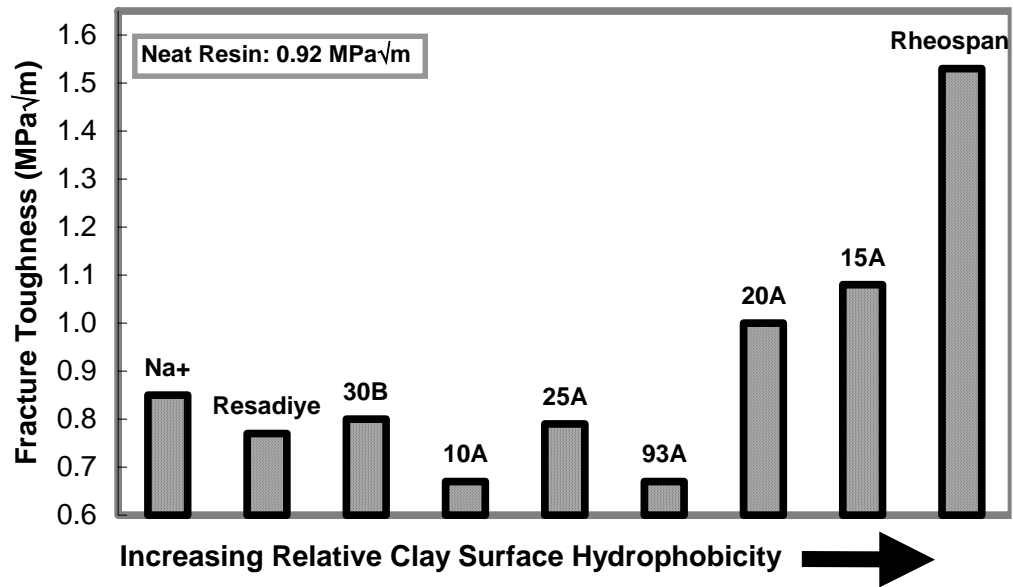


(b)

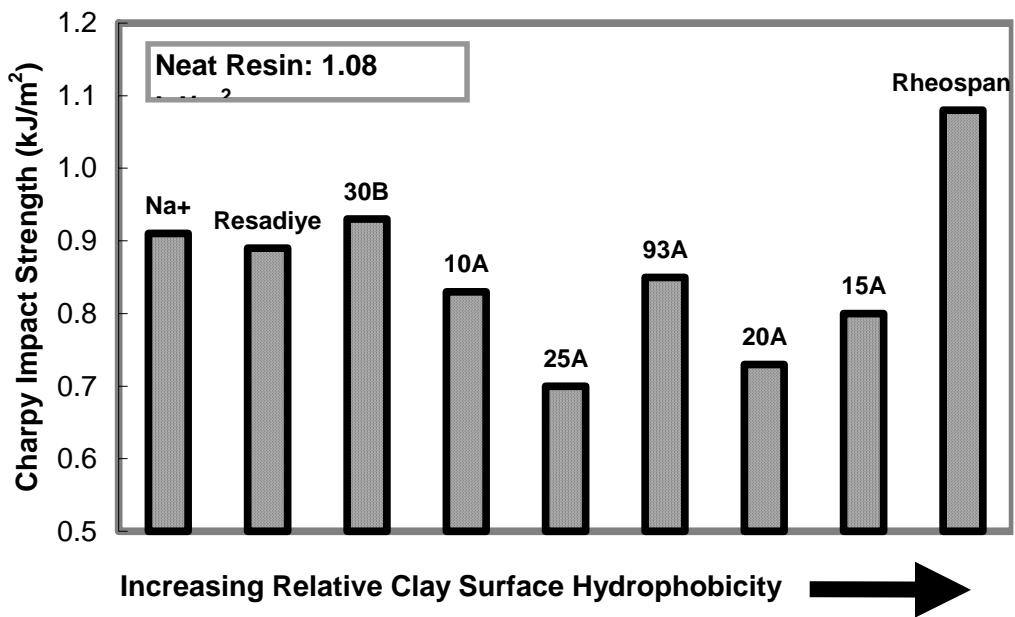


(c)

Figure 3.26 (cont.)



(d)



(e)

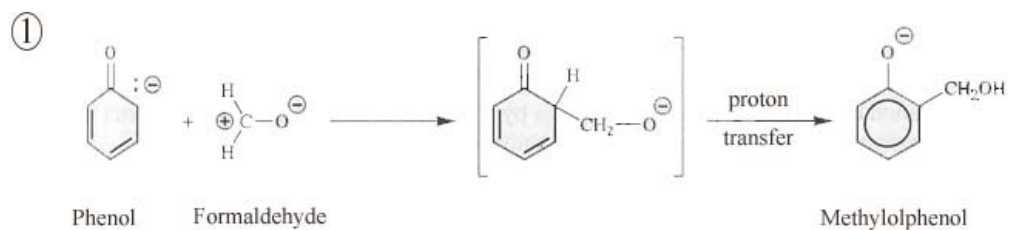
Figure 3.26 (cont.)



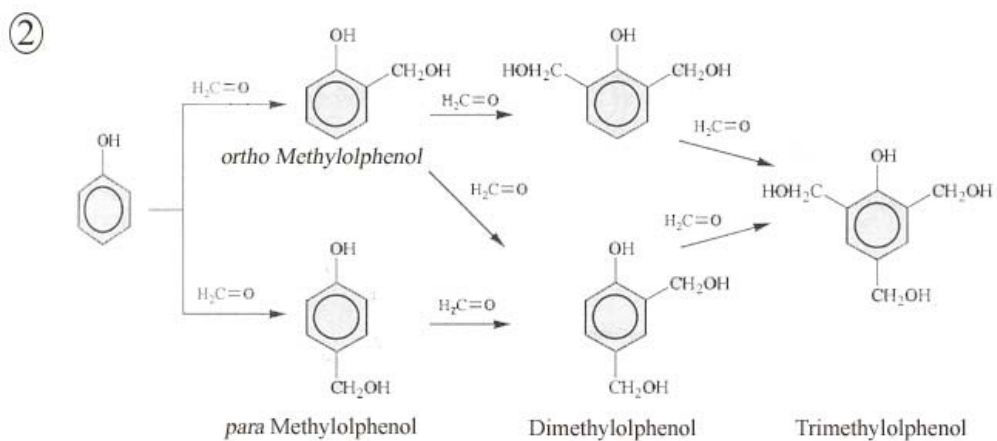
Figure 3.26 shows that, mechanical properties of the specimens reinforced with the clays having relatively high hydrophobicity levels (e.g. Rheospan and Cloisite 15A) were improved compared to the neat resin specimens. This improvement was for example ~6% in Flexural Strength, ~11% in Flexural Strain at Break, and ~66% in Fracture Toughness for the specimens with Rheospan clay, having relatively high hydrophobicity level. For the specimens with Cloisite 15A, which is another clay having relatively high hydrophobicity level, these improvements were ~7% in Flexural Modulus, and ~16% in Fracture Toughness.

In the specimens with other organoclays (Cloisites 30B, 10A, 25A, 93A, 20A) having relatively lower hydrophobicity levels, mechanical properties were not improved compared to the values of neat resin specimens. Figure 3.26 also shows that, specimens with unmodified clays (Cloisite Na<sup>+</sup>, Resadiye) having relatively the lowest hydrophobicity level, generally had higher mechanical properties compared to the specimens with other organoclays (Cloisites 30B, 10A, 25A, 93A, 20A), but still lower values compared to neat resin specimens. This unexpected result could be due to the changes in the microstructure of the polymer matrix that occur during the crosslinking reaction. The steps of the curing reaction between phenol and formaldehyde are given in Figure 3.27.

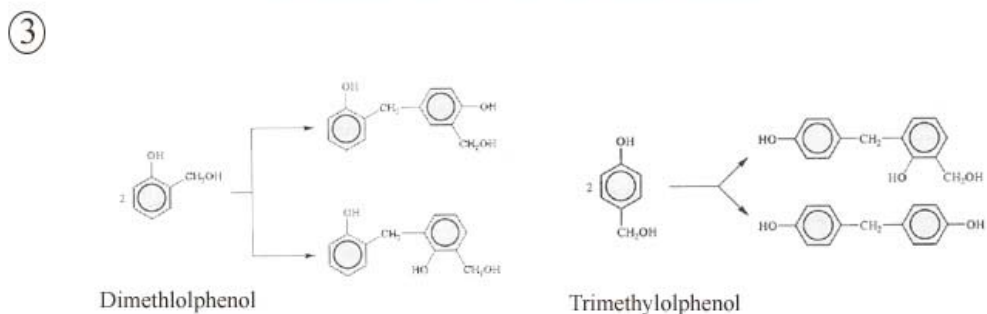
As shown in the figure, when phenol anion is added to formaldehyde either *ortho* or *para* methylolphenols form. Since phenol is very reactive, the reaction continues and di- and tri- methylolphenols occur rapidly. As reaction further continues, methylolphenols condense with each other to form methylene bridges. This occurs for both *para* and *ortho* substituted methylolphenols. A typical liquid resol is quite low in molecular weight, i.e. it contains no more than two or three benzene rings. If the reaction is carried further, condensation yields a solid structure via crosslinking [40].



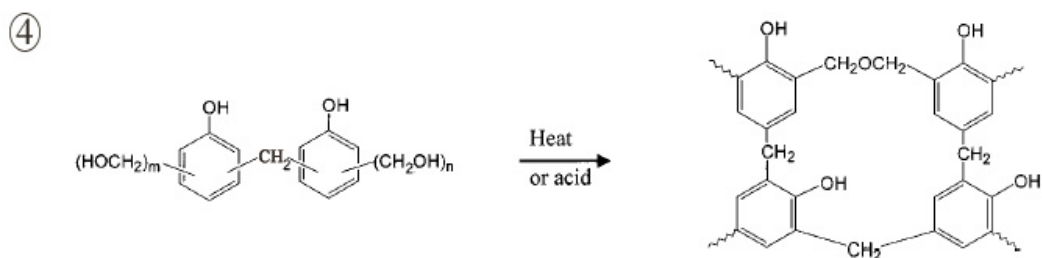
**Addition of Phenol to Formaldehyde**



**Formation of Di- and Tri- Methylolphenols**



**Methylene Bridge Formation**



**Crosslinking Reaction**

**Figure 3.27** Curing reaction steps between phenol and formaldehyde [40, 35]

The critical point in the curing reaction of this study was the changes in the polarity of the resin. At the beginning of the cure (Figure 3.27, step 3), the hydrophobicity of the resin was very low due to the high number of methylol groups, which have a polar structure. However, as the crosslinking reaction proceeds these methylol groups were lost, which results in the formation of a nonpolar, thus hydrophilic resin structure. This might be interpreted as the better compatibility of the hydrophilic clays (e.g. Cloisite Na<sup>+</sup> and Resadiye) at the initial stages of resin curing; and better compatibility of the hydrophobic clays (e.g. Rheospan and Cloisite 15A) especially at the final stages of resin curing; both leading to some degree of intercalation and/or exfoliation. Relatively high mechanical properties of unmodified hydrophilic clays (Figure 3.26), when compared to more hydrophobic clays (Cloisites 30B, 10A, 25A, 93A, 20A), are thought to be due to higher degrees of intercalation occurring at the initial stages of curing reaction.

#### **(ii) Effect of Clay Interlayer Spacing**

The interlayer thicknesses of all the clays used are given in Table 3.10. It is seen that, modification treatment increases the interlayer spacing significantly. The interlayer spacing of unmodified clays Cloisite Na<sup>+</sup> and Resadiye are 11.7 and 12.6 nanometers, respectively. However, after modification *d*-spacing may increase up to 31.5 nm as indicated for Cloisite 15A.

Hydrophobicity is the degree of polarity of the molecules; and the polarity increases with increasing clay gallery distance. It is due this fact that *d*-spacing of the clay layers are directly related to the clay surface hydrophobicity (Figure 3.28). Therefore, this correlation shown in Figure 3.28 will be also valid for the correlation between the clay interlayer spacing and the mechanical properties of the specimens given in Figure 3.26.

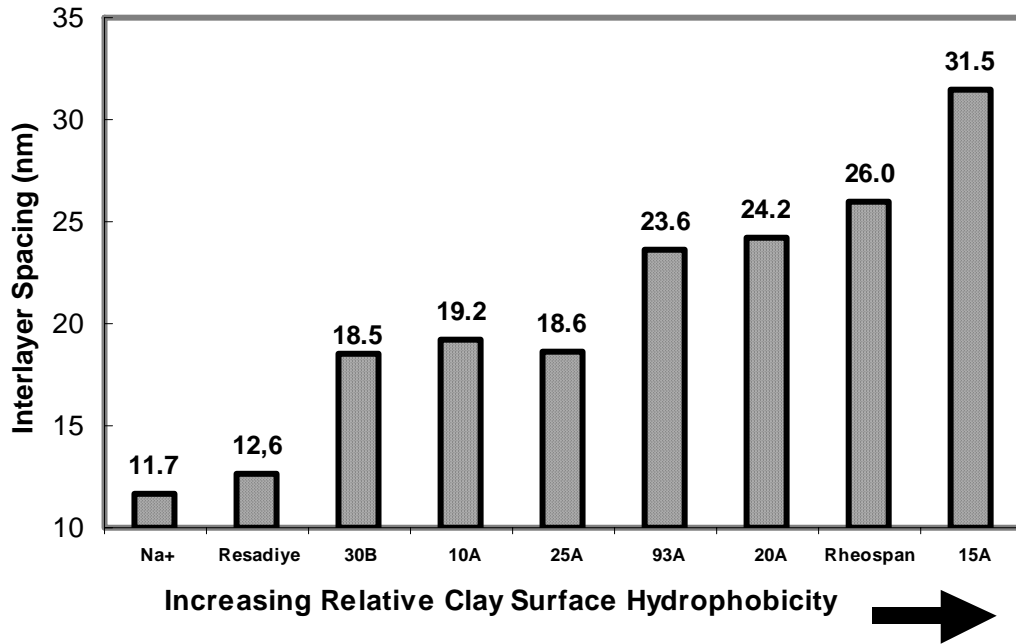


**Figure 3.28** Correlation between the clay interlayer spacing and their relative surface hydrophobicity levels

The increase in the interlayer distance is related closely to the size of the modifier; since as the size of the modifier molecules increases, the interlayer distance also increases. Such an increase in interlayer distance affects polymer intercalation positively. However, inserting large molecules in between the clay layers has also an opposing effect on intercalation. When relatively larger molecules reside in between the clay layers, then the polymer may not have enough space to intercalate into. It is due to these two opposing effects that, the modifier should have an optimum size; opening the clay layers sufficiently while not hindering the polymer intercalation.

Therefore, the high performance of the specimens at low gallery distance may be attributed to the small modifier size not hindering the polymer intercalation; whereas the high performance at high gallery distances may be attributed to the large modifier molecule providing a high interlayer gallery for the polymer to intercalate into.

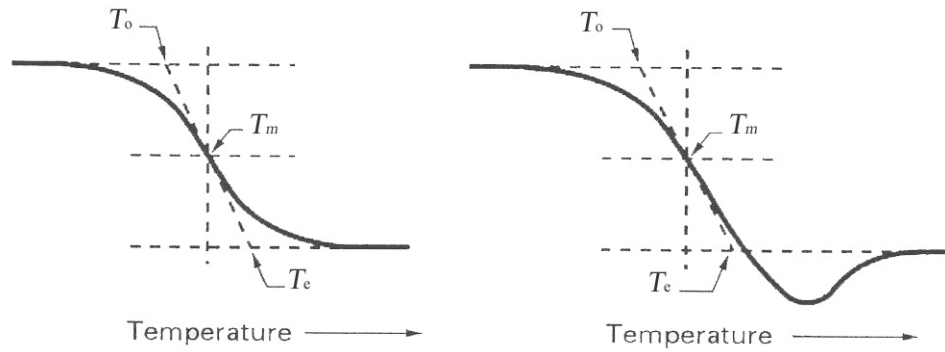
### **(iii) Effect of Using Curing Catalysts**

A helpful approach to improve intercalation cited in the literature [21, 31] was to place catalyst molecules in between the clay galleries. With such an approach, the rate of polymerization in between the galleries becomes much faster than those outside the clay layers; which means intercalation occurs efficiently. The clays used in this study were purchased in chemically modified condition; and neither of the modifier chemicals were catalysts for the polymerization reaction of resol type phenolic resins. This approach will be considered in further studies.

### 3.2.3 Thermal Analysis

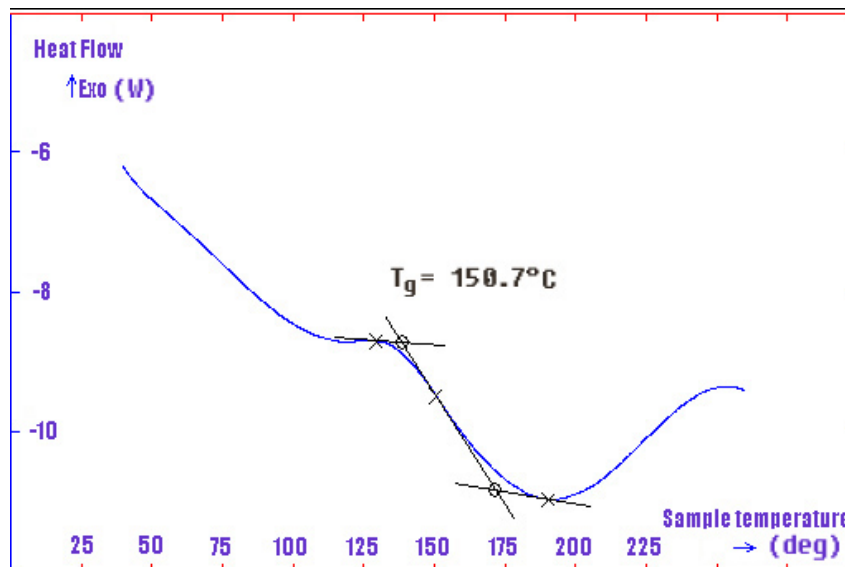
In this study, in order to observe the effect of clay loading on the thermal behavior of the specimens, Differential Scanning Calorimetry (DSC) experiments were carried out. In DSC, the difference between the heat flux into a test specimen and that into a reference specimen is measured as a function of temperature and/or time, while the test specimen and the reference specimen are subjected to a controlled temperature program under a specified atmosphere [41]. The glass transition of polymers is observed by DSC as an endothermic step in the heat capacity of the sample, and the glass transition temperature is the approximate midpoint of the temperature range over which the glass transition takes place. The determination of glass transition temperature by this method is carried out as shown in Figure 3.29. Here,  $T_o$  refers to the onset temperature and  $T_e$  refers to the end temperature.  $T_m$ , the midpoint temperature, is the point at which the curve is intersected by a line that is equidistant between the two extrapolated baselines.

Thermal stability is one property that phenol formaldehyde is almost unrivalled among other polymers, which gives rise to its wide use as a thermal insulation material. Thus, it is difficult to properly observe the effect of clay loading on the thermal properties of the resol type resin. The studies in the literature show that the insertion of low amounts of clay generally improves thermal properties of thermosetting resins; such as glass transition temperature or thermal degradation temperature, flame resistance and thermal stability [42]. However, the works on phenol formaldehyde resin based nanocomposites have shown that it was not the case. As the phenolic resin had almost awesome thermal properties before addition of clay; the composites did not have much improvement on thermal properties [23, 30]; although some groups have observed slight improvements in  $T_g$  values [31].



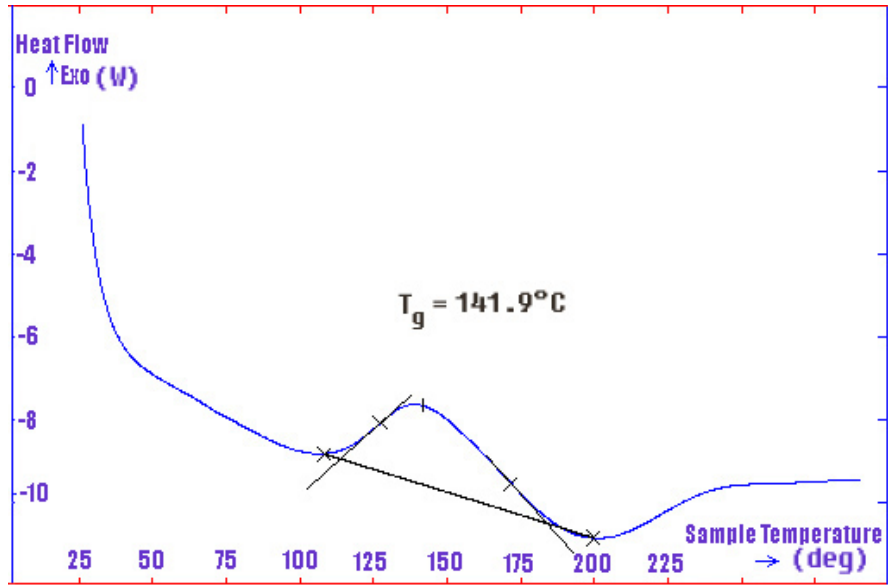
**Figure 3.29** Two typical examples of glass transition temperature determination [41]

Figure 3.30 gives the DSC curves of three specimens chosen for this purpose; neat PF76TD resin specimen and the composite specimens containing 0.5 and 1.5 % Rheospan clay. Then, in Figure 3.31, their DSC curves are drawn on the same chart for comparison. The influence of two parameters can be observed in these figures, as discussed below.

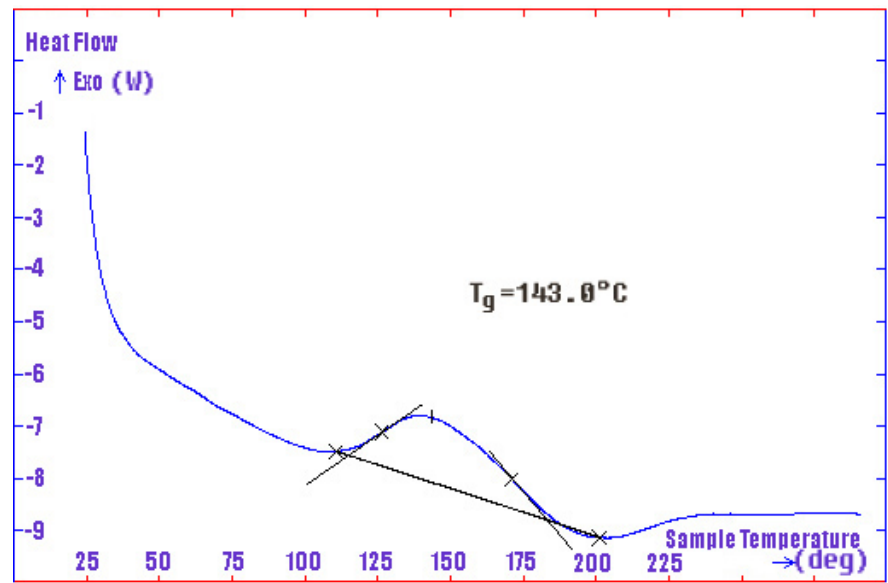


(a)

**Figure 3.30** DSC curves of PF76TD resin specimens with (a) no clay content (b) 0.5% and (c) 1.5% Rheospan clay. Note that the  $T_g$  calculations were carried out by the software of the equipment.



(b)



(c)

Figure 3.30 (cont)



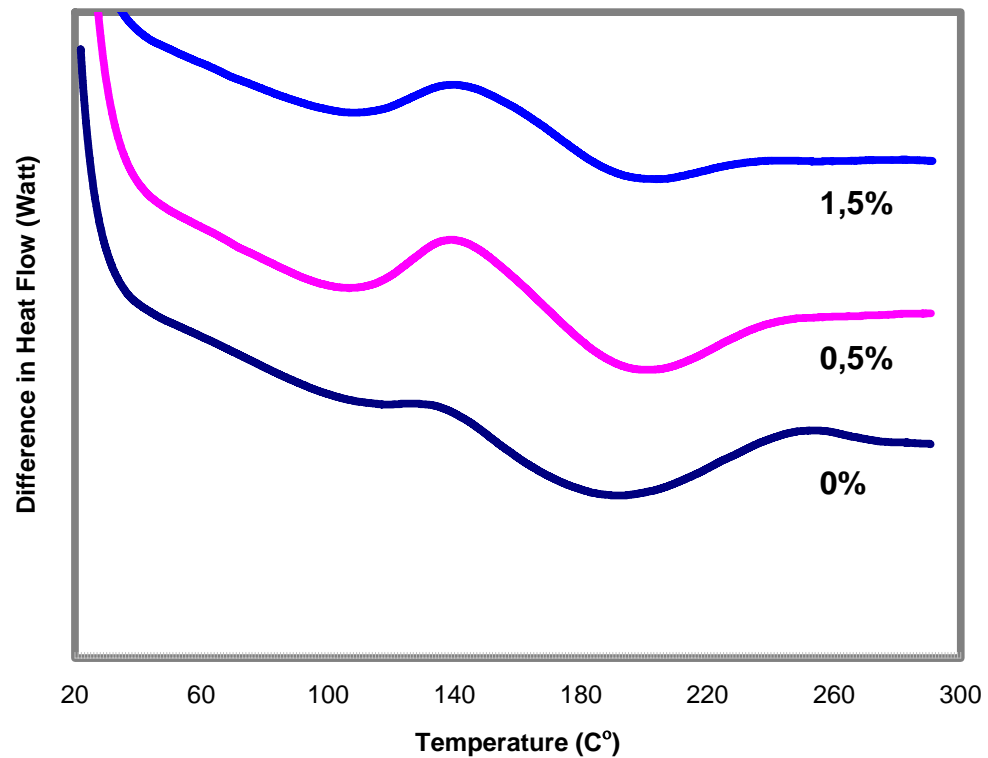


**Figure 3.31** Comparison of the DSC curves of three acid cured PF76TD resin specimens of increasing Rheospan clay concentration. Y-axis values of the specimens has been modified for easy comparison of the curves

#### (i) Effect of Clay Content

Figure 3.30(a) shows that the glass transition temperature of the resol type phenol formaldehyde resin specimen is around 150°C. When 0.5% Rheospan clay was added to the matrix (Figure 3.30(b)), the glass transition temperature shifted to 142°C, and when the clay amount was further increased to three times this value (Figure 3.30(c)), it was observed at 143°C. It is stated in literature that  $T_g$  determinations of thermosetting resins have rather large scattering range [43]. Thus, the shift of the glass transition peak from 150°C to 143° C could be regarded within the scattering range of the experiment. Therefore, it can be concluded that, use of 0.5 or 1.5% Rheospan clay has no significant effect on the glass transition temperature of PF76TD resin.

## **(ii) Effect of Degree of Crosslinking**

In thermosetting resins one of the most important parameters is *degree of crosslinking*; as it is highly effective on the final mechanical properties of the resin. As the degree of crosslinking increases, the macromolecules of the resin are more strongly connected to each other, due to the formation of a network of covalent bonds. However, decrease in the degree of crosslinking results in relatively lower mechanical properties; due to the less covalent bonds present. In polymer / layered silicate specimens, the degree of crosslinking may be affected when a clay phase is present during curing.

Figure 3.30 (b) and (c) show that, specimens with 0.5 and 1.5% clay have certain exothermic peaks at the onset of glass transition. This might be due to the rather incomplete crosslinking of these specimens. On the other hand neat resin specimen (Figure 3.30 (a)) had no similar exothermic peak. It can therefore be interpreted that crosslinking was nearly complete for the neat resin specimen.

## CHAPTER 4

### CONCLUSIONS

After comparing the effects of several different production parameters on the microstructural morphology, mechanical properties and thermal properties of the specimens produced, the following conclusions were drawn:

#### (A) Production of the Specimens

##### (i) Curing Stage

- Since the phenolic resins used were water based and since the condensation polymerization reaction occurring during curing also produces water; the biggest problem in the curing of the resin was the formation of microvoids in the final microstructure. With *heat curing* this problem could be overcome, by keeping the gel time long enough for the slow water vapor release to occur completely, preventing microvoid formation.
- However, heat curing required very long heating schedules (as long as 3 days) leading to formation of separate clay-rich and resin-rich layers due to the density differences.
- In acid curing route crosslinking was much quicker (4 hours), preventing the agglomeration or phase separation of the clay.
- Ethylene glycol modified resol type phenolic resin PF76TD was much easier to cure. The required cure cycle was much shorter than that for PF76. Macro and micro void formation was less likely; and even when formed, these voids were smaller in size compared to those formed in PF76.

(ii) Mixing Stage

- Mechanical mixing of the two constituents was most effective when it was carried out in increasing steps of 50, 100 and 150 rpm at a temperature of 55°C. Slower rates resulted in insufficient mixing while faster rates increased the amount of air getting trapped in the resin.
- Ultrasonic mixing was observed to be necessary in obtaining a more homogeneous mixture of the two constituents. It was most effective at 55°C for a period of one hour.

**(B) Characterization of the Specimens**

(i) X-ray Diffraction Analysis

- XRD diffractograms showed that the layered structure of the Rheospan clay had been dismantled and the peak at around  $2\theta=3.4^\circ$  has been lost when it was used in the composites specimens. This might be interpreted as the occurrence of exfoliation.
- Intensity of XRD peaks increased with the increase in the clay content of the specimens.
- Using bulk XRD specimens resulted in lower intensity peaks compared to those obtained from powder specimens. However, use of powder form has the possibility of destruction of the layered silicate structure during grinding which may lead to improper results.

(ii) Electron Microscopy Analysis

- SEM analysis showed that specimens of both phenolic resins contained micro voids. But, neat PF76TD specimens contained finer and less amount of micro voids compared to neat PF76 specimen.
- With the clay addition, micro void density decreased significantly.
- Clay addition also increased the fracture surface roughness of the specimens considerably indicating a higher amount of energy absorption during cracking and fracturing.
- Although heat cured specimens had relatively low amount of micro voids, there was the problem of clay-rich and resin-rich layer formation. This problem was not observed in acid cured specimens.
- Type of clay modification influenced the compatibility at the clay polymer interface. Some of the modified clays (e.g. Cloisite 15A and Rheospan) showed much better compatibility compared to others (e.g. Cloisite 10A and Cloisite 30B).
- SEM fractographs also showed that several polymer toughening mechanisms were effective in compatible clay-polymer systems. These mechanisms increased the fracture toughness of the specimens mainly by decreasing the rate of crack propagation.
- TEM analysis revealed that clay intercalation might have occurred especially in the specimens with Rheospan clay. TEM micrographs showed that clay interlayer distance increased from 26 nm up to 40-80 nm.

(iii) Mechanical Tests

- 3-point bending, fracture toughness and Charpy impact test results showed that neat PF76TD specimens, which is the phenolic resin having some amount of ethylene glycol, had much better mechanical properties than neat PF76 resin specimens.

- Acid cured composite specimens, although they contain some amount of micro voids, were much stronger and tougher than the heat cured specimens having separate clay-rich and resin-rich layers due to their very long cure cycle.
- Mechanical properties of unmodified Na-montmorillonite clays of different sources (Cloisite Na<sup>+</sup> and Resadiye) were approximately the same.
- Flexural strength, flexural strain at break, Charpy impact strength and fracture toughness of the composites specimens were the highest when the clay concentration was 0.5wt%. Above 1% these properties started to decrease. The reason for this behavior was attributed to the degree of intercalation of the clay layers by the phenolic resin. At low clay loadings intercalation could be more readily achieved while increasing clay contents resulted in the formation of clay tactoids.
- Either very hydrophobic (Rheospan and Cloisite 15A) or very hydrophilic (Cloisite Na<sup>+</sup> and Resadiye) clays were most compatible with the resol type phenolic resin. This was thought to be due to the altering hydrophobicity of the resin during the crosslinking reaction. The polymer resin, being hydrophilic at the initial stages of curing, was compatible with hydrophilic clays; and being hydrophobic at the final stages of curing, was compatible with hydrophobic clays.
- The highest improvement in the mechanical properties of the composite specimens obtained was the 66% increase in fracture toughness.

(iv) Thermal Analysis

- DSC curves revealed that there was no significant effect of clay on the glass transition temperature of the composite specimens.

## CHAPTER 5

### FURTHER STUDIES

The research carried out in this work can be further studied by investigating the following topics:

#### **Modification of Resadiye Clay**

In this present study Reşadiye bentonite was purified to yield pure Na-montmorillonite, which was then used as an unmodified clay reinforcement in the polymer resin. A further study can be carried out on modification of Reşadiye clays using different modifiers. Modified Na-montmorillonite clays can then be placed in different resins and characterized using the same methods used in this study. By comparing the properties of modified Resadiye clay reinforced nanocomposites with others in the literature, the applicability of the approach can be revealed.

#### **Flammability of Phenolic Resin / Layered Silicate Nanocomposites**

Phenolic resins have wide applications due to their high thermal properties. The resol type resins used in this study, PF76 and PF76TD are already used in the industry as refractory materials. There are several works in the literature on the flammability of polymer / layered silicate nanocomposites, but the effect of clay addition on the flammability of phenolic resins have not been studied so far. Further work can be carried out on testing the flammability of the phenolic resins based nanocomposites produced in this study, using a cone calorimeter.

### **Synthesis of Phenol Formaldehyde / Layered Silicate Nanocomposites, Using Modified Montmorillonite as Catalyst**

An effective method to enhance intercalation of clay by the polymer is to place the catalyst of the polymerization reaction inside the clay galleries, simply by modifying the clay with suitable chemicals. Purified Na-montmorillonite clays of Resadiye region can be modified with this purpose, using the catalyst of the reaction between phenol and formaldehyde. Then, the reaction between these two base materials can be carried out in presence of suitably modified montmorillonite clay, possibly yielding an intercalated and/or exfoliated structure.

### **Production of Phenolic Resin / Layered Silicate Nanocomposites, by Hot Pressing Method**

The studies carried out on phenolic resin / layered silicate nanocomposites in the literature generally involves the use of hot pressing the solid resin with the layered silicate. When this production route is followed, characterization tools such as XRD are more efficiently used, as samples can be examined at different stages of curing. Such observations lead to a better understanding of the intercalation phenomena. A similar study can be carried out by providing solid novolac resin, which is available commercially; or by freeze drying the available liquid resol resin, to obtain a solid resol resin.



## REFERENCES

- [1] ASM Handbook, vol.20 Material Selection And Design, 1997
- [2] Dubois P. and Alexandre M., “Polymer-layered silicate nanocomposites: preparation, properties and uses of a new class of materials”, Material Science and Engineering, vol.28, 1-63, 2000
- [3] Xing X.S. and Li R.K.Y., “Wear behavior of epoxy matrix composites filled with uniform sized sub-micron spherical silica particles”, Wear, vol.256, 21-26, 2004
- [4] Thostenson E.T., Ren Z., Chou T., “Advances in the science and technology of carbon nanotubes and their composites: a review”, Composites Science and Technology, vol.61, 1899-1912, 2001
- [5] Samir M.A.S.A, Alloin F., Sanchez J.Y., Dufresne A., “Cellulose nanocrystals reinforced poly (oxyethylene)”, Polymer, vol.45, 4149-4157, 2004
- [6] Schmidt D., Shah D., Giannelis E.P., “New advances in polymer/layered silicate nanocomposites”, Current Opinion in Solid State and Materials Science, vol.6, 205-212, 2002
- [7] Matthews F.L. and Rawlings R.D., “Composite Materials: Engineering and Science”, First Edition, Chapman & Hall Inc., London, 1993
- [8] Fischer H., “Polymer nanocomposites: from fundamental research to specific applications”, Material Science and Engineering C, vol.23, 763-772, 2003
- [9] LeBaron P.C., Wang Z., Pinnavaia T.J., “Polymer-layered silicate nanocomposites: an overview”, Applied Clay Science, vol.15, 11-29, 1999
- [10] Levitt A.P., “Whisker Technology”, Wiley-Interscience, Massachusetts, 1970
- [11] Usuki A., Kawasami, M., Kojima, Y., Okada, A., “Swelling behavior of montmorillonite cation exchanged for w-amino acids by e-caprolactam”, J.Mater.Res., vol.8, 1174-1178, 1993
- [12] Gao F., “Clay / polymer composites: the story”, Materialstoday, 50-55, November 2004

- [13] Arajan P.M., Schadler L.S., Braun P.V., "Nanocomposite Science and Technology", First Edition, Wiley-Vch, Weinheim, 2003
- [14] Fischer H., "Polymer nanocomposites: from fundamental research to specific applications", Materials Science and Engineering: C, Volume 23, 763-772, 2003
- [15] Kojima Y., Usuki A., Kawasumi M., Okada A., Kurauchi T., Kamigaito O., "Synthesis of nylon 6-clay hybrid by montmorillonite intercalated with  $\epsilon$ -caprolactam", Journal of Polymer Science A, vol. 31, 983-986, 1993
- [16] Chen C., Khobaib M., Curliss D., "Epoxy layered-silicate nanocomposites", Progress in Organic Coatings, vol.4, 376-383, 2003
- [17] Delozier D.M., Orwoll R.A., Cahoon J.F., Johnston N.J., Smith Jr J.G., Connell J.W., "Preparation and characterization of polyimide/organoclay nanocomposites", Polymer, vol.43, 813-822, 2002
- [18] Yao K.J., Song M., Hourstonb D.J., Luo D.Z., "Polymer/layered clay nanocomposites: 2 polyurethane nanocomposites", Polymer, vol.43, 1017-1020, 2002
- [19] Alexandre M., Dubois P., Sun T., Garces J.M., Jerome R., "Polyethylene-layered silicate nanocomposites prepared by the polymerization-filling technique: synthesis and mechanical properties", Polymer, vol. 43, 2123-2132, 2002
- [20] Morgan A.B., Harris J.D., "Exfoliated polystyrene-clay nanocomposites synthesized by solvent blending with sonication", Polymer, vol. 45, 8695-8703, 2004
- [21] Wang H., Zhao T., Zhi L., Yan Y., Yu Y., "Synthesis of novalac/layered silicate nanocomposites by reaction exfoliation using acid-modified montmorillonite", Macromolecular Rapid Communications, vol. 23, 44-48, 2002
- [22] Wu Z., Zhou C., Qi R., "The preparation of phenolic resin/montmorillonite nanocomposites by suspension condensation polymerization and their morphology", Polymer Composites, vol. 23, no.4, 634-646, 2002
- [23] Choi M.H., Chung I.J., Lee J.D., "Morphology and curing behaviors of phenolic resin-layered silicate nanocomposites prepared by melt intercalation", Chemistry of Materials, vol.12, 2977-2983, 2000

- [24] Choi M.H., Chung I.J., “Mechanical and thermal properties of phenolic resin-layered silicate nanocomposites synthesized by the melt intercalation”, Journal of Applied Polymer Science, vol.90, 2316-2321, 2003
- [25] Grim R.E., “Clay Mineralogy”, McGraw-Hill, New York, 1953
- [26] Clauer N., Chaudhuri S., “Clays in Crustal Environments: Isotope Dating and Tracing”, Springer-Verlag, New York, 1995
- [27] Ray S.S. and Okamoto M. “Polymer/layered silicate nanocomposites: a review from preparation to processing”, Progress in Polymer Science, vol.28, 1539-1641, 2003
- [28] [http://www.nanocor.com/benefits\\_tech.asp](http://www.nanocor.com/benefits_tech.asp)
- [29] Vaia R.A., Ishii H., Giannelis E.P., “Synthesis and properties of two-dimensional nanostructures by direct intercalation of polymer melts in layered silicates”, Chemistry of Materials, vol.5, 1694-1696, 1993
- [30] Byun H.Y., Choi M.H. and Chung I.J., “Synthesis and characterization of resol type phenolic resin/layered silicate nanocomposites”, Chemistry of Materials, vol.13, 4221-4226, 2001
- [31] Wang H., Zhao T., Yan Y., Yu Y., “Synthesis of resol-layered silicate nanocomposites by reaction exfoliation with acid-modified montmorillonite”, Journal of Applied Polymer Science, vol.92, 791-797, 2004
- [32] Fried J.R., “Polymer Science and Technology”, First Edition, Prentice-Hall PTR, USA, 1995
- [33] Fornes T.D., Hunter D.L., Paul D.R., “Effect of sodium montmorillonite source on nylon 6/clay nanocomposite”, Polymer, vol.45, 2321-2331, 2004
- [34] Kornmann X., Lindberg H. and Berglund L. A., “Synthesis of epoxy-clay nanocomposites: influence of the nature of the clay on structure”, Polymer, vol. 42, 1303-1310, 2001
- [35] Wolfrum J. and Ehrenstein G.W., “Interdependence between the curing, structure and the mechanical properties of phenolic resins”, Journal of Applied Polymer Science, vol. 74, 3173-3185, 1999

- [36] Morgan A.B, Gilman J.W., “Characterization of polymer-layered silicate (clay) nanocomposites by transmission electron microscopy and x-ray diffraction: A comparative study”, Journal of Applied Polymer Science, vol.87, 1329-1338, 2003
- [37] Cullity B.D, “Elements of X-ray Diffraction”, First Edition, Addison –Wesley Publishing Company, Inc., USA, 1967
- [38] Alger, M., “Polymer Science Dictionary”, Second Edition, Chapman & Hall, London, 1997
- [39] Singh K.P., Palmese G.R., “Enhancement of Phenolic Polymer Properties by Use of Ethylene Glycol as Diluent”, Journal of Applied Polymer Science, vol. 91, 3096-3106, 2004
- [40] Ravve A., “Principles of Polymer Chemistry”, Plenum Press, New York, 1995
- [41] International Standard ISO 11357-2, “Plastics - Differential Scanning Calorimetry”, 1999
- [42] Beyer G., “Nanocomposites: A new class of flame retardants for polymers”, Plastics Additives & Compounding, October 2002
- [43] Pascault J.P., “Thermosetting Polymers”, Marcel Dekker Incorporated, USA, 2002

## APPENDIX A

### XRD Diffractograms of the 9 Different Clays Used

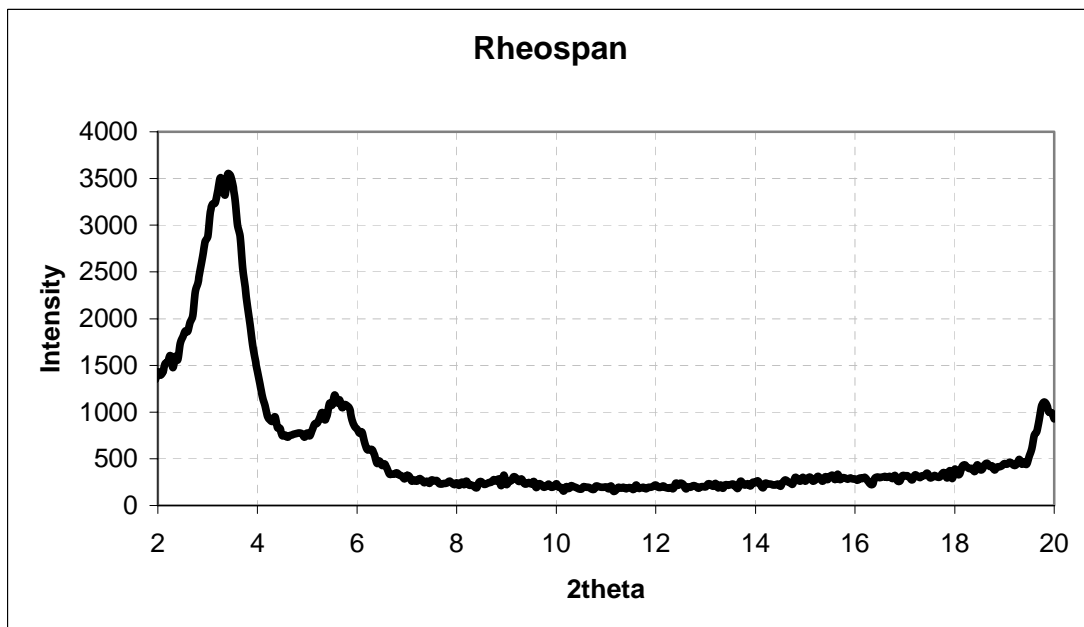


**Figure A.1** XRD diffractogram of Rheospan clay ( $2\theta = 3.4^\circ$ )

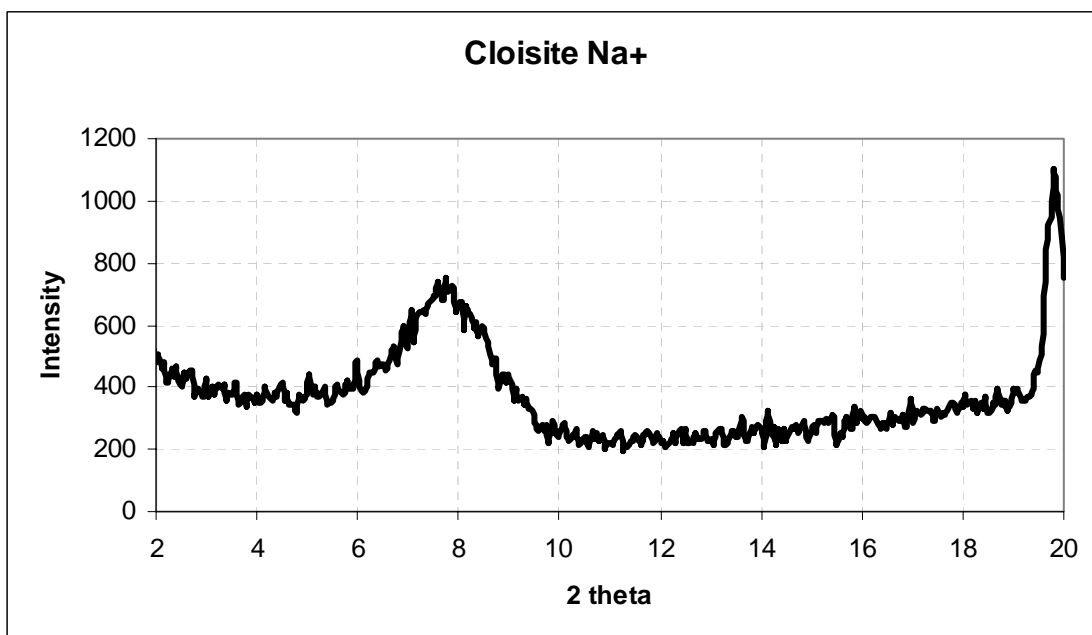


**Figure A.2** XRD diffractogram of Cloisite Na+ clay ( $2\theta = 7.8^\circ$ )

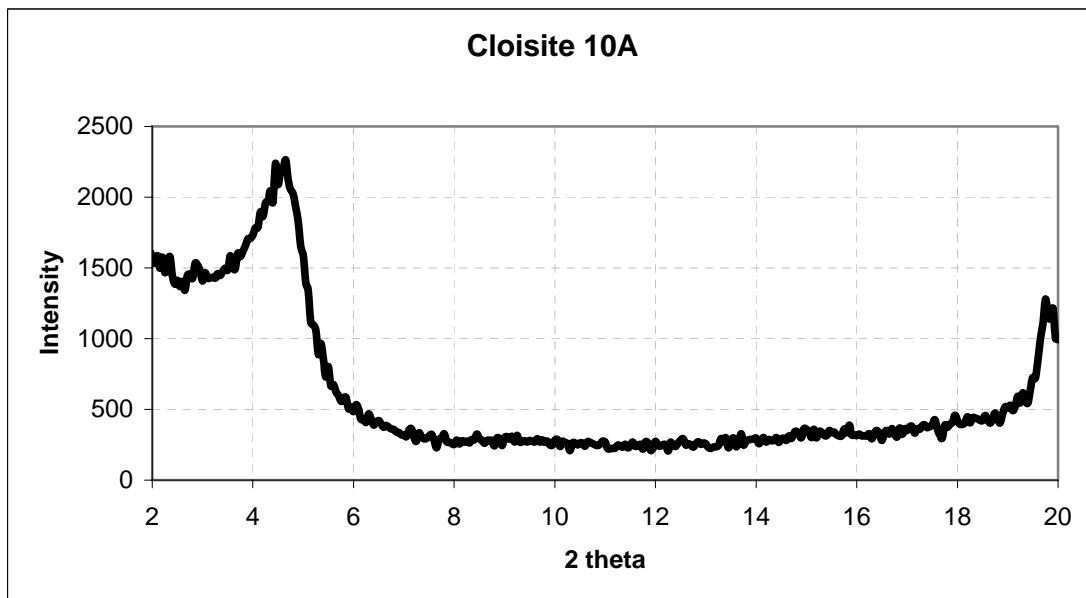


**Figure A.3** XRD diffractogram of Cloisite 10A clay ( $2\theta = 4.7^\circ$ )

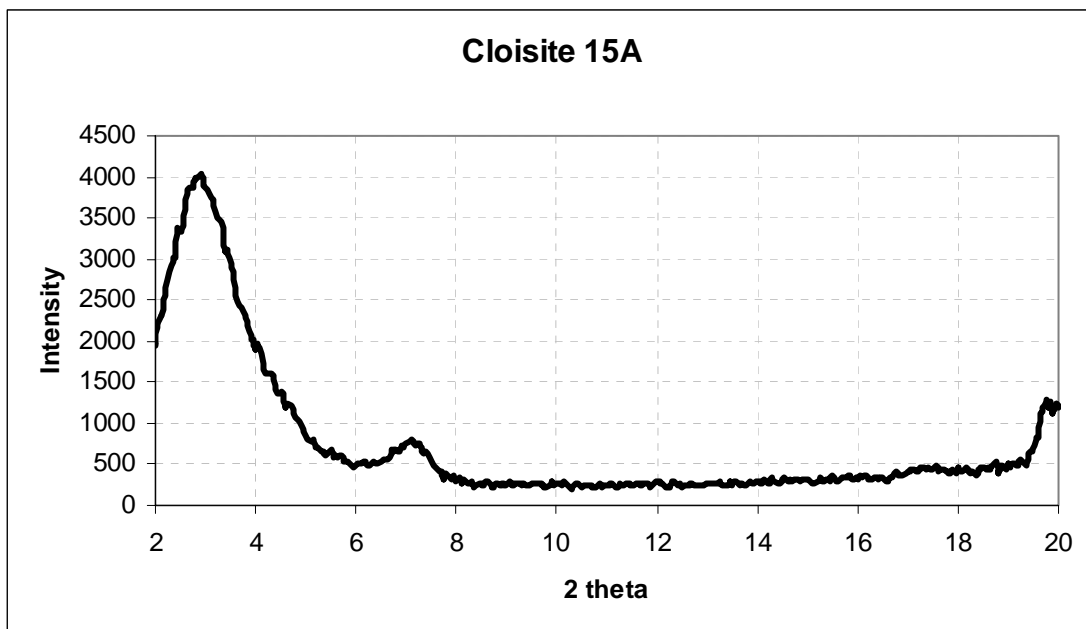


**Figure A.4** XRD diffractogram of Cloisite 15A clay ( $2\theta = 2.9^\circ$ )

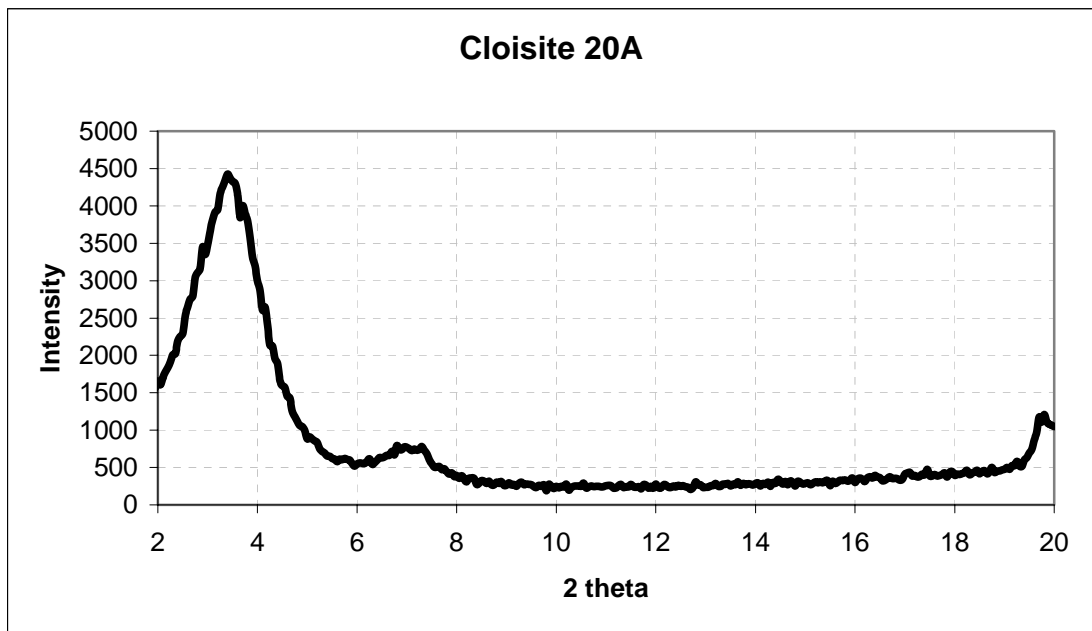


**Figure A.5** XRD diffractogram of Cloisite 20A clay ( $2\theta = 3.4^\circ$ )

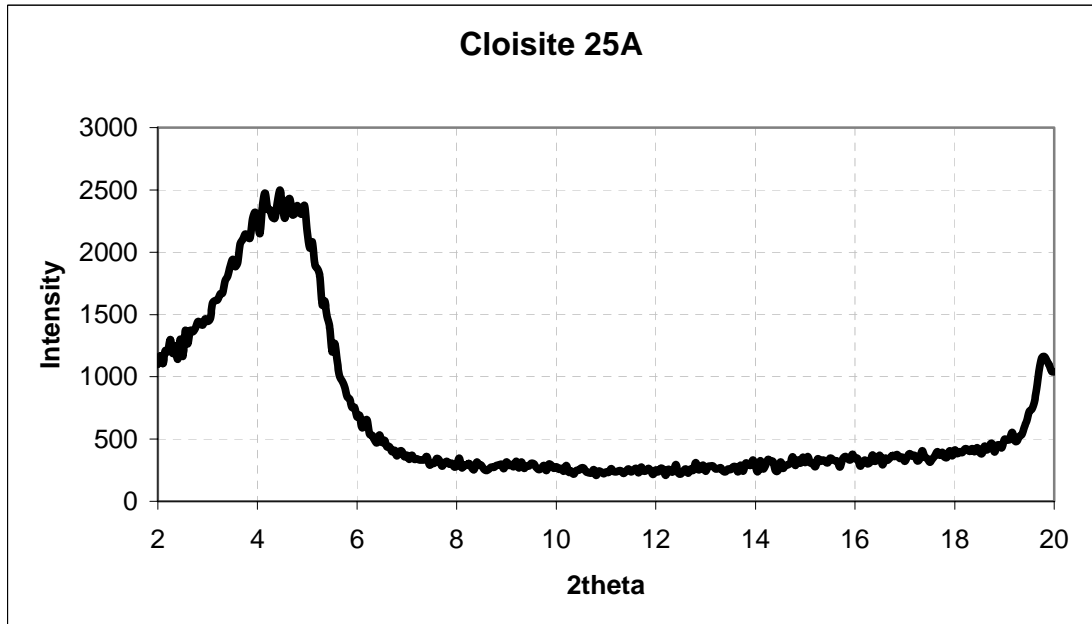


**Figure A.6** XRD diffractogram of Cloisite 25A clay ( $2\theta = 4.4^\circ$ )

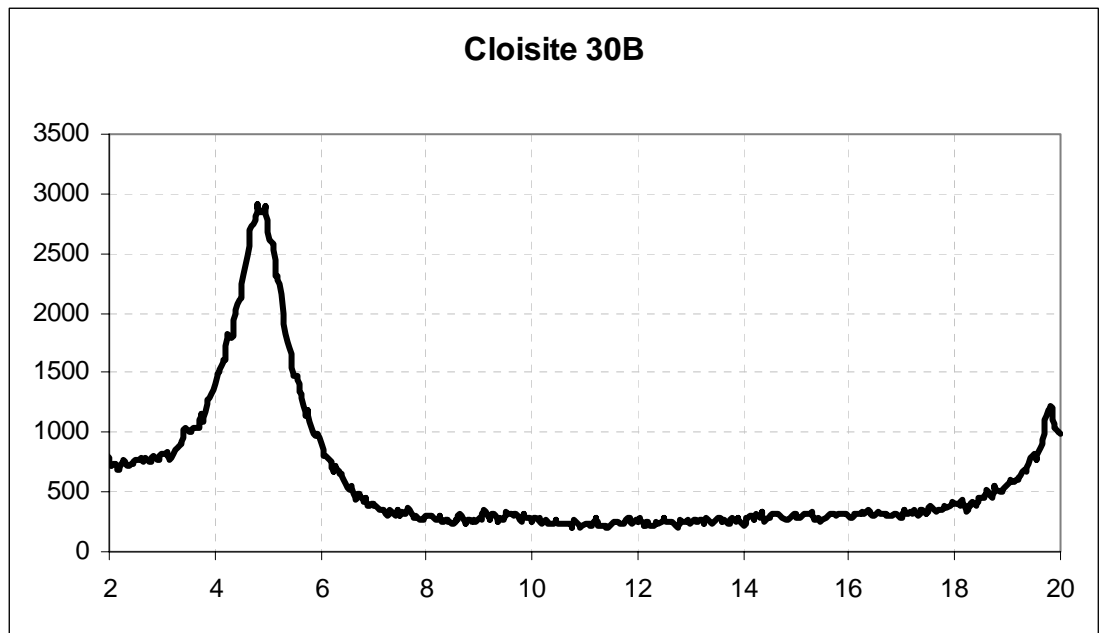


**Figure A.7** XRD diffractogram of Cloisite 30B clay ( $2\theta = 4.8^\circ$ )

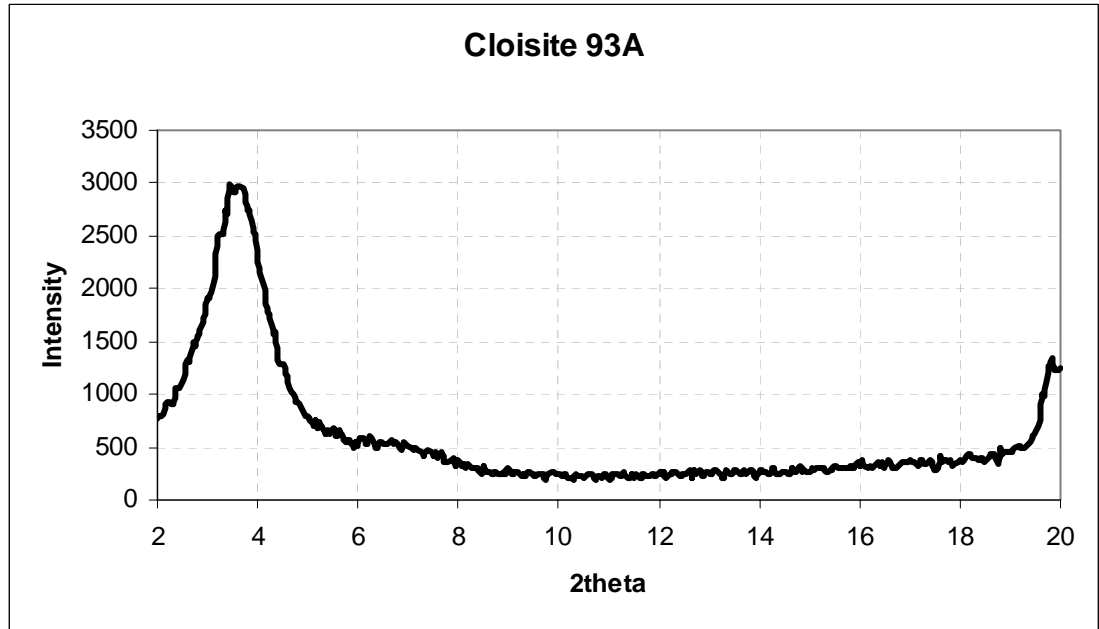


**Figure A.8** XRD diffractogram of Cloisite 93A clay ( $2\theta = 3.6^\circ$ )



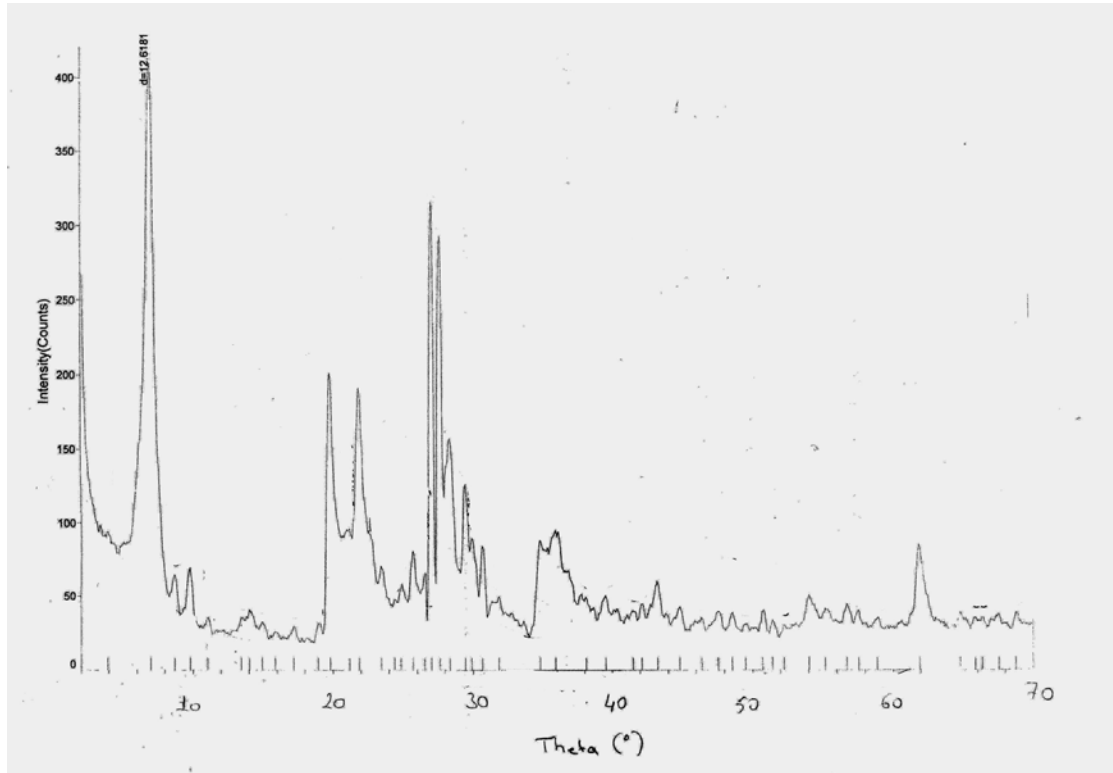


**Figure A.9** XRD diffractogram of Resadiye clay ( $d = 12.62\text{nm}$ )

## APPENDIX B

### XRD Diffractograms of the 14 Different Specimens Produced

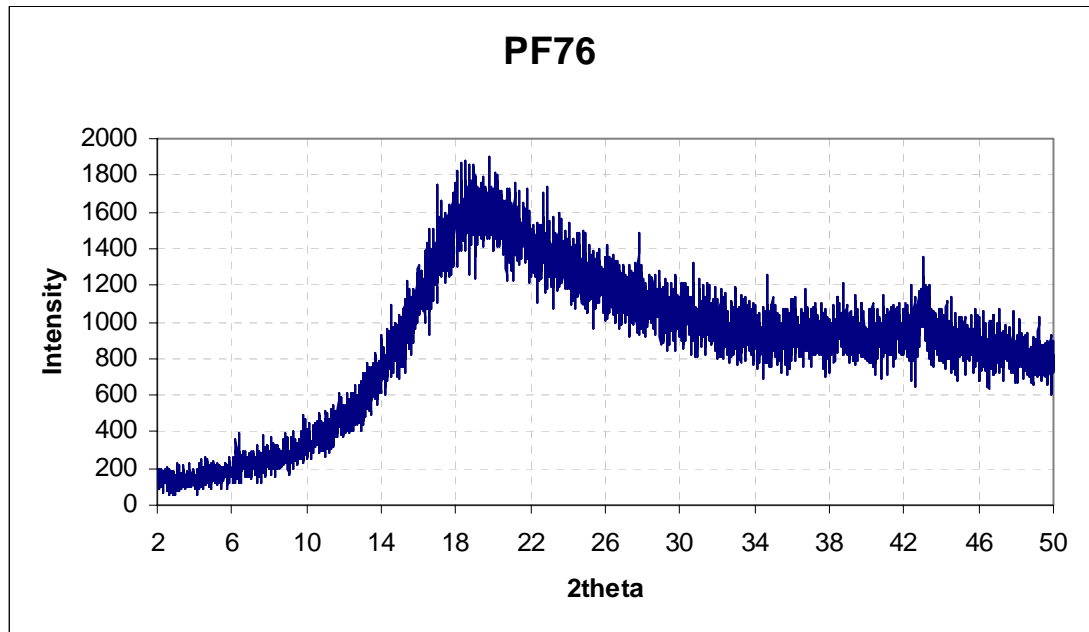


Figure B.1 XRD diffractogram of PF76 neat resin specimen

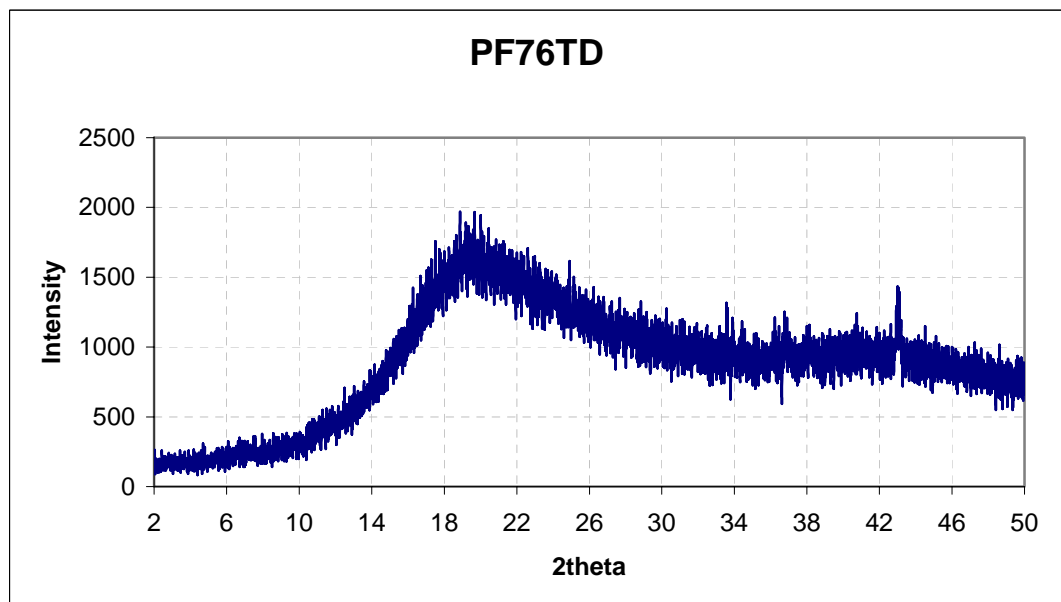
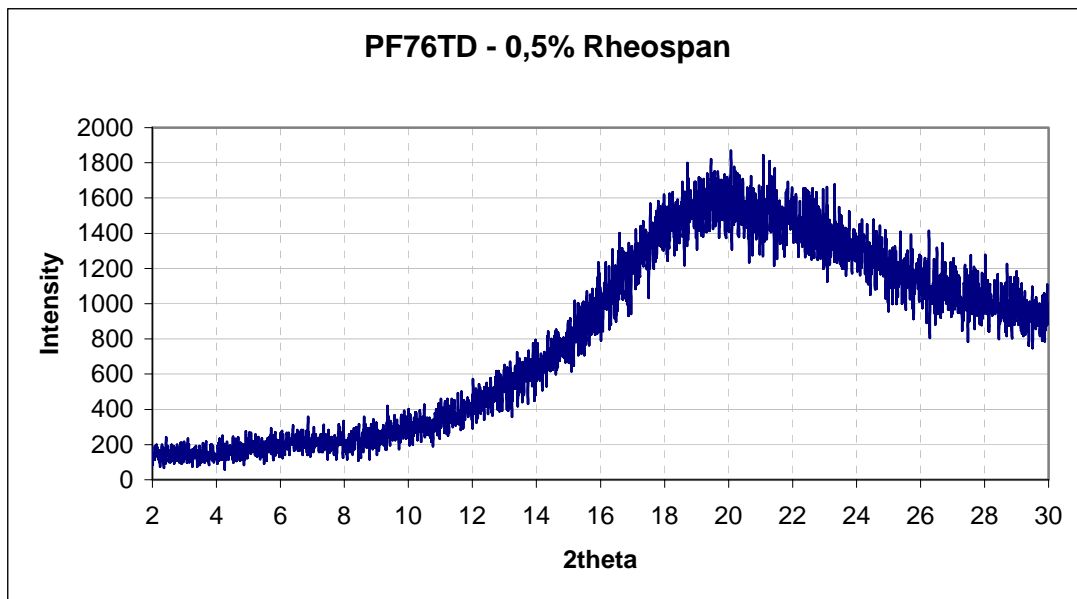
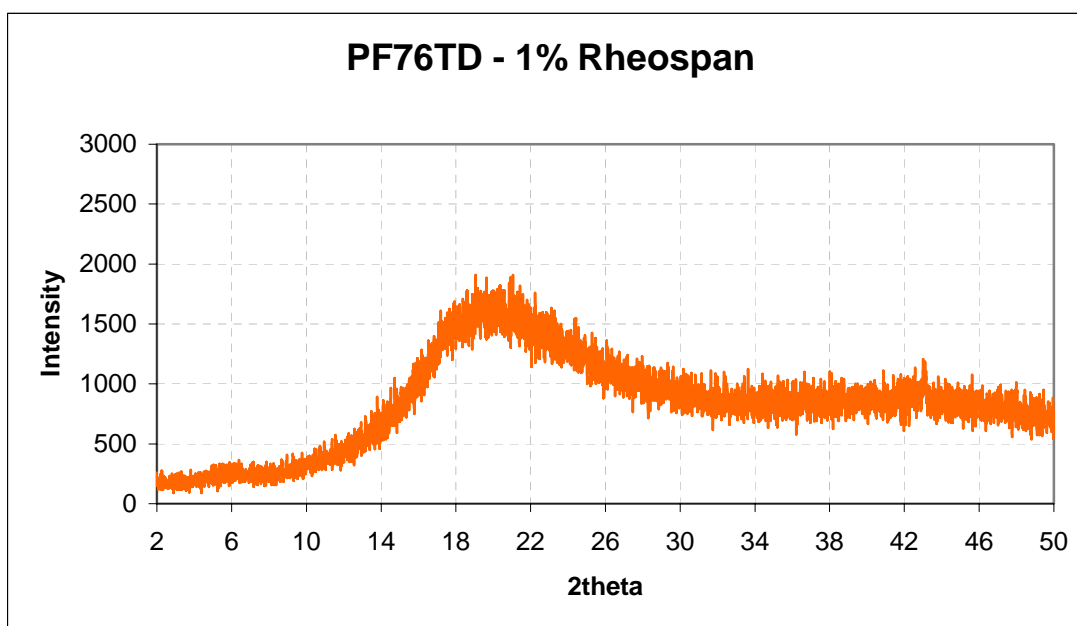


Figure B.2 XRD diffractogram of PF76TD neat resin specimen



**Figure B.3** XRD diffractogram of PF76TD-0,5% Rheospan specimen



**Figure B.4** XRD diffractogram of PF76TD-1,0% Rheospan specimen

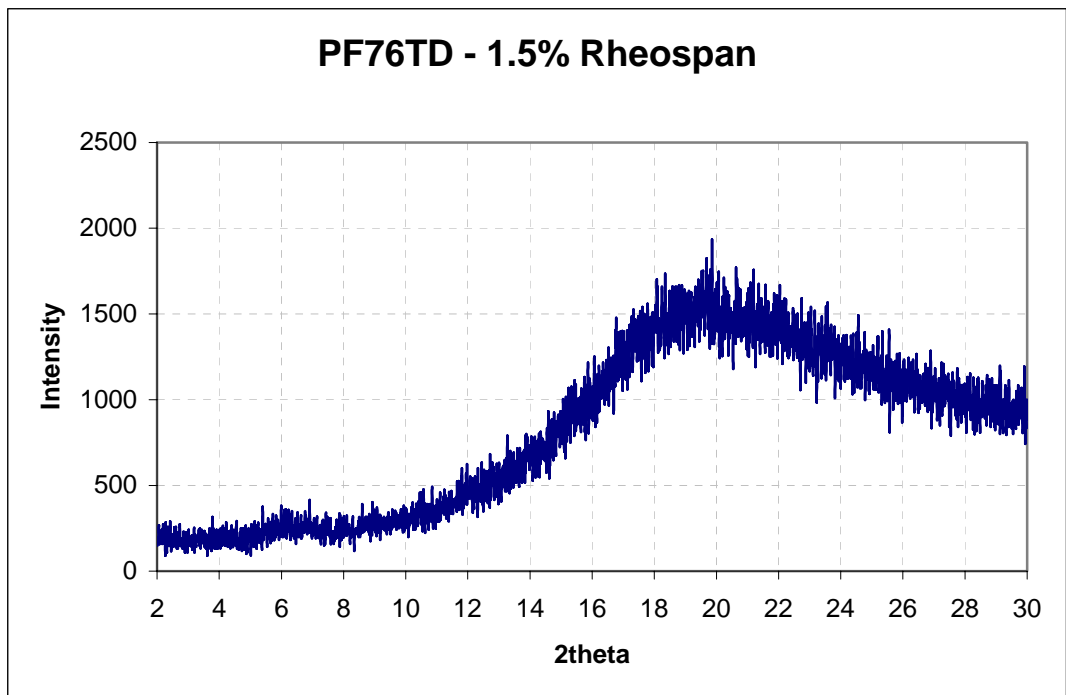


**Figure B.5** XRD diffractogram of PF76TD-1,5% Rheospan specimen

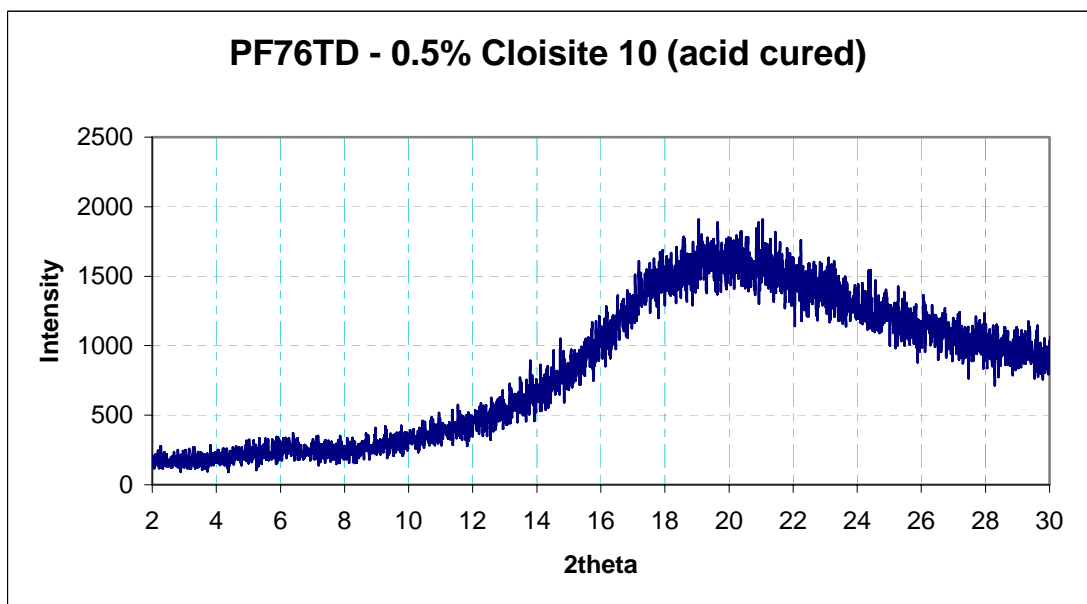


**Figure B.6** XRD diffractogram of PF76TD-0,5% Cloisite 10A (acid cured) specimen

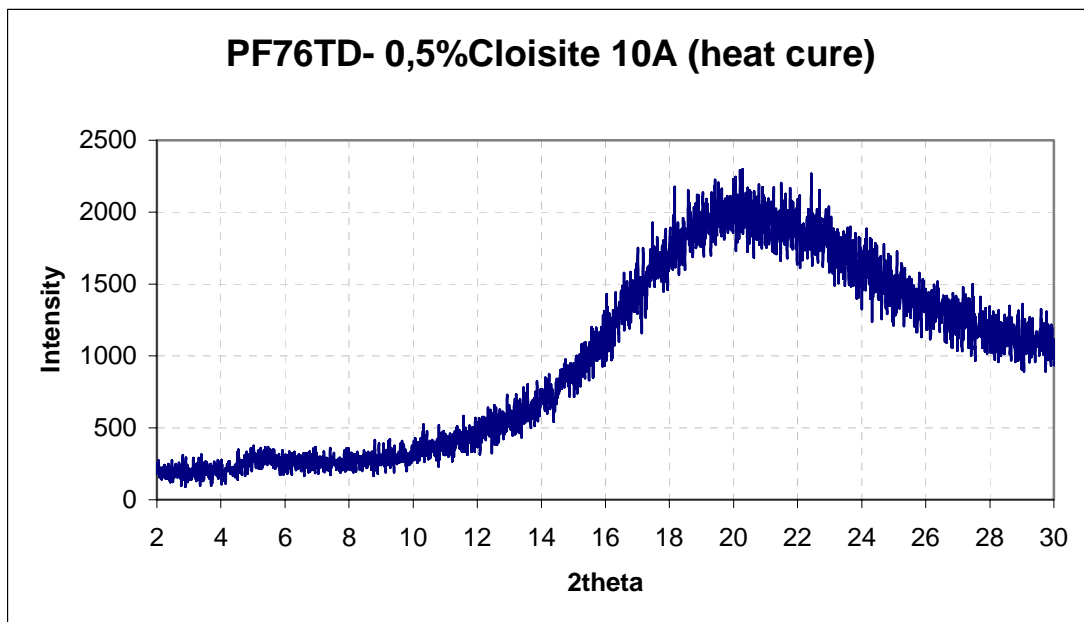


**Figure B.7** XRD diffractogram of PF76TD-0,5% Cloisite 10A (heat cured) specimen

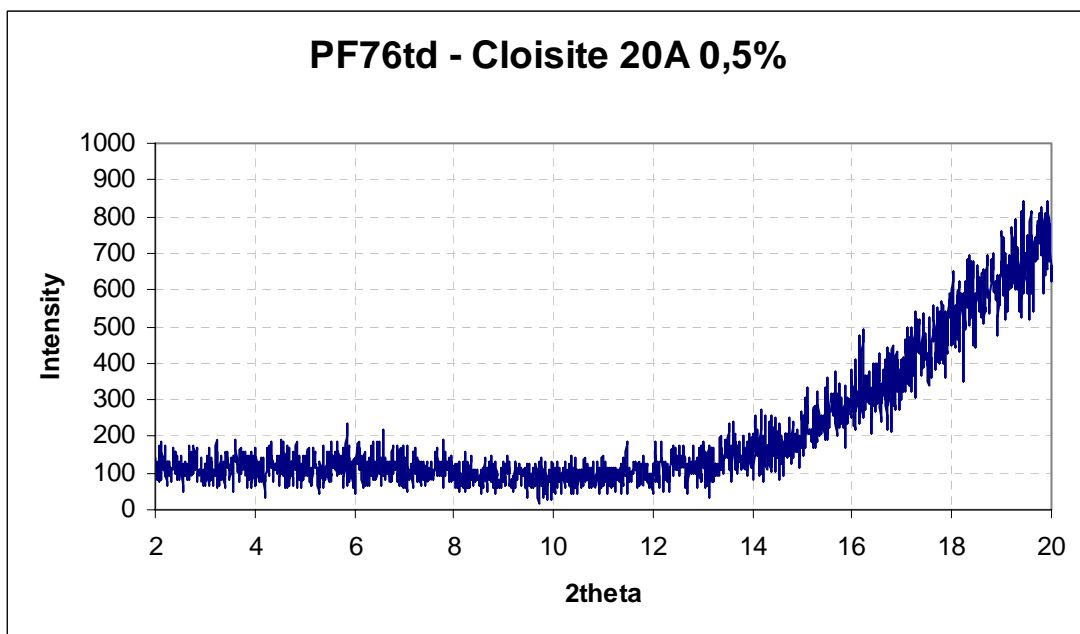


**Figure B.8** XRD diffractogram of PF76TD-0,5% Cloisite 20A specimen

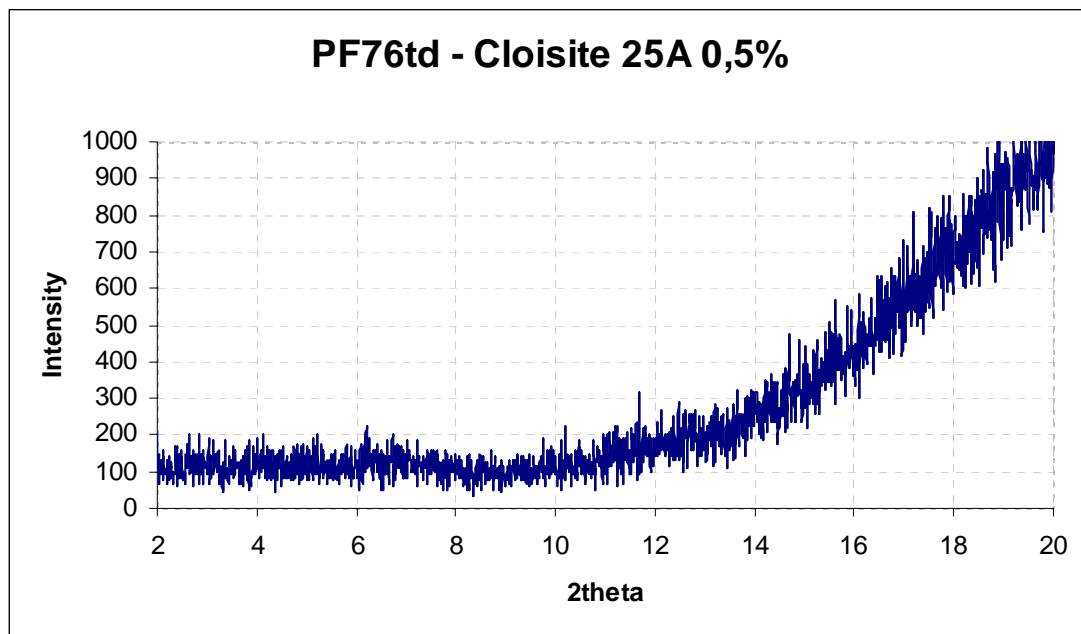


**Figure B.9** XRD diffractogram of PF76TD-0,5% Cloisite 25A specimen

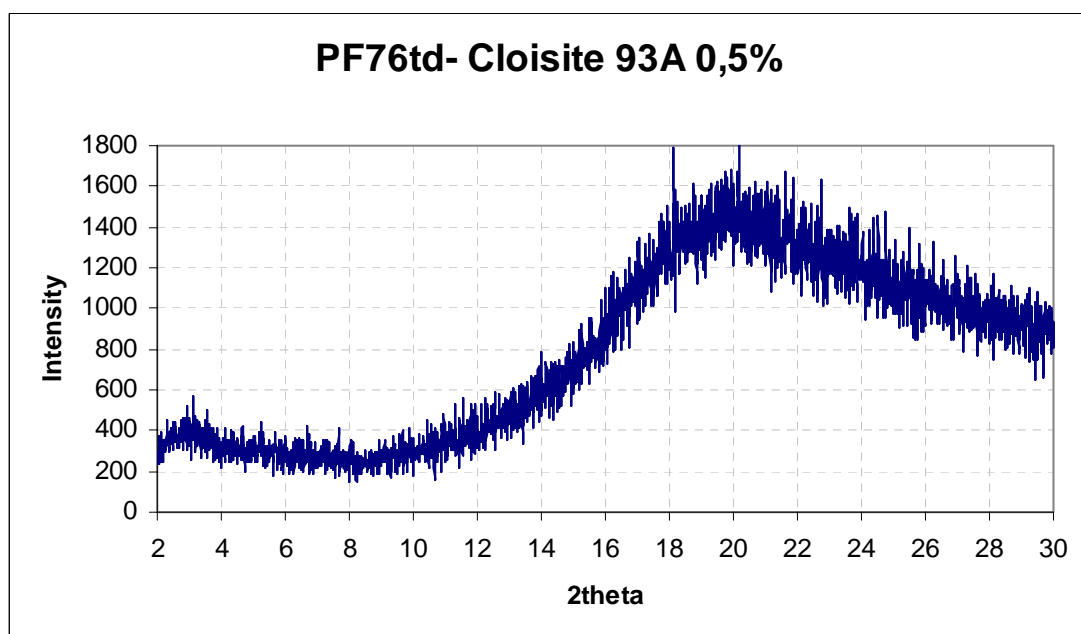


**Figure B.10** XRD diffractogram of PF76TD-0,5% Cloisite 93A specimen

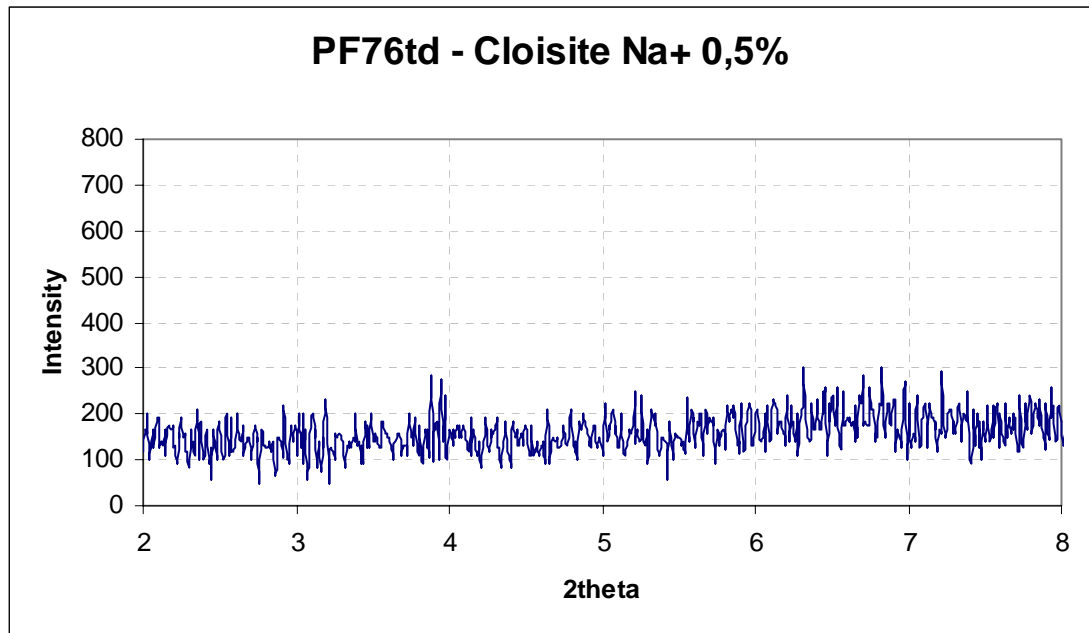


**Figure B.11** XRD diffractogram of PF76TD-0,5% Cloisite Na+ specimen

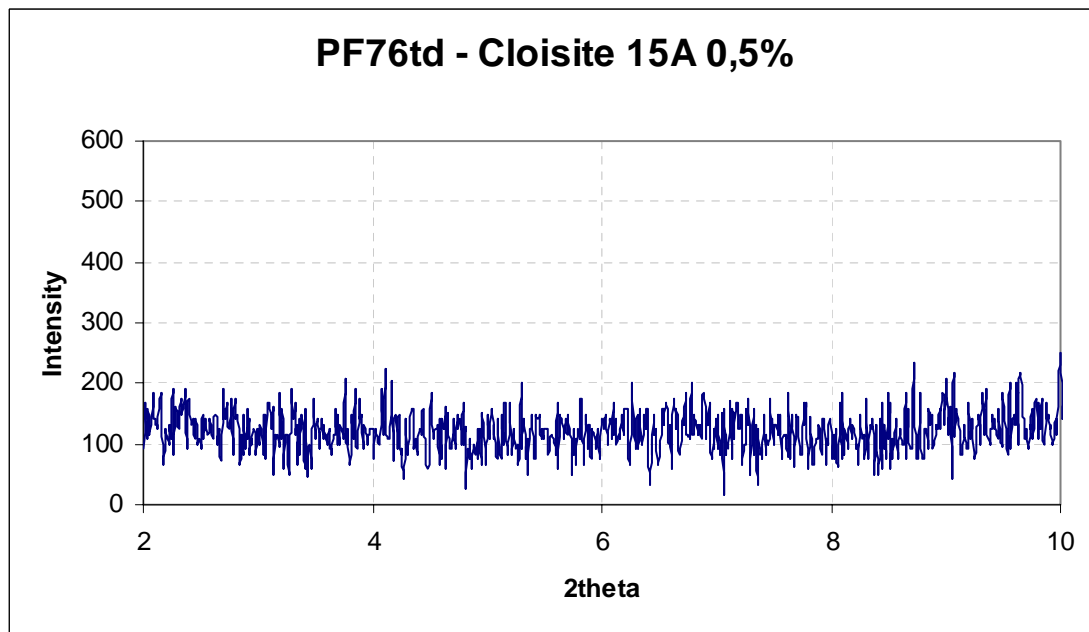


**Figure B.12** XRD diffractogram of PF76TD-0,5% Cloisite Na+ specimen

## APPENDIX C

### Examples of Flexural Stress vs Strain Curves of the 14 Different Specimens

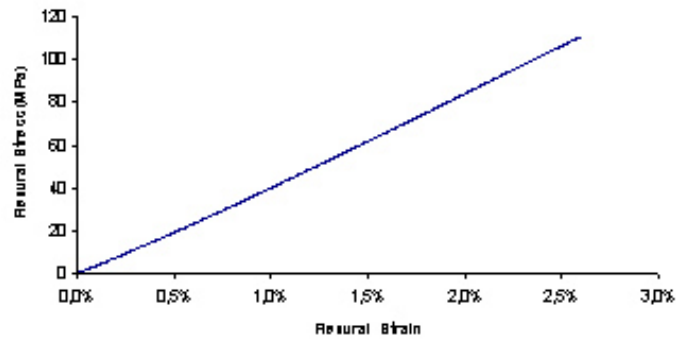


Figure C.1 Flexural Stress vs Strain Curves of neat PF76 specimen

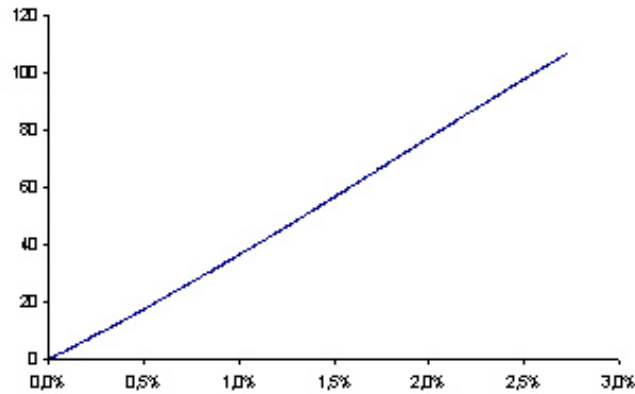


Figure C.2 Flexural Stress vs Strain Curves of neat PF76TD specimen

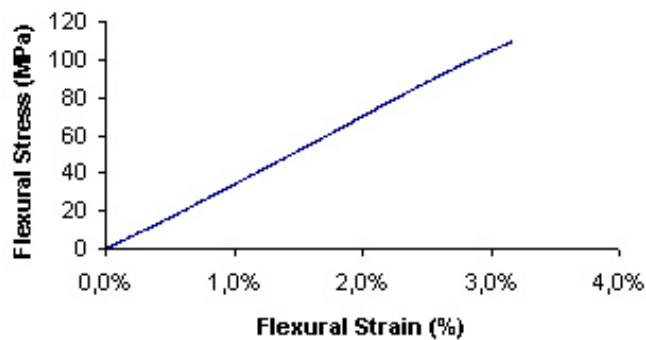
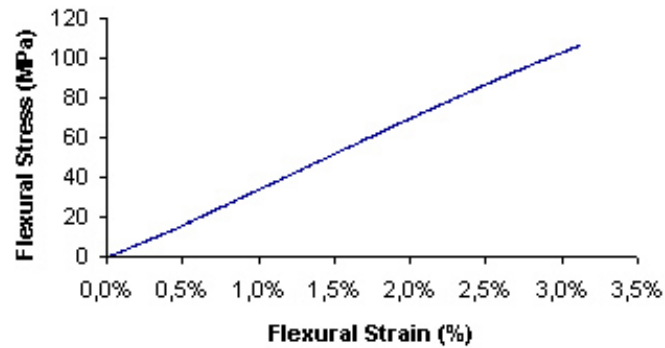
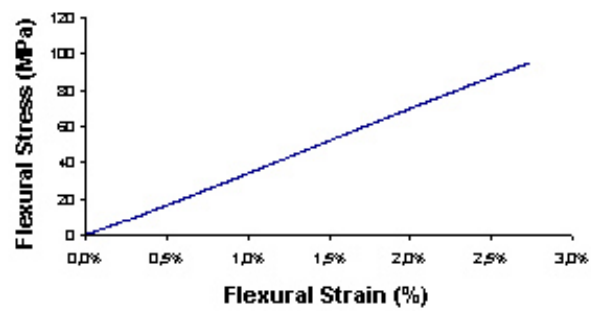


Figure C.3 Flexural Stress vs Strain Curves of PF76TD - 0,5% Rheospan





**Figure C.4 Flexural Stress vs Strain Curves of PF76 TD – 1,0% Rheospan specimen**



**Figure C.5 Flexural Stress vs Strain Curves of PF76 TD – 1,5% Rheospan specimen**

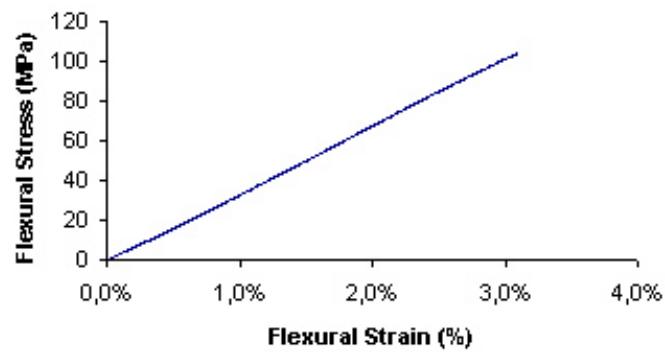


**Figure C.6 Flexural Stress vs Strain Curves of PF76 TD – 0,5% CloisiteNa+ specimen**

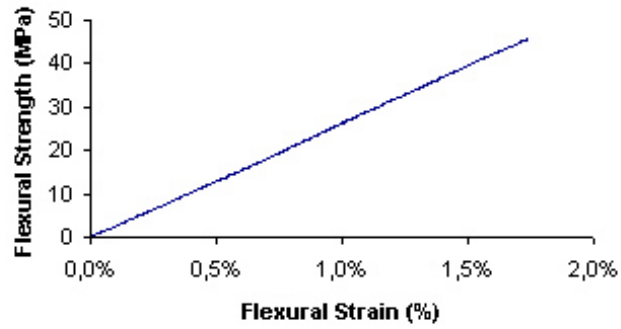


**Figure C.7 Flexural Stress vs Strain Curves of heat cured PF76TD – 0,5% Cloisite10A specimen**

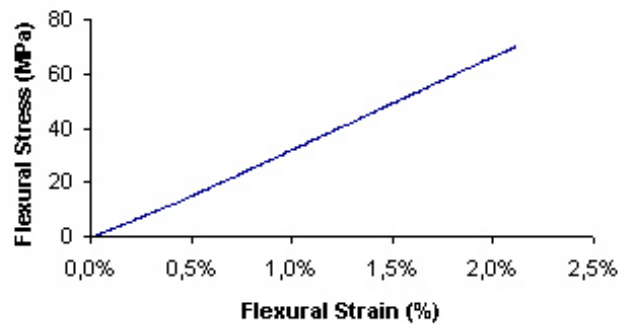


**Figure C.8 Flexural Stress vs Strain Curves of acid cured PF76TD – 0,5% Cloisite10A specimen**

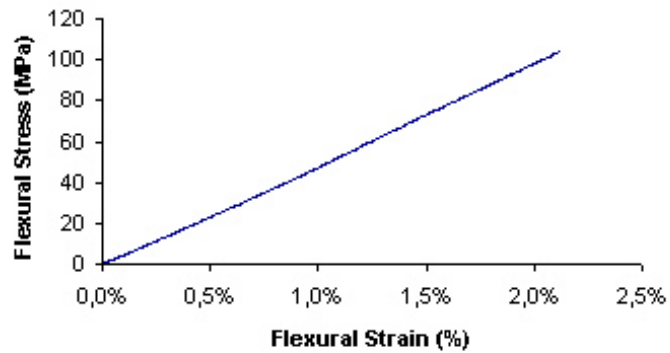


**Figure C.9 Flexural Stress vs Strain Curves of PF76TD – 0,5% Cloisite 15A specimen**

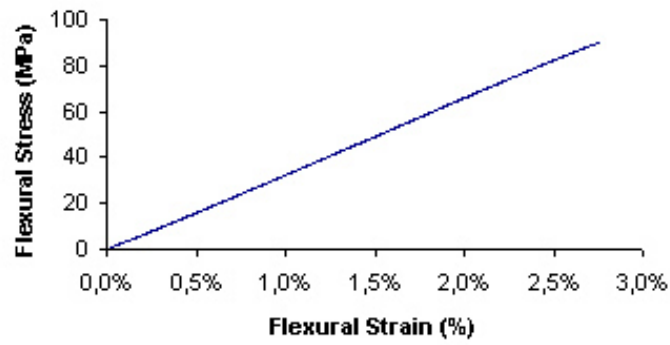


**Figure C.10 Flexural Stress vs Strain Curves of PF76 TD-0,5% Cloisite20A**

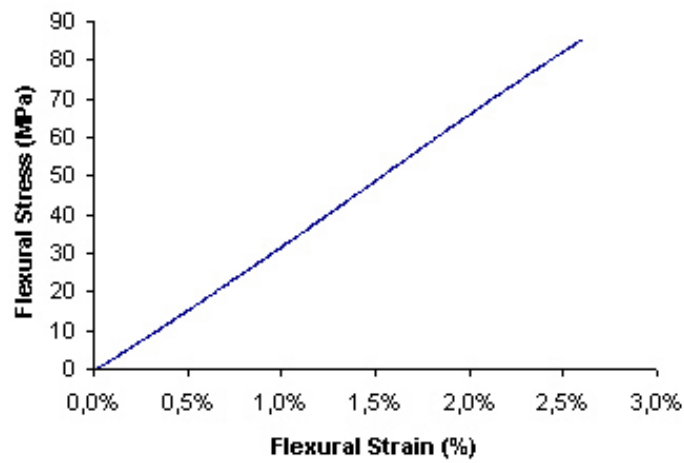


**Figure C.11 Flexural Stress vs Strain Curves of PF76 TD-0,5% Cloisite 25A**

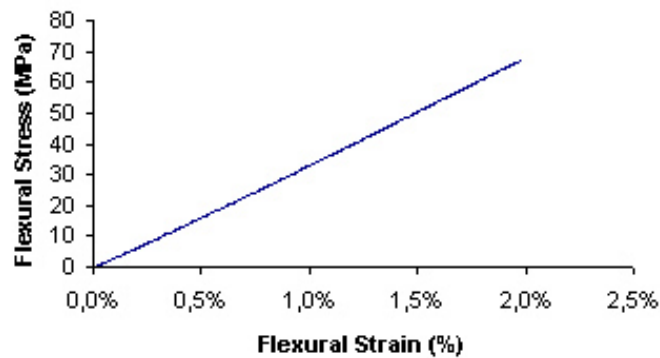


**Figure C.12 Flexural Stress vs Strain Curves of PF76 TD-0,5% Cloisite 30B**

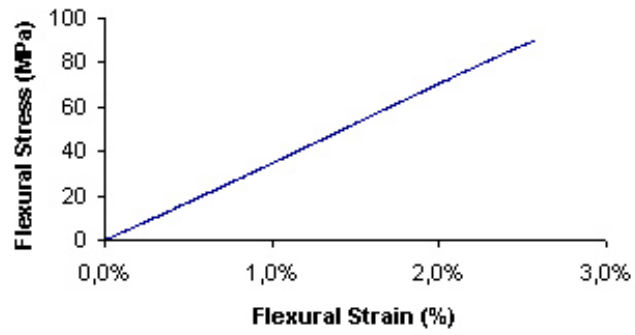


**Figure C.13 Flexural Stress vs Strain Curves of PF76 TD -0,5% Cloisite 93A specimen**

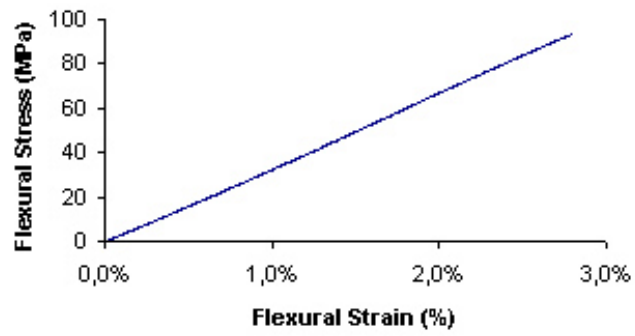


**Figure C.14 Flexural Stress vs Strain Curves of PF76 TD -0,5% Resadiye specimen**

## APPENDIX D

### Examples of Load vs Deflection curves of the 14 Different Specimens

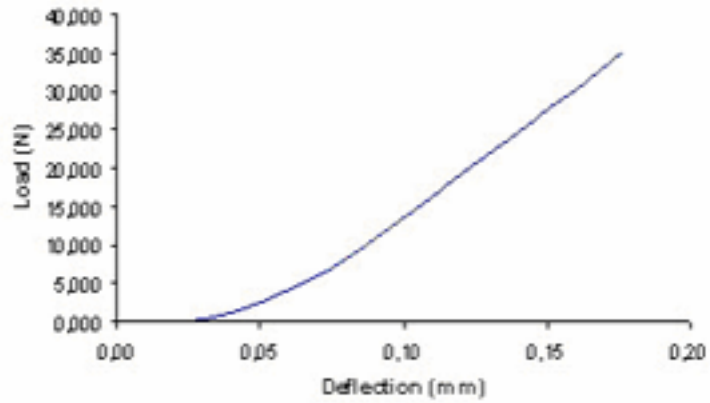


Figure D.1 Flexural Load vs Deflection Curves of neat PF76 specimen

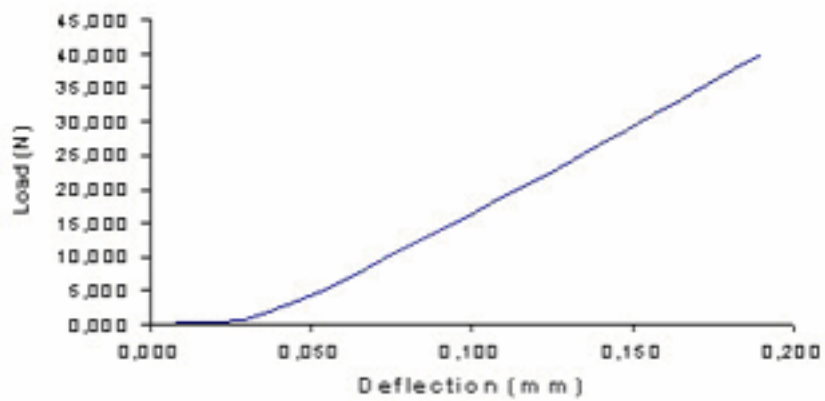


Figure D.2 Flexural Load vs Deflection Curves of neat PF76 TD specimen

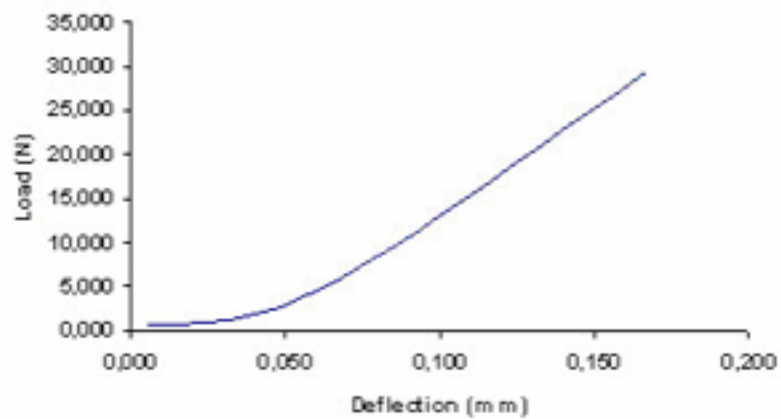
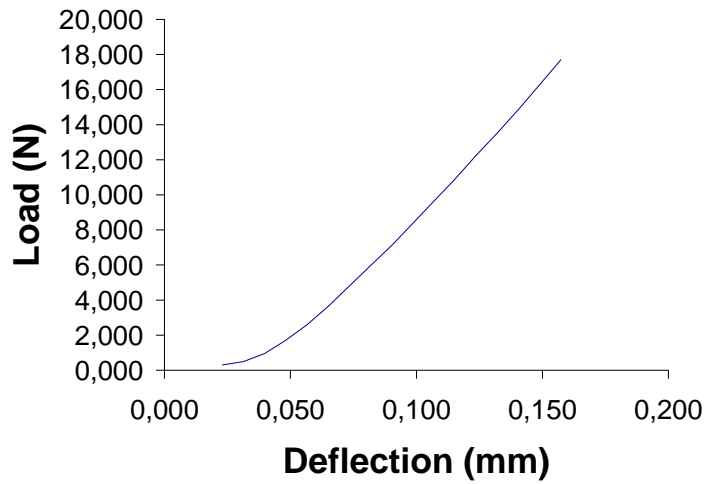
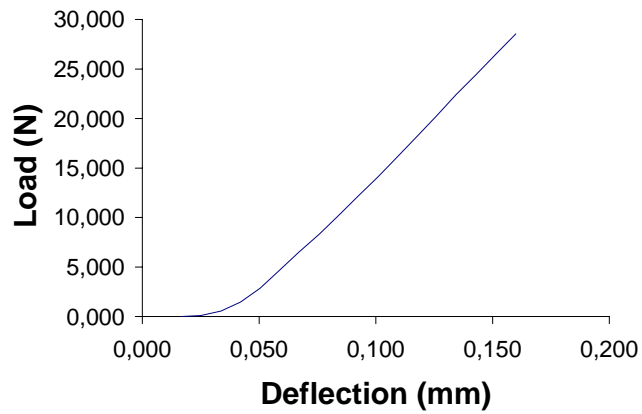


Figure D.3 Flexural Load vs Deflection Curves of PF76TD - 0,5% Rheospan



**Figure D.4** Flexural Load vs Deflection Curves of heat cured PF76TD – 0,5% Cloisite 10A specimen



**Figure D.5** Flexural Load vs deflection Curves of acid cured PF76TD – 0,5% Cloisite 10A specimen

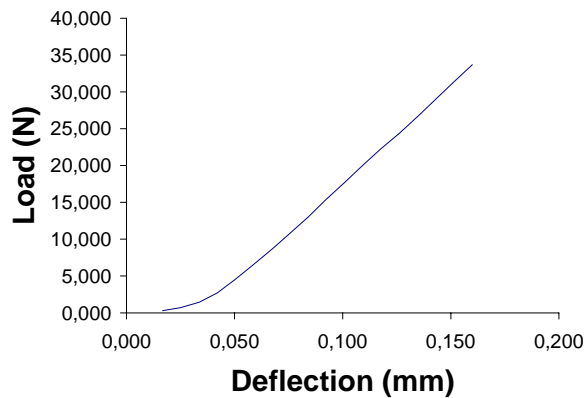


**Figure D.6** Flexural Load vs deflection Curves of PF76TD – 0,5% CloisiteNa+ specimen

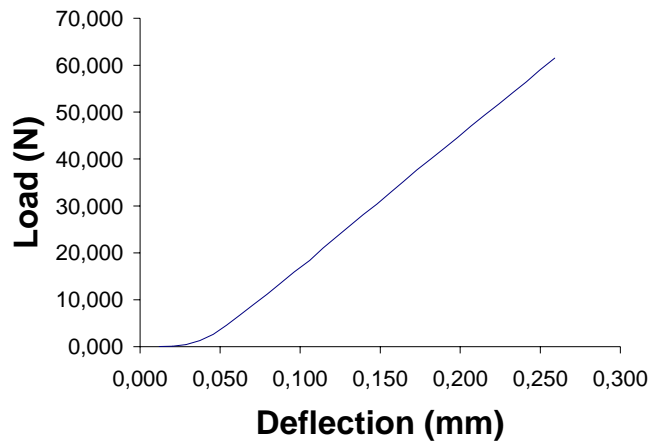


**Figure D.7** Flexural Load vs Deflection Curves of PF76TD – 1,0% Rheospan specimen

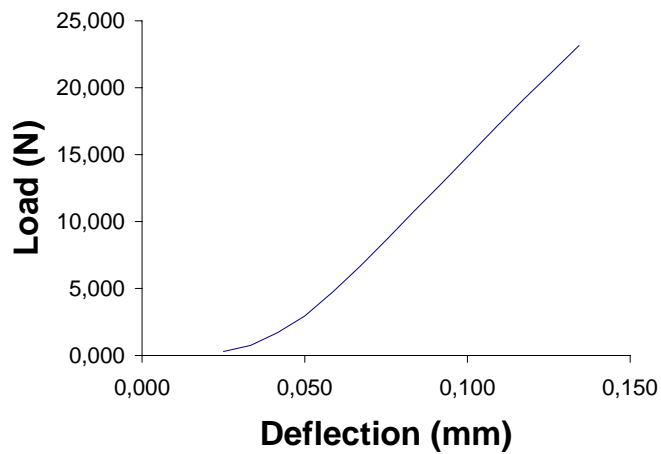


**Figure D.8** Flexural Load vs Deflection Curves of PF76TD – 1,5% Rheospan specimen

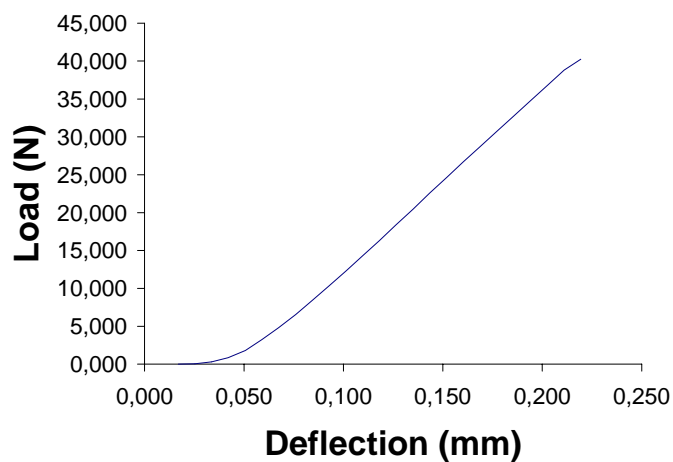


**Figure D.9** Flexural Load vs Deflection Curves of PF76TD – 0,5% Cloisite 15A specimen

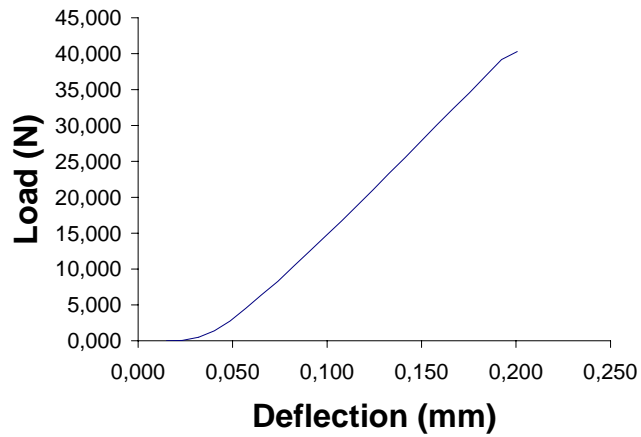


**Figure D.10** Flexural Load vs Deflection Curves of PF76TD – 0,5% Cloisite20A specimen

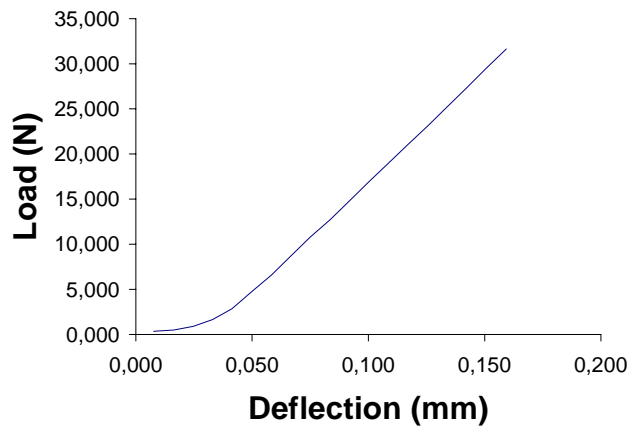


**Figure D.11** Flexural Load vs Deflection Curves of PF76TD – 0,5% Cloisite 25A specimen

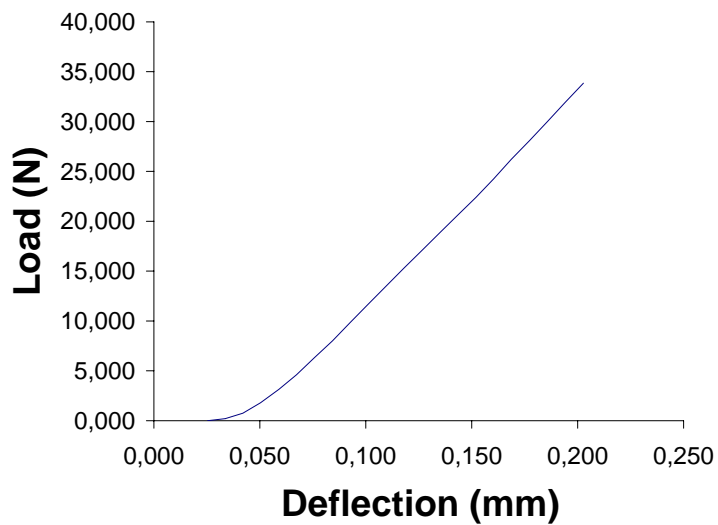


**Figure D.12** Flexural Load vs Deflection Curves of PF76TD – 0,5% Cloisite 30B specimen



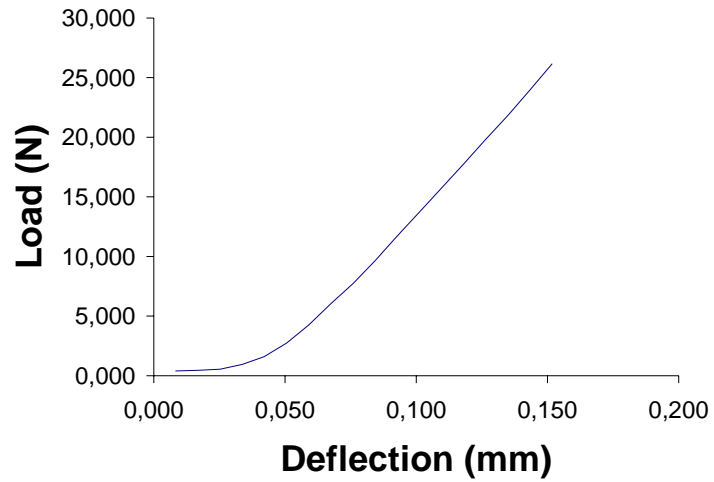


**Figure D.13** Flexural Load vs Deflection Curves of PF76TD –0,5% Cloisite 93A specimen

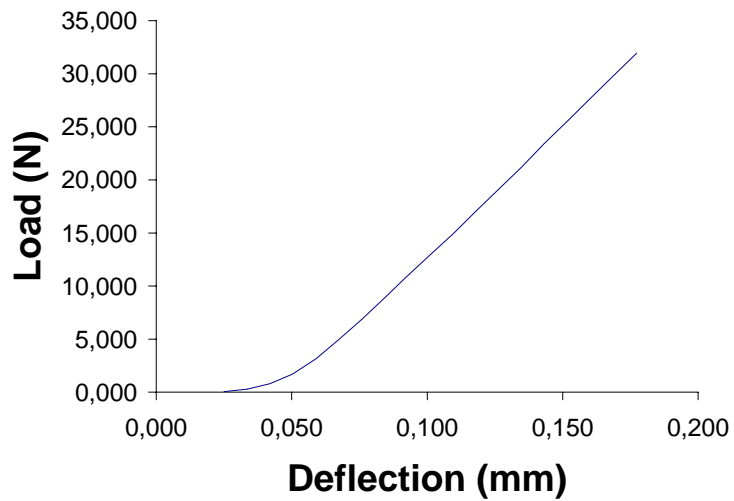


**Figure D.14** Flexural Load vs Deflection Curves of PF76TD – 0,5% Resadiye specimen